# A Novel Continuous Homogeneous Catalytic Process for Fluorous Biphasic Systems

by

**Evangelia Perperi**

A thesis submitted for the degree of Doctor of Philosophy of the University of London

Department of Chemical Engineering,
University College London
London, NW1 7JE

September, 2004

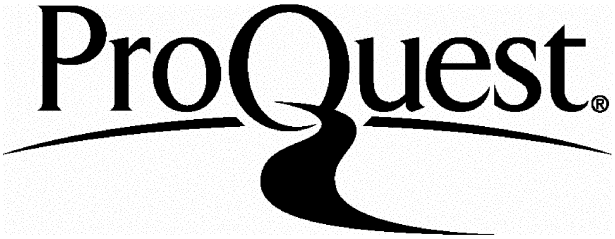

Dedicated to my parents,

Dimitris and Katerina.

# ABSTRACT

Homogeneous catalysts can provide very high activity and selectivity towards industrial desirable products at relatively mild conditions, but their commercialisation has been so far hampered by the problem of their separation from reaction mixture and solvent and hence the difficulties associated with their recycling. To overcome this problem a new concept of fluorous biphasic homogeneous catalysis has been developed to facilitate the separation and recycling of the catalyst. In these systems the catalyst is dissolved in a fluorous solvent. Under ambient conditions the fluorous phase is immiscible with the organic one containing the reaction components, facilitating catalyst separation and recycling. At reaction conditions only one phase is formed allowing excellent contact between substrate and catalyst and eliminating mass transfer limitation. This is a generic technology with high potential for industrialisation that is applicable to a wide variety of homogeneous catalytic systems.

In this work a continuous reaction system is developed, which includes a chemical reactor that is connected via a heat exchanger with a gravity settler, where from the catalyst phase is continuously recycled to the reactor. The work is focused on the hydroformylation of higher alkenes, a reaction system of great industrial importance.

The liquid – liquid equilibrium of the fluorous solvent – organic phase was studied. A proof of concept separation study in a continuous system was also carried out demonstrating the efficiency of the separation of the two phases.

Finally, reaction studies were carried out in the presence of a fluorous modified rhodium catalyst. Conversion levels up to 70% were observed, with linear to branched

product ratios being around 12, while the fluorous catalyst was successfully recycled to the reactor. Efficient stirring was essential for high conversions for minimising alkene isomerisation. Leaching of the ligand, rhodium and the fluorous solvent into the organic product phase was significant.

# ACKNOWLEDGEMENTS

First of all, I would like to thank my supervisor Dr. George Manos for giving me the opportunity to be part of this research. I learnt a lot from his knowledge, experience and expertise, while his personal guidance, enthusiasm and interest made it possible for me to complete the project. I would also like to express my appreciation because he was always there not only to provide his advice in my work but, above all, even his personal concern in all aspects of everyday life.

I would also like to thank Yulin, Clare, Dr. Adams, Dr. Angeli and Prof. Hope without the help of which the completion of the project would not have been possible. A special thanks to Prof. Cole – Hamilton for sharing with me his chemistry expertise. His personal interest and enthusiasm through out the project is very much appreciated.

I would also like to thank EPSRC for the financial support of the project.

I will certainly miss the people I shared my office with over the past four years at UCL and St. Andrews University. I would like to thank them for creating a pleasant atmosphere with their different personalities and enlightening discussions. I owe special thanks to Marcello for our long technical conversations and his brilliant ideas.

I would also like to thank Giannis, Lia, Karolina and Emily for their emotional support during all this trying time.

Last but not least I would like to thank my family for their support and encouragement during all my academic years.

# Contents

# List of Figures

**Chapter 4: Experimental Set – Up**



**Chapter 5: Phase Equilibrium Experiments**

# CHAPTER 1:

# Introduction

Homogeneous catalysts can provide very high activity and selectivity towards industrial desirable products at relatively mild conditions but their commercialisation has been so far hampered by the problem of their separation from reaction mixture and solvent and hence the difficulties associated with their recycling [Frohling and Kohlpaintner, 1996]. The new concept of Fluorous Biphasic Systems (FBS) has been developed for the easy separation and recycling of the homogeneous catalysts. In these systems the catalyst is dissolved in a fluorous solvent, which under reaction temperature is miscible with an organic solvent that contains the reaction components, while under ambient conditions is immiscible with the reaction mixture [Horvath and Rabai, 1994]. This is a generic technology that is applicable to a wide variety of homogeneous catalytic systems, but this work is focused on the hydroformylation of higher alkenes, a reaction system of great industrial importance [Frohling and Kohlpaintner, 1996].

Hydroformylation of long chain alkenes produces aldehydes, which are subsequently used as raw materials for the manufacture of soaps and detergents.

Currently, hydroformylation process is carried out using cobalt based catalysts, which require very harsh operating conditions. Considerable advantages in selectivity and operating conditions can be obtained using rhodium based catalysts, but conventional separation of the products by distillation is impossible because the boiling points of the products, even at low pressure, are well above the decomposition temperature of the catalyst [Frohling and Kohlpaintner, 1996]. The fluorous biphasic approach has high potential for industrialisation as it is monophasic under the catalytic conditions allowing excellent contact between substrate and catalyst and eliminating mass transfer limitation, while biphasic at ambient temperature facilitating product recovery and catalyst recycling [Hope and Stuart, 1999].

In this work, for the first time a continuous reaction system that facilitates catalyst recycling has been developed and used for the continuous hydroformylation of higher olefins, i.e. 1 – octene, to linear and branched aldehydes under fluorous biphasic conditions. Besides the chemical reactor it includes a heat exchanger at the reactor outlet and a separator at its end. The phase behaviour and the mass transfer characteristics of the system are essential for the design of the reactor and the separator. The nature of the fluorous and organic solvents, the nature and concentration of the substrate, products, catalyst and gaseous components, the temperature and pressure, the reaction mechanism and phase separation are studied and they provide criteria for the units' design.

Initially, separation studies of the fluorous solvent from the organic reactants and products in the absence of catalyst were undertaken that verified the separation principle of the system. Fast and efficient separation of the two phases was observed. The more polar products present in the organic phase the less was the leaching of the fluorous solvent in the organic phase.

A continuous reaction system was subsequently studied. These reaction runs in the presence of a fluorous modified rhodium catalyst proved that the developed experimental set – up can be successfully used for the continuous hydroformylation of higher alkenes under fluorous biphasic conditions, giving satisfactory conversion and selectivity to the desired product. Catalyst and ligand concentration, as well as efficient stirring, are essential for high conversions. The main drawback of the process is the significant leaching of ligand and catalyst in the organic phase, which is continuously removed from the system, leading thus to deactivation of the catalytic system in the long term.

# Chapter 2:

# Literature Survey

## 2.1 HYDROFORMYLATION

### *2.1.1 Introduction*

Hydroformylation is the reaction between olefins and a mixture of hydrogen and carbon monoxide (synthesis gas), which leads to linear (l) and branched (b) aldehydes as primary products, Figure 2.1. This reaction is the oldest and most widely used homogeneous catalytic reaction of olefins [Parsall and Ittel, 1992].

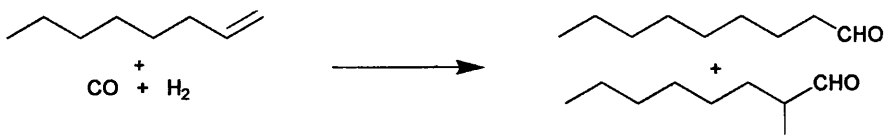


**Figure 2.1:** Hydroformylation of 1-octene to $C_9$ aldehydes.

The product linear aldehydes are used as intermediates to produce many different compounds, such as alcohols, diols, carboxylic acids, acroleins, acetals, ethers and

amines. Alcohols are by far the largest group in the range of such products and are mainly consumed as plasticizers in the polymer and detergent industry [Frohling and Kohlpaintner, 1996]. Thus, high selectivity towards linear aldehydes is desirable.

Many metal complexes have been stated to catalyse the hydroformylation reaction. A general form of these catalysts is $H_xM_y(CO)_zL_n$, where (M) is a transition metal – which enables the formation of a metal carbonyl hydride species – and (L) is a ligand. When, $n=0$ the catalyst is called "unmodified", whereas a ligand other than CO and $H_2$ is coordinated at the metal centre, the catalyst is "modified" [Frohling and Kohlpaintner, 1996]

So far cobalt, rhodium, platinum and ruthenium are the four transition metals used as hydroformylation catalysts in research but only Co and Rh are used in commercial processes. The first hydroformylation catalysts used in industries were based on Co without a modifying ligand. Harsh conditions were used and the reactivity was slow. Rh based catalysts have better selectivity to the linear products and demand milder reaction conditions, but due to catalyst separation problems they are not preferred to currently used cobalt complexes [Frohling and Kohlpaintner, 1996; van Leeuwen, 2000].

Higher selectivity towards *n* – aldehydes and better activity on hydroformylation of long chain olefins can be achieved by modifying the metal catalyst. The main classes of ligands used in industrial hydroformylation are phosphorous (III) ligands, such as phosphines $PR_3(R=C_6H_5, n-C_4H_9)$ [van Rooy *et al.*, 1996; Horvath *et al.*, 1998; Paganelli *et al.*, 2000; Wang *et al.*, 2000; van Leeuwen, 2000] and phosphites $P(OR)_3$ [ van Rooy *et al.*, 1996; Kamer *et al.* 2000].

### *2.1.2 Unmodified catalysts mechanism*

The mechanism for the hydroformylation of olefins using unmodified cobalt catalyst was proposed by Heck and Breslow [Heck and Breslow, 1961] and is shown in Figure 2.2. Though the cycle was initially proposed for cobalt complexes, it is also valid for unmodified rhodium complexes [Frohling and Kohlpaintner, 1996].

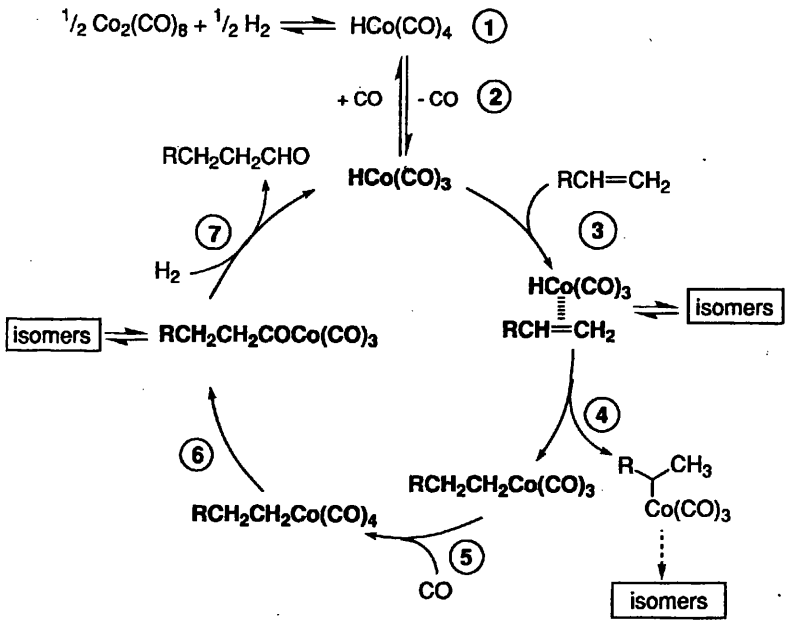


**Figure 2.2:** Catalytic cycle of hydroformylation with unmodified cobalt catalysts.

The main steps involved in the cycle are the following [Heck and Breslow, 1961]:

1. reaction of the metal carbonyl $Co_2(CO)_8$ with $H_2$ to form the hydridometal carbonyl species $HCo(CO)_4$
2. dissociation of $CO$ to generate the unsaturated 16e species $HCo(CO)_3$
3. coordination of the olefin $RCH=CH_2$ (18e)
4. formation of the alkylmetal carbonyl species (16e)
5. coordination of $CO$ (18e)

6. insertion of CO to form the alkylmetal carbonyl $RCH_2CH_2COCo(CO)_3$ (16e)

7. reaction of the acylmetal species with hydrogen to form the aldehyde and regeneration of the hybridometal carbonyl $HCo(CO)_3$.

The suggested hydroformylation mechanism, though generally accepted, is still under investigation and many different pathways have been proposed for the initial formation of the hydridometal carbonyl species $HCo(CO)_3$, as well as, the final reaction of the acylmetal species to form the aldehyde and regenerate the hydridometal carbonyl species [Frohling and Kohlpaintner, 1996 and references within].

The linear to branched ratio of the adlehydes formed by unmodified catalysts depends on the selective reaction of the hybridocobalt carbonyl with the olefin via *Markovnikof* and *anti- Markovnikof* addition. The less sterically demanding $HCo(CO)_3$ favours the formation of the branched isomer, where $HCo(CO)_4$ leads mainly to the formation of the linear isomer. This is in accordance with the increased selectivity observed at higher carbon monoxide partial pressures, when according to step 2 in Figure 2.2 more $HCo(CO)_4$ species are available. The catalytic activity drops at the same time, as $HCo(CO)_4$ is the less reactive catalyst species [Frohling and Kohlpaintner, 1996].

### *2.1.3 Modified catalysts*

The Heck – Breslow cycle can be also applied at the hydroformylation mechanism of the phosphine-modified rhodium catalysts with minor modifications [Frohling and Kohlpaintner, 1996].

The most known catalyst precursor, $RhH(PPh_3)_3CO$, was first applied to hydroformylation by Wilkinson [Evans *et al.*, 1968]. The key intermediate complex $HRh(CO)_2(TPP)_2$ can be generated by several equilibria, as shown in Figure 2.3. Starting with the key intermediate complex two possible pathways are proposed: the associative and the dissociative mechanism.

The associative mechanism – pathway 2 in Figure 2.4 – starts with the coordination of the olefin to $HRh(CO)_2(TPP)_2$, which leads to the fast and irreversible formation of the alkylrhodium complex $RRh(CO)_2(TPP)_2$. The latter is an intermediate derived through the dissociative mechanism as well. The dissociative mechanism is initiated by the dissociation of a carbon monoxide ligand from the initial complex, $HRh(CO)_2(TPP)_2$, to give $HRh(CO)(TPP)_2$. Olefin coordination, formation of the alkyl complex and coordination of a carbon monoxide ligand leads to the formation of the alkylrhodium complex $RRh(CO)_2(TPP)_2$. The next steps are the same for the two mechanisms: CO insertion to form the acyl complex $RC(O)Rh(CO)(TPP)_2$, oxidative addition of hydrogen and reductive elimination to form the aldehyde followed by the final coordination of an additional $CO$ ligand to regenerate the key complex.

The above described mechanism is very simplified. Usually, metal species containing one to four molecules of ligand will participate in the cycle depending on the concentration and the nature of the ligand and the CO partial pressure. When, alkenes higher than ethene are used, both the linear and the branched region – isomers may be coordinated to the metal complex leading to the formation of the linear or branched aldehyde respectively. Furthermore, the alkylrhodium complex

$RRh(CO)_2(TPP)_2$ may lead to the formation of internal alkenes through $\beta$ – hydride elimination.

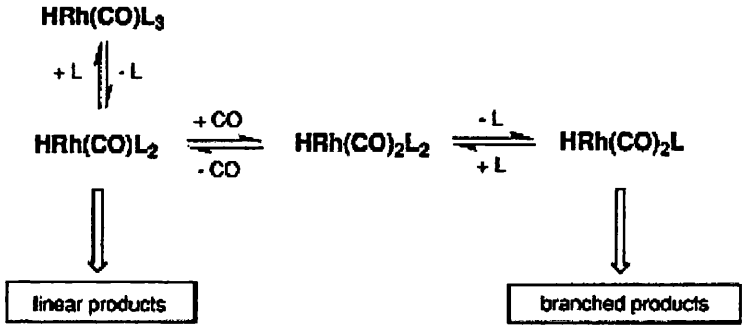


**Figure 2.3:** Initial equilibrium forming the active catalyst species, $L = TPP$.

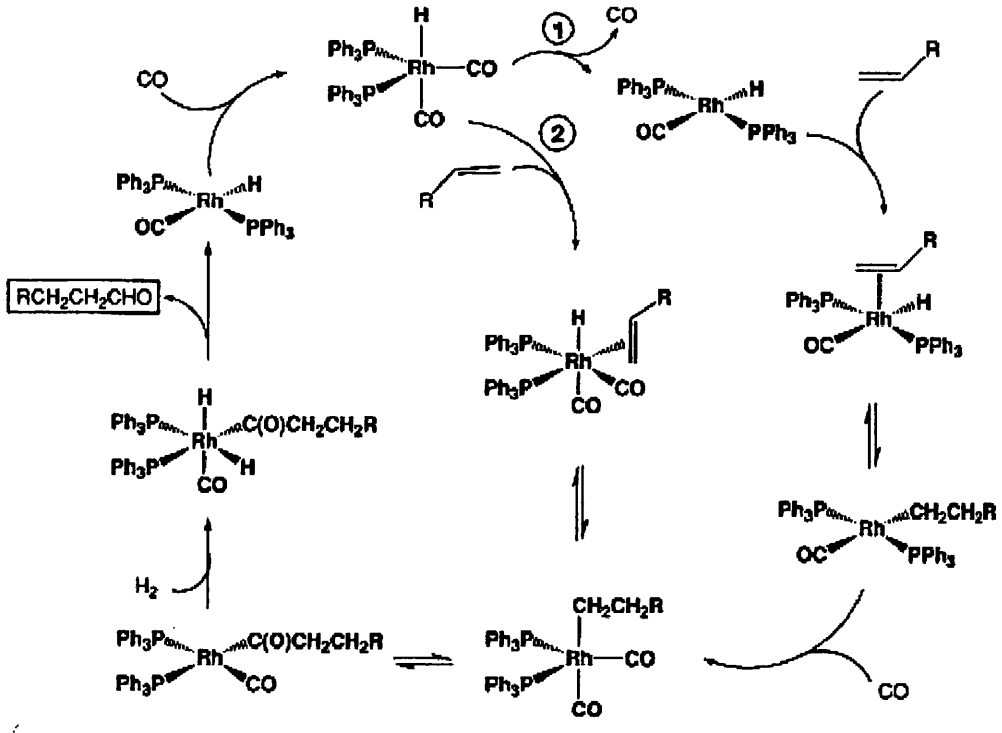


**Figure 2.4:** The hydroformylation cycle for modified rhodium catalyst: (1) dissociative and (2) associative mechanism [Frohling and Kohlpaintner, 1996].

Mechanistic and kinetic studies of rhodium catalysed hydroformylation have given contradictory results in respect of the rate determining step in the catalytic cycle [Frohling and Kohlpaintner, 1996; van Leeuwen *et al.*, 2000]. Initially, it was suggested that the oxidative addition of hydrogen was the rate determining step [Parsall and Ittel, 1992; Divekar *et al.*, 1993; Deshpande *et al.*, 1996; Bhanage *et al.*, 1997; Chaudhari *et al.*, 2001; Haumann *et al.*, 2002], while other studies suggest that the alkene coordination to the metal complex or the insertion of the alkene in the R–H bond is the rate determining step [van Rooy *et al.*, 1996; van Leeuwen *et al.*, 2000]. Bearing in mind that hydroformylation is a reaction depending a lot on the experimental conditions such as catalyst, substrate and phosphine concentration, as well as CO and $H_2$ partial pressure, the above mentioned contradiction is easily understood. Moreover, the above mentioned studies were done not only in homogeneous, but biphasic systems as well, where mass transfer limitations may be very important for the drawn conclusions.

The regioselectivity (linear to branched aldehydes ratio) of the modified catalysts is enhanced at higher ligand concentrations and low pressures of carbon monoxide. At these conditions, the equilibrium in Figure 2.3 is shifted towards the formation of the $HRh(CO)L_3$ complex, where the metal centre is coordinated by more than one phosphine ligand. This is a more sterically hindered environment leading to the formation of linear isomers [Frohling and Kohlpaintner, 1996; van Leeuwen *et al.*, 2000].

### *2.1.4 Kinetics of hydroformylation using modified rhodium catalyst*

Parameters like temperature, partial pressures of CO and $H_2$, as well as catalyst, ligand and substrate concentration, determine the kinetics of hydroformylation. The general reaction rate is given by Equation 2.1:

$$r = k * [substrate]^{\alpha} * [catalyst]^{\beta} * [p(H_2)]^{\gamma} * [p(CO)]^{\delta} * [ligand]^{\varepsilon} \qquad \text{(Eq.2.1)}$$

In most cases, the reaction rate is positively influenced by increases in the concentration of catalyst, olefin and hydrogen, while carbon monoxide has a negative effect. The actual numeric values for the exhibitors depend on the reacting system, catalyst, olefin, organic or aqueous solvent and ligand [Divekar *et al.*, 1993; Purwanto and Delmas, 1995; van Rooy *et al.*, 1995; Frohling and Kohlpaintner, 1996; van Rooy *et al.*,1996; Deshpande *et al.*, 1996; Bhanage *et al.*, 1997; Palo and Erkey, 1999; Lekhal *et al.*, 1999; Paganelli *et al.*, 2000; Wang *et al.*, 2000; Haumann *et al.*, 2002; Zhang *et al.*, 2002; Yang *et al.*, 2002, a; Yang *et al.*, 2002, b]. More details about their effect are given below.

*Temperature:* Higher temperatures increase the initial reaction rate, like in most homogeneous catalytic reactions [van Rooy *et al.*, 1995; Frohling and Kohlpaintner, 1996; Wang *et al.*, 2000; Yang *et al.*, 2002, b]. On the other hand, higher temperatures lead to lower to linear to branched aldehydes ratios for most olefins. This is probably because less coordinated metal species are involved in the catalytic cycle and these less sterically hindered metal centres lead to an increased formation of the branched isomers. Moreover, the formation of by-products, such as isomerised olefins, parafins, alcohols and water, generally increases with temperature [van Rooy *et al.*, 1995; Frohling and Kohlpaintner, 1996].

*CO partial pressure:* in general hydroformylation rates are inversely proportional to the partial pressure of CO for higher pressures, while for modified processes the

hydrogenation activity at low $p(CO)$ sets a lower limit for $p(CO)$. These effects are the same for both homogeneous and biphasic systems [Divekar *et al.*, 1993; Purwanto and Delmas, 1995; Frohling and Kohlpaintner, 1996; Deshpande *et al.*, 1996; Bhanage *et al.*, 1997; Haumann *et al.*, 2002]. Inhibition of the reaction rate due to increasing $p(CO)$ is owned to the side reactions that lead to the formation of the inactive species $(RCO)Rh(CO)_2L_2$ and $(RCO)Rh(CO)_3L$, competitive reactions to the reductive addition of hydrogen, Figure 2.4. As a consequence, the effective concentration of the active catalytic species is reduced thus reducing the reaction rate.

*$H_2$ partial pressure:* hydroformylation reaction rate and activity is increased with higher pressures of hydrogen. Generally, a first order dependency of the reaction rate from $p(H_2)$ is observed, enhancing further the belief that the oxidative addition of $H_2$ to the acyl Rh carbonyl species is the rate controlling step [Divekar *et al.*, 1993; Purwanto and Delmas, 1995; Deshpande *et al.*, 1996; Bhanage *et al.*, 1997; Haumann *et al.*, 2002].

In most cases, the ratio of the partial pressure of the two gases is 1:1 and the overall pressure is determined by the combination of the effect of the partial pressures [Divekar *et al.*, 1993; Frohling and Kohlpaintner, 1996; Wang *et al.*, 2000]. Unmodified cobalt based industrial processes run under high pressures, 250-300 bar, while modified rhodium based processes use low pressures, 15-18 bar [Frohling and Kohlpaintner, 1996].

*Catalyst and ligand concentration:* the olefin conversion and the aldehyde yield are affected by the catalyst concentration. High catalyst concentration leads to high reaction rates and high conversions. This behaviour is expected since an increase in the catalyst concentration will increase the active catalyst species. Usually a linear dependency of the reaction rate from the catalyst concentration is observed [Divekar

*et al.*, 1993; Purwanto and Delmas, 1995; van Rooy *et al.*, 1995; Deshpande *et al.*, 1996; Bhanage *et al.*, 1997; Palo and Erkey, 1999; van Leeuwen *et al.*, 2000; Haumann *et al.*, 2002]. No general rule for the catalyst concentration effect on the reaction selectivity has been found yet, as the latter also depends on the modifying ligand concentration [Frohling and Kohlpaintner, 1996].

For modified catalysts, increase in the ligand concentration is in favour of the reaction rate leading to a maximum. High excesses of ligand do not influence the reaction rate. The ligand/metal ratio influences selectivity to *n* – aldehydes. In general, an increase in the ligand/metal ratio at the modified methods increases the *n/i* ratio. Coordination of the ligands to the metal centre enhances steric bulkiness and linear products are favoured. This effect is more or less pronounced, depending on the ligand structure. Hydrogenation and isomerisation reactions are hindered by an excess of ligand [Divekar *et al.*, 1993; Frohling and Kohlpaintner, 1996; van Rooy *et al.* 1996; Palo and Erkey, 1999].

*Substrate concentration:* in homogeneous catalytic systems, used for the hydroformylation of linear alkenes, the reaction rate varies linearly at lower olefin concentrations. According to the catalytic cycle, an increase in substrate concentration will increase the coordination of olefin to the active metal species, to form the alkyl metal complex, hence will increase the reaction rate. At higher concentrations the effect is marginal [Divekar *et al.*, 1993; Purwanto and Delmas, 1995; van Rooy *et al.*, 1995; van Rooy *et al.*, 1996; Deshpande *et al.*, 1996; Bhanage *et al.*, 1997; Palo and Erkey, 1999]. For phosphine modified catalyst the rate of hydroformylation decreases with the increase of substitution of the olefin due to steric effects. Two methyl groups in the $4^{th}$ carbon atom have a greater impact than on in the $3^{rd}$. It was observed that a higher degree of substitution closer to the double bond gave progressively more linear

products, but at lower rates [van Rooy *et al.*, 1996]. Higher reaction rates of substituted alkenes can be achieved by using bulky phosphite ligands [van Rooy *et al.*, 1996; van Leeuwen *et al.*, 2000]. Due to steric bulkiness phosphites form metal complexes with just one ligand, complexes from which it is easy to lose a CO ligand, making the coordination of a substitute alkene easier, hence increasing the reaction rate [van Rooy *et al.*, 1996; Kamer *et al.*, 2000].

As hydroformylation reaction comprises at least two gases, carbon monoxide and hydrogen - in the cases of $C_2 - C_4$ even the third reactant is in the gaseous phase – and the catalyst is always dissolved in a liquid, there are expected to be limitations at the reaction rate involving the dissolution of the gases to the liquid phase. When water is used as the catalyst solvent the two phase system turns to three phase system. In order to have the required mass transfer from the gas phase through the phase boundary to the liquid phase intimate contact between the phases is necessary. However, the mass transfer of the gases to the liquid phase is not the limiting step for the space – time – yield of the process as process improvements have been implemented. Sparging of the synthesis gas at the liquid and additional mechanical agitation are sufficient for the quick dissolution of the gases at the low pressure processes [Frohling and Kohlpaintner, 1996]. Studies of the stirrer speed effect on the reaction rate show that the latter is increased with increased speeds reaching a maximum. Increasing the stirrer speed enhances the sparging of the gases, their transfer to the liquid phase and thus their effective dissolution rate in the reaction mixture until the mixture becomes saturated. After the equilibrium value is achieved, further increase of the speed does not influence the rate value. For homogeneous and biphasic systems this equilibrium is achieved at 400 rpm and 1500 rpm respectively [Bhanage *et al.*, 1997; Lekhal *et al.*, 1999].

### *2.1.5 Modifying ligands*

Most of the papers published today in the area of hydroformylation are dealing with the development of new phosphine structures and their obtained catalytic results [Buhling *et al.*, 1995; Bhattacharyya *et al.*, 1997; Hanson *et al.*, 1998; Osuna *et al.*, 2000; Bonafoux *et al.*, 2001; Bischoff and Kant, 2001; Suomalainen *et al.*, 2002; Pinault and Bruce, 2003]. It is generally accepted that electron donating ligands, like alkylphosphines lead to slower catalysis [Mac Dougal *et al.*, 1996], while arylphosphines, containing electron-withrdrawing substituents give higher reaction rates [Buhling *et al.*, 1995]. Moreover, phosphites usually show high activities especially in the hydroformylation of long – chain aldehydes [van Rooy *et al.*, 1996]. The electronic effects of these ligands can explain their effect on the reaction rate. Electron withdrawing ligands decrease the back – donation to carbon monoxide, thus carbonyls are bonded weaker to the metal centre, favouring the formation of active metal species, Figure 2.4. Additionally, alkene complexion is also favoured [van Leeuwen *et al.*, 2000].

One of the drawbacks of the modified catalysts is that whereas unmodified cobalt carbonyl catalysts tolerate a certain level of impurities, ligand modified rhodium catalysts are prone to oxidation, which is also catalysed by the transition metal. Therefore, oxygen, hydrogen peroxides, hydrogen sulphides and halogen compounds have to be carefully removed from synthesis gas and olefin to ensure the long term stability of Rh – TPP complexes [van Leeuwen, 2000]. Alkynes and dienes may also affect ligand – modified catalysts by formation of complexes, thus diminishing their activity, so only traces of these compounds should be present in the olefin feed [Frohling and Kohlpaintner, 1996]. Freeze pump thawing of the used solvents and treatment of the alkene over natural alumina to remove oxygen and peroxides and

over sodium potassium to remove alkynes and dienes are the common practices used to have a more stable system. The addition of excess of ligand in the reacting system is another common practice to avoid oxidation [van Leeuwen, 2000].

The combination of the available modifying ligands with the different separation techniques in catalysis – homogeneous, aqueous biphasic, fluorous biphasic, $scCO_2$, ionic liquids, supported catalysts – provides a big variety of systems for the hydroformylation of linear and branched alkenes. Of our particular interest are the results obtained when fluorous ponytails, i.e. $C_nF_{2n+1}$, are added at the phosphine ligands in order to get the catalyst dissolved in a fluorous solvent (Fluorous Biphasic Systems) [Horvath *et al.*, 1998; Foster *et al.*, 2002, b]. Ligands such as $P(4-C_6H_4C_6F_{13})_3$ and $P(O-4C_6H_4C_6F_{13})_3$ have been studied, giving high conversions and linear to branched ratios [Foster *et al.*, 2002, b]. These systems will be discussed in detail in the following paragraphs.

### *2.1.6 Commercial applications*

The conditions and results of some major industrially applied hydroformylation processes are summarised in Table 2.1. Cobalt and rhodium are the only metals used as catalysts at the industrial processes. Cobalt based processes demand very high pressures and with few exceptions are used for the hydroformylation of longer chain olefins. Rhodium based processes (Low Pressure Processes) use milder reaction conditions, regarding the temperature and mainly the pressure. Besides, they give good conversion and aldehyde yields, but their commercialisation is hampered by

problems regarding the catalyst separation from the product aldehydes [Frohling and Kohlpaintner, 1996].

**Table 2.1:** Typical data for major industrial hydroformylation processes [Frohling and Kohlpaintner, 1996].

| Process | *BASF* | *Exxon* | *Shell* | *UCC* | *RCH/RP* | *BASF* |
|---|---|---|---|---|---|---|
| *Olefin* | $C_3H_6$ | $C_6 - C_{12}$ | $C_7 - C_{14}$ | $C_3H_6$ | $C_3H_6$ | $C_3H_6$ |
| *Catalyst* | Co | Co | Co | Rh | Rh | Rh |
| *Ligand* | None | None | phosphine | TPP | TPPTS | TPP |
| *Temperature, °C* | 120-150 | 160-190 | 150-190 | 90-95 | 110-130 | 110 |
| *Pressure, bar* | 270-300 | 290-300 | 40-80 | 15-18 | 40-60 | 16 |
| *$CO/H_2$ ratio* | 1:1 | 1:1.16 | ≤1:2 | 1:1.07 | 1.01:1 | 0.9:1.1 |
| *Ligand/metal* [1] | | | 1-3:1 | n/a | n/a | 100:1 |
| *Conversion, %* | 88-92 | 96 | n/a | 85-89 | 95 | 84-86 |
| *Aldehyde yield,%* | 70-75 | 72 – 75 | n/a | n/a | 99 | n/a |
| *n/i ratio* | 2.1-2.6 | n/a | 5.7-9 | n/a | 21 | 5.25 |

[1]molar ratio, n/a: not available

Fortunately, the variety of ligands allows extensive catalyst variation and optimisation. New, more stable catalytic systems with better activity and selectivity are designed to meet the feedstock and product specifications [Arnoldy, 2000]. Table 2.2 lists the known commercial applications of the Rh – catalysed hydroformylation processes for linear terminal alkenes [Arnoldy, 2000].

**Table 2.2:** Commercial applications of the Rh – catalysed hydroformylation processes for linear terminal alkenes [Arnoldy, 2000].

| *Alkene* | *Products* | *developed by* | *Ligand* | *kt/a* |
|---|---|---|---|---|
| Ethene | Propanol | Celanese, Union Carbide | TPP[a] | 400 |
| Propene | butanol, iso-butanol, 2 - ethyl -1- hexanol, neopentyl glycol | BASF, Celanese, Union Carbide, Mitsubishi | TPP | 4000 |
| Propene | butanol, iso-butanol, 2 - ethyl -1- hexanol, neopentyl glycol | Ruhrchemie-RhonePoulenc | TPPS[b] | 600 |
| 1-hexene/ 1-octene | carboxylic acids | Celanese | TPP | 18 |
| 1-butene | 2-propyl-1-heptanol | Hoechst | TPPTS | 40 |
| 1-butene/ 2-butenes | 2-propyl-1-heptanol | Union Carbide | Diphosphite | 80 |
| higher 1-Alkenes | detergent alcohols | Kvaerner | DPBS[c] | 120 |

[a] TPP = triphenylphosphine [b] TPPS = tris(m-sulfonyl)triphenylphosphine, [c] DPBS = ω-diphenylbutane-α-sulfonates

## 2.2 CATALYTIC SYSTEMS IN HYDROFORMYLATION

### *2.2.1 Homogeneous vs. heterogeneous catalysis*

*Homogeneous* catalytic systems are the systems where at least one of the compounds present is miscible with the catalyst. Consequently in a continuous reactor the catalyst is removed together with the reaction mixture. *Heterogeneous* systems use a solid catalyst that is in contact with the fluid reactants. The catalytic effect takes place on the catalytic surface, external and/or internal [Frohling and Kohlpaintner, 1996].

Heterogeneous systems are successfully used in many industrial processes, i.e. mineral oil processes. The main advantages of catalyst – product separation, as well as, long catalyst life can explain the wide use of these systems. On the other hand, problems related to slow diffusion and vigorous reaction conditions limit their applications.

**Table 2.3:** Homogeneous versus heterogeneous catalysis [Frohling and Kohlpaintner, 1996].

| | *Homogeneous catalysis* | *Heterogeneous catalysis* |
|---|---|---|
| Activity (relative to active component content) | High | Variable |
| Selectivity | High | Variable |
| Reaction conditions | Mild | Harsh |
| Service life catalyst | Variable | Long |
| Sensitivity towards catalyst poison | Low | High |
| Diffusion problems | May influence biphasic systems | May be important |
| Catalyst recycling | Expensive | Not necessary |
| Variation of steric and electronic properties of catalysts | Possible | Very difficult |

The main advantage of homogeneous systems is the considerably higher activity and selectivity achieved at lower temperatures. Thus, more temperature sensitive catalysts can be used and the system demands less energy consumption. One of the major obstacles for practical applications of homogeneous systems is the separation of the products and the catalyst recycling [Horvath and Rabai, 1994; Frohling and Kohlpaintner, 1996]. Table 2.3 summarises the main characteristics of homogeneous and heterogeneous catalytic systems.

To date, many strategies and techniques for product separation from the catalyst in homogeneous systems have been developed, leading to an extensive use of organometallic complexes in homogeneous catalysis.

### *2.2.2 Heterogenisation of hydroformylation catalysts*

Many new processes under investigation attempt the immobilisation of homogeneous catalysts in order to facilitate easy product separation. In these processes the catalyst is anchored to some kind of soluble or insoluble support and the separation is carried out by a filtration technique [Tzschucke *et al.*, 2002; Cole-Hamilton, 2003]. Dendrimer supported catalysts are an example of such a technique [Reek *et al.*, 2000; Oosterom *et al.*, 2001; Niu and Crooks, 2003]. These systems have a precise distribution of catalytic sites. They are efficient and tunable by ligand design and can be easily separated by nanofiltration. The problems of metal leaching and catalyst decomposition, as well as the cost of the dendrimers, need to be addressed before they become an attractive commercial alternative [Reek *et al.*, 2000; Oosterom *et al.*, 2001; Niu and Crooks, 2003]. Another interesting approach is the polymer supported catalysts. The most widely studied polymers for catalyst – immobilisation are organic polymers such as cross - linked polystyrenes [Reek *et al.*, 2000]. The asymmetric hydroformylation of styrene using polystyrene supported rhodium catalyst clearly showed the drawback of these types of polymers, with high catalyst leaching and poor mechanical properties [Nozaki *et al.*, 1998]. Inorganic supports, such as silica, alumina, glasses, clays and zeolites, do not suffer from these drawbacks [Reek *et al.*, 2000]. A great example of the immobilisation of an active and selective hydroformylation catalyst into a silicate matrix monoliths that were constructed as the

blades of a mechanical stirrer has been reported recently [Sandee *et al.*, 2001]. Moreover, "smart polymers" that show temperature depended solubility properties have successfully been developed [Bergbreiter, 1996]. Nonetheless, smart polymers have not been tested so far for the hydroformylation reaction.

A second type of processes under investigation is the biphasic systems. In these systems the catalyst is designed to be soluble in a solvent that, under some conditions, is immiscible with the reaction product, thus enabling easy catalyst – product separation [Cole-Hamilton, 2003]. The aqueous biphasic system is very effective in catalyst separation and recycling and is industrially used for the hydroformylation of lighter olefins [Kohlpaintner *et al.*, 2001]. Fluorous biphasic systems [Horvath and Rabai, 1994], supercritical fluids [Palo and Erkey, 1999], ionic liquids [Dupont *et al.*, 2002] and supercritical fluid – ionic liquids biphasic systems [Sellin *et al.*, 2001] have been extensively used for the hydroformylation reaction.

### *2.2.3 Liquid – liquid biphasic systems*

A liquid – liquid biphasic catalytic process is a process in which a catalyst is designed to reside in one of the liquid phases while reactants and products form the other liquid phase. These systems are frequently used in synthetic, catalytic and separation processes [Horvath and Rabai, 1994; Horvath, 1998; Tzschucke *et al.*, 2002; Cole-Hamilton, 2003]. The formation of the two phases is caused by the different intermolecular forces between molecules of the one liquid phase in comparison to forces between molecules of the other liquid phase. So, the selection of a reagent or catalyst phase depends on the properties of the product solution at high conversion values. For example, if the product is apolar, the reagent or catalyst phase

should be polar and vice versa. The success of a biphasic system depends on whether the reagent or catalyst could be designed to remain preferentially in its phase. The easiest way to achieve the desired solubility is by designing the catalyst to be catalyst phase like; for example, by attaching appropriate solubilising ligands to the catalyst [Horvath and Rabai, 1994; Frohling and Kohlpaintner, 1996; Horvath, 1998; Horvath *et al.*, 1998]. Biphasic catalysis offers the chance for homogeneous catalysis, with the advantages of mild reaction conditions, high activity and selectivity coupled with easy catalyst and reaction products separation just by decantation, overcoming this way the main drawback of homogeneous catalysis [Frohling and Kohlpaintner, 1996].

The principle of the biphasic homogeneous catalytic reactions is shown in Figure 2.5. The ligand, $L$, attached to the catalyst ensures that the latter remains dissolved at the catalyst containing phase. Depending on the solubility of the reagents at the catalyst phase, the reaction can take place either at the interface of the two phases or at the bulk of the catalyst phase. The products formed during the reaction have very low or no miscibility with the catalyst phase, thus leading to their easy separation from the catalytic system and the recycling of the catalyst.

The most common homogeneous biphasic systems are aqueous systems, where the active catalyst is and remains dissolved in water. The reactants and reaction products, which are organic and relatively non – polar, can be separated off after the reaction is complete by simply separating the second phase from the catalyst solution, so the latter can be recycled [Kohlpaintner *et al.*, 2001].

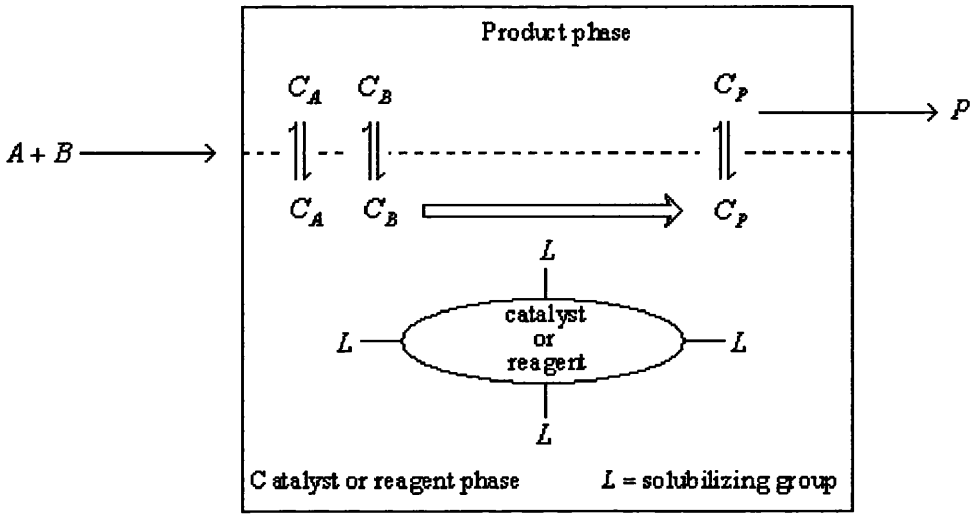


**Figure 2.5:** Biphasic homogeneous reaction concept [Horvath, 1998].

The aqueous system is the only liquid – liquid biphasic system used successfully at the industrial hydroformylation of lower olefins – propene and butene [Frohling and Kohlpaintner, 1996; Cornils, 1998; Hanson and Zoeller, 1998; Kohlpaintner *et al.*, 2001]. The ligand used for the modification of the rhodium catalyst is TPPTS, tri(*m*-sulfonyl)triphenylphopshine. The catalyst formed after preactivation, [HRh(CO)- $\{(m\text{-}SO_3NaC_6H_4)_3P\}_3$ has nine sulfonate substitutes and is accordingly readily soluble in water [Cornils, 1998]. This simple in term of apparatus oxo – process has high selectivity, producing up to 98% linear aldehydes and it utilises the heat of reaction producing a net steam supplier system by means of the "heat transfer medium" *n* – butyraldehyde [Cornils, 1998; Kohlpaintner *et al.*, 2001]. The products are easily separated by simple decantation and the catalyst is recycled to the reactor by immobilisation using water as the "mobile support" [Cornils, 1998; Kohlpaintner *et al.*, 2001]. The great economics of this process, due to minimum catalyst loss, as well as the process's potential from a safety and an environmental point of view make its application even more attractive.

Despite the advantages of the aqueous biphasic catalytic systems, they are not without disadvantages. Some reactants or catalysts hydrolyse when exposed to water, resulting in the production of unwanted byproducts and decreased performance. Moreover, because of the two phase nature of the system, the reaction occurs at the interface of the two phases and the reactants have to cross the phase boundary, which may lead to mass transfer limitations, resulting in lower reaction rates compared to single phase homogeneous systems [Wachsen *et al.*, 1998]. This effect is enhanced by the normally low miscibility of organic compounds in water [de Wolf *et al.*, 1998; Horvath, 1998]. The low solubility of higher olefins in water limits the application of the oxo – process to the hydroformylation of olefins higher than pentene [Horvath *et al.*, 1990; Horvath, 1998]. Several attempts have been made to overcome the problem of low miscibility including: the design of various ligands [Buhling *et al.*, 1995; Hanson *et al.*, 1998] , the use of co – solvents such as methanol [Monteil *et al.*, 1994; Purwanto and Delmas, 1995], the design of thermoregulated phase transfer ligands [Wang *et al.*, 2000; Webb *et al.*, 2003], the use of microemulsions [Tic *et al.*, 2001; Haumann *et al.*, 2002], the use of cyclodextrines [Kalck *et al.*, 1998; Reek *et al.*, 2000], the use of ionic liquids (molten salts) [Dupont *et al.*, 2001; Tzschucke *et al.*, 2002; Cole-Hamilton, 2003], as well as supported aqueous phase catalysts [Kalck *et al.*, 1998; Hanson and Zoeller, 1998; Reek *et al.*, 2000].

Supercritical $CO_2$, ($scCO_2$), on its own or in combination with ionic liquids has also been used to overcome some of the limitations of aqueous biphasic systems [Palo and Erkey, 1999; Sellin *et al.*, 2001; Webb *et al.*, 2003]. The absence of a gas – liquid phase boundary and the ability of $scCO_2$ to dissolve large quantities of gases combined with the facile product and catalyst separation simply by reducing the pressure makes $scCO_2$ a useful tool for homogeneous catalysis. A continuous

hydroformylation process for higher olefins using $scCO_2$ and ionic liquids has successfully been developed [Webb *et al.*, 2003].

One of the most interesting non – aqueous biphasic systems developed are the fluorous biphasic systems, where the catalyst is dissolved in a solvent rich in $C-F$ bonds [Horvath and Rabai, 1994; de Wolf *et al.*, 1998]. These systems, which are the main topic of this thesis, are discussed in detail in the following paragraphs.

### *2.2.4 Fluorous Biphasic Systems, FBS*

The FBS concept is based on the limited miscibility of partially or fully fluorinated compounds with non fluorinated compounds [Zhu, 1993]. A *fluorous biphasic system* consists of a fluorous phase containing preferentially fluorous soluble catalyst and a second organic phase containing reactants and products with limited solubility in the fluorous phase [Horvath and Rabai, 1994; Horvath, 1998]. The term fluorous was first introduced by Horvath and Rabai [Horvath and Rabai, 1994] as the analogue to the term aqueous to emphasise the fact that the reaction is mainly controlled by a reagent or a catalyst designed to dissolve preferentially in the fluorous phase and the term has been extensively used since then.

A *fluorous medium* could be any perfluoroalkane, perfluorodialkylether, perfluorotrialkylamine, or similar non – polar species that share key physical properties with these species. This definition was recently given by Gladysz and Curran [Gladysz and Curran, 2002]. *Fluorous phase* is defined as the rich in fluorocarbons phase [Horvath and Rabai, 1994]. The most effective fluorous solvents are perfluorinated alkenes that may contain functional groups, provided there are minimal attractive interactions between those groups. As perfluoroaryl groups offer

dipole-dipole interactions, they are less compatible with the FBS concept than perfluoroalkyl groups [Horvath and Rabai, 1994].

The success of the FBS is due to the unique properties of perfluorinated hydrocarbons. They are inert, apolar and thermally stable, allowing vigorous reaction conditions [de Wolf *et al.*, 1998]. Moreover, they lack hydrogen – bonding capabilities, which makes them relatively insoluble in their hydrocarbon analogues and they dissolve various gases such as oxygen, hydrogen and carbon dioxide [Zhu, 1993; Fish, 1999]. The fact that fluorocarbon solvents are non toxic and even biocompatible [Fish, 1999] – fluorocarbons have successfully been used as oxygen transport media or "blood substitutes", as well as for diagnosis and drug delivery [Horvath, 1998] – is another advantage of their use as solvents. Nevertheless, it was the realisation of the low miscibility of perfluoroalkanes, perfluorordialky ethers and perfluorotrialkyl amines with even the common organic solvents like toluene and acetone that led to the development of the fluorous biphasic chemistry [Horvath, 1998].

Numerous perfluorinated solvents are commercially available with a wide selection of boiling points and densities that are always greater than those of common organic solvents. As demand increases, the prices of these solvents are being reduced accordingly [Barthel Rosa and Gladysz, 1999; Dobbs and Kimberley, 2002]. The use of PerFluoroMethylCyclohexane (PFMC), though a more expensive solvent has been used in the majority of the published exploratory work. As many cheaper perfluorinated alkenes are sold as mixtures of isomers or by boiling point range, their use could be compromised on the reproducibility and the interpretation of the measurements [Barthel Rosa and Gladysz, 1999].

The use of perfluorocarbons, however, may also have some disadvantages. The $C_1$ – $C_2$ fluorocarbons (freons) are green house gases and cause ozone depletion and their inertness is a major environmental problem [de Wolf *et al.*, 1998]. Their boiling points, however, are much lower than those of the higher perfluoroalkanes. Consequently, higher perfluoroalkanes have lower vapour pressures and might cause less environmental problem. Moreover, because of their exceptional stability, they have an extremely long life in the atmosphere (>2600 years) [de Wolf *et al.*, 1998; Cavazzini *et al.*, 1999]. Bearing all these in mind, the PFC users must make every effort possible to ensure that any PFC release into the environment is minimised and that its dispersion is contained.

Fluorous biphasic systems are well suited for converting apolar reactants to products of higher polarity, as the partition coefficient of reactants and products is high and low respectively in the fluorous phase. The net result is no or little solubility limitation on the reactants and easy separation of the products. Furthermore, as the conversion level increases, the amount of polar products increases as well, enhancing further separation [Horvath, 1998]. One of the most important advantages of the fluorous biphasic catalyst concept is that with the appropriate choice of organic and fluorous phases, either by heating or by increasing the pressure the two-phase system becomes a single-phase one, as shown in Figure 2.6. Thus, catalysis occurs under genuine homogeneous conditions, with all the advantages of high conversion and selectivity. After the completion of the reaction and when the system is cooled and/or depressurised the two phases are quickly re – established, for facile catalyst – product separation [Hope and Stuart, 1999]. Fluorous-organic solvent miscibility data can be found in literature [Sorensen, 1979].

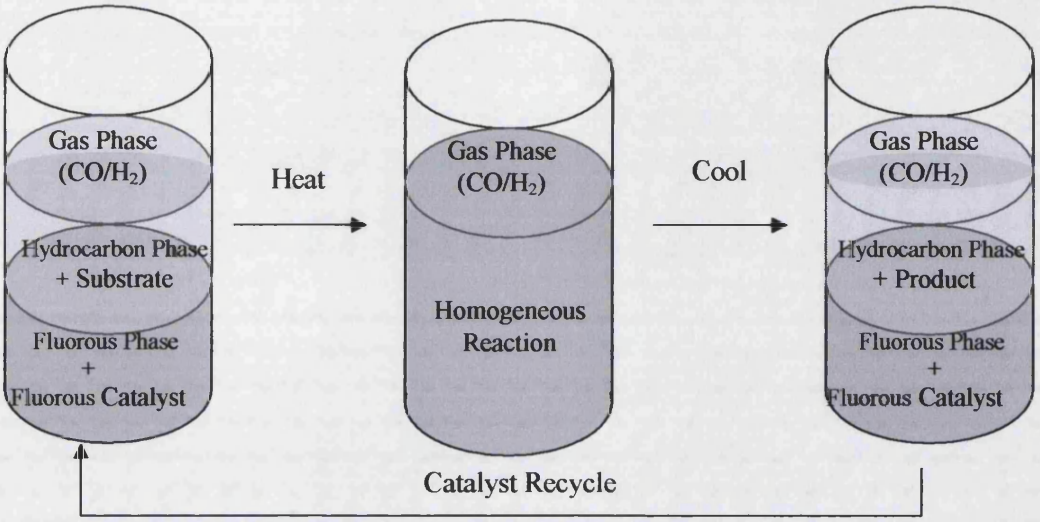


**Figure 2.6:** Catalysis within a Fluorous Biphasic System (FBS).

It should be emphasised that many well – established hydrocarbon soluble reagents and catalysts can be converted to fluorous soluble by the addition of fluorous ligands [Horvath, 1998]. These are molecules that are specifically designed in order to mimic the reactivity of conventional organic molecules, yet be readily soluble in fluorous solvents by virtue of their high fluorine content [Dobbs and Kimberley, 2002].

The fluorous biphasic concept has been successfully used in the liquid – liquid extraction technique, for the isolation and purification of air and water sensitive organometallic compounds [Horvath, 1998; Spetseris *et al.*, 1998; Tzschucke *et al.*, 2002], the multistep organic synthesis [Horvath, 1998; Curran, 2000], as well as the phase separable homogeneous catalysis [Horvath, 1998; Cole-Hamilton, 2003].

### *2.2.5 Fluorous Biphasic Catalysis, FBC*

Most molecular catalysts could be made fluorous soluble by attaching fluorous ponytails to the catalyst core in appropriate size and number. However, this modification has only been applied to transition metal complexes. In general, a fluorous compatible organometallic catalyst, $M_x\{L[(R)_n(Rf)_m]_y\}_z$ contains at least one metal centre to which at least one fluorous ligand, $L[(R)_n(Rf)_m]_y$ is bonded, which includes the hydrocarbon domain, $(R)_n$, and the fluorous domain, $(Rf)$. The fluorous domain controls the fluorous solubility of the molecule, while the organic domain, which resembles the conventional organic molecule, directs the reactivity of the compound. The fluorous partition coefficients ($P_{FBS} = c_{fluorousphase} / c_{otherphase}$) of such complexes depend on the type and size of both the fluorous and the hydrocarbon domain [Horvath, 1998; Dobbs and Kimberley, 2002]. The most effective fluorocarbon moieties, also known as fluorous ponytails, are linear and branched perfluoroalkyl chains with high carbon number, like perfluorohexyl ($C_6F_{13}$) and perfluorooctyl ($C_8F_{17}$) groups [Horvath and Rabai, 1994; de Wolf *et al.*, 1998]. The fluorous partition coefficients can be increased by increasing the number of perfluoroalkyl groups attached to the ligand.

However, the strong electron – withdrawing properties of perfluoroalkyl moieties can have a dramatic effect on the catalytic activity when compared to non – substituted systems. Although it is difficult to predict the exact effect of these groups, it is easily understood that a decrease of electron density on the metal centre is expected to have a significant effect on bonding of catalytically important substrates, such as CO, $H_2$ and olefins [de Wolf *et al.*, 1998]. Thus, the insertion of two or three methylene, $(-CH_2-)$, groups before the fluorous ponytails is necessary to decrease

this strong electronic influence [Horvath and Rabai, 1994; Hope and Stuart, 1999]. Studies have shown that even very long hydrocarbon inserts do not completely insulate the metal atoms from the electronic influence of the fluorinated units, but beyond a $C_3H_6$ group the variation with additional $-CH_2-$ units is minimal [Horvath *et al.*, 1998]. It should be noted that for the ligands with longer spacer groups it is necessary to incorporate longer perfluoroalkyl substituents in order to confer preferential perfluorocarbon solubility, as the total fluorine content of a fluorous compatible complex should be above 60% [Horvath *et al.*, 1998; Hope and Stuart, 1999; Fish, 1999].

Ever since the introduction of the fluorous biphasic concept a lot of attention has been given to the synthesis of the fluorous ponytails and their effect on the catalyst activity. Fluorous soluble complexes like phosphines [Horvath *et al.* 1998; Bhattacharyya *et al.*, 1997; Bhattacharyya *et al.*, 2000; Richter *et al.*, 2000], phosphates [Bhattacharyya *et al.*, 1997; Bhattacharyya *et al.*, 2000; Richter *et al.*, 2000], biphanols [Adams *et al.*, 2003], porphyrins [Horvath *et al.*, 1998], pthalocyanines [Horvath *et al.*, 1998], diketonates [Klement *et al.*, 1997], tris(pyrazolyl)borates [Horvath *et al.*, 1998], bipyridines [Horvath *et al.*, 1998], cyclopentadienes [Hope and Stuart, 1999] and 1,4,7 – triazacyclononane [Horvath *et al.*, 1998] have been prepared and used for the modification of the catalysts. The fluorous analogues of several transition metal complexes have also been synthesized including $HRh(CO)\{P[CH_2CH_2(CF_2)_5CF_3]_3\}_3$ [Horvath *et al.*, 1998], the fluorous Wilkinson catalyst, $ClRh\{P[CH_2CH_2(CF_2)_5CF_3]_3\}_3$ [Juliette *et al.*, 1997], the fluorous Vaska complex, $ClIr(CO)\{P[CH_2CH_2(CF_2)_5CF_3]_3\}_2$ [Guillevic *et al.*, 1997] and $HRh(CO)\{P[-4-C_6H_4(CF_2)_5CF_3]_3\}_3$ and $HRh(CO)\{P[O-4-C_6H_4(CF_2)_5CF_3]_3\}_3$ [Foster *et al.*, 2002, a; Foster *et al.*, 2002, b]. Fluorous biphasic catalysis has been

used in a variety of catalytic reactions including hydroformylation [Horvath *et al.*, 1998; Foster *et al.*, 2002, b; Mathivet *et al.*, 2002, a], hydrogenation [Richter *et al.*, 1999; Hope *et al.*, 1999], alkene oligomerisation [Benvenuti *et al.*, 2002], transesterification [Xiang *et al.*, 2002], hydroboration [Juliette *et al.*, 1997], hybride reaction, alkene epoxidation and alkane and alkene functionalisation [Fish, 1999]. Of our particular interest is the hydroformylation of higher olefins, which was the first reaction to be demonstrated in fluorous biphasic systems [Horvath *et al.*, 1998].

### *2.2.6 Hydroformylation of olefins in Fluorous Biphasic System*

Hydroformylation of higher olefins using FBC was reported for the first time by Horvath and Rabai, who carried out hydroformylation of 1 – decene using a fluorous modified Rh catalyst [Horvath and Rabai, 1994]. In a later publication [Horvath *et al.*, 1998], the above mentioned system was described in more detail, reporting experimental results and comparing them with non – fluorous systems. Hydroformylation of ethylene was also tested in the same system, thus, proving that FBS can be used for the hydroformylation of both lower and higher alkenes [Horvath *et al.*, 1998].

In the above mentioned study, the hydroformylation of 1 – decene was carried out under fluorous biphasic conditions, using perfluoromethylcyclohexane as the fluorous solvent and toluene as the organic solvent. The rhodium catalyst was modified using $P[CH_2CH_2(CF_2)_5CF_3]_3$ fluorous phosphine ligand. The reaction was carried out in a batch autoclave at 100 °C and 10 bar of $CO/H_2$ (1:1), in a 50/50 vol% of toluene / perfluoromethylcyclohexane. The concentration of Rh ranged from 0.02 to 2.2 mmol/l and an excess of ligand was used (P/Rh > 3). Under these reaction conditions the

solvent mixture formed a single homogeneous phase. After the end of the reaction the reaction mixture was cooled and the formed phases were allowed to separate [Horvath *et al.*, 1998].

The selection of the $P[CH_2CH_2(CF_2)_5CF_3]_3$ phosphine ligand was done after the electronic properties of several trialkylphosphines were calculated. The insertion of two methylene (- $CH_2$ -) groups was enough to lower the electron withdrawing effect of the fluorous ponytails, while the three perfluorohexyl groups provided a fluorous domain of about 75% of the total volume of the phosphine and high fluorous solubility [Horvath *et al.*, 1998]. Moreover, the solution structure of $HRh(CO)\{P[CH_2CH_2(CF_2)_5CF_3]_3\}_3$, which is in equilibrium with $HRh(CO)_2\{P[CH_2CH_2(CF_2)_5CF_3]_3\}_2$, is similar to that of $HRh(CO)(PPh_3)_3$ and $HRh(CO)\{Pm-C_6H_4SO_3Na)_3\}_3$, the latter being used in the aqueous biphase hydroformylation of olefins [Horvath *et al.*, 1998].

The experimental results showed that while hydroformylation of 1 – decene was inhibited by increased concentrations of $P[CH_2CH_2(CF_2)_5CF_3]_3$, the l:b ratio of the aldehyde increased. The TurnOver Frequency[a] (TOF) of 1 – decene and the l:b ratio of the product aldehydes changed from 0.60 l/mol/s and 3.21 to 0.04 l/mol/s and 7.84 respectively, for phosphine concentrations increasing from 22.1 mmol/l to 304 mmol/l [Horvath *et al.*, 1998]. This was easily explained based on the reaction mechanism, as shown in Figure 2.3. The distribution of Rh intermediates with different CO/phosphine ligand ratios depends on the relative concentrations of CO and phosphine. At constant partial pressure of CO the ligand concentration becomes the determining factor. Thus, kinetic and selectivity data should be expressed as a

[a] TOF is defined as the rate of olefin conversion by 1 mole of rhodium and is expressed as the moles of olefin converted to aldehyde per mole of catalyst per sec.

function of ligand concentration rather than Rh/P ratio that is usually reported in literature [Horvath *et al.*, 1998]. The main side reaction was the olefin isomerisation, about 10%, and was not affected by the concentration of the ligand. Since the hydroformylation rate of internal alkenes is much lower than terminal alkenes [Evans *et al.*, 1968] the formed internal alkenes remained unconverted in the reactor. Moreover, less than 1% of 1 – decene was hydrogenated to decane. The catalytic activity of the $Rh/P[CH_2CH_2(CF_2)_5CF_3]_3$ catalyst was similar to that of the non fluorous analogue $Rh/P[(CH_2)_7CH_3]_3$ and an order of magnitude lower than that of the $Rh/PPh_3$ catalyst. In contrast, the l:b product selectivity of $Rh/P[CH_2CH_2(CF_2)_5CF_3]_3$ was closer to that of $Rh/PPh_3$ rather than that of $Rh/P[(CH_2)_7CH_3]_3$ [Horvath *et al.*, 1998].

The fluorous biphasic catalyst recovery concept was tested in a cycle of batch experiments, where the products, after the batch reactions, were separated from the catalyst and the latter was recycled to the reactor. In 9 consecutive runs, a total TurnOver Number[b] (TON) of more than 35000 was measured with 4.2% Rh loss. This loss represented 1.18 ppm Rh loss per mol of aldehyde and was due to the low but finite solubility of the $Rh/P[CH_2CH_2(CF_2)_5CF_3]_3$ catalyst in the product phase. Furthermore, the changes in activity and selectivity during the experiment indicated some ligand leaching as well, which was not quantified [Horvath *et al.*, 1998].

One problem with these results was that the selectivity to the desired linear products was modest unless high concentrations of the expensive fluorous modified ligand were employed (ligand concentrations of 152 and 304 mmol/l, at rhodium to

[b] TON is expressed as the moles of olefin converted to aldehyde per mole of catalyst used.

ligand ratios of 103 and 102 respectively, gave the best l:b ratios of 6.3 and 7.8 respectively. In addition the alkene isomerisation, *ca.* 10%, was quite high as well.

In a following study, Hope and co-workers [Bhattacharyya *et al.*, 2000] have synthesised $P(4-C_6H_4C_6F_{13})_3$ triphenylphosphine and $P(OC_6H_4-4-C_6F_{13})_3$ triphenylphosphite and tested their activity in 1 – hexene hydroformylation. They showed that the aryl unit is a better electronic insulator than the $C_2H_4$, albeit not perfect; even the $C_6H_2OCH_2$ unit does not completely insulate the P atom. In addition, the electronic influence through the aryl ring is purely inductive whereby a *meta* – substituent has a greater effect than a *para* – substituent. Moreover, *ortho* – and *meta* – substitutions can generate steric interactions [Bhattacharyya *et al.*, 2000]. Improved reaction rates and selectivities were obtained when $P(OC_6H_4-4-C_6F_{13})_3$ was used, which was further studied in the hydroformylation of other higher terminal alkenes [Bhattacharyya *et al.*, 2000; Foster *et al.*, 2002].

Another group reported results for the fluorous biphasic hydroformylation of 1 – decene using novel perfluoroctyl substituted triphenylphosphites [Mathivet *et al.*, 2002, b]. The standard reaction conditions used were: 80 °C, 40 bar $CO/H_2$ (1:1), Rh:P = 5 and 1*H*-perfluorooctane as fluorous solvent. Though all the catalytic systems studied exhibited high activity with TOF>3000 $h^{-1}$, there was a great difference of reactivity according to the position and number of substituents on the aromatic ring of the phosphite used. The aldehyde selectivity and l:b ratio were also very different depending on the nature of the phosphine. *Ortho* – substituted phosphite and to greater extent, o,o' – disubstituted phosphates induce lower aldehyde selectivities and lower l:b ratios than their *meta* – or *para* – substituted counterparts. From a catalyst recycle point of view, the presence of a perfluorosubstituent in the *ortho* position is essential in order to avoid the attack of the phopshite by the aldehyde formed. With

bulky *ortho* – substituted phosphates, the catalytic species contains only one phopshite per rhodium and the fluorous partition coefficient of this species is too low to prevent rhodium leaching during separation.

More recent publications [Foster *et al.*, 2002, a; Foster *et al.*, 2002, b] examined the hydroformylation of 1 – octene under fluorous biphasic conditions, where the rhodium catalyst was modified using four different fluorous ligands, $P[O4-C_6H_4C_6F_{13}]_3$, $P[O3-C_6H_4C_6F_{13}]_3$, $P[O2-C_6H_4C_6F_{13}]_3$ and $P[4-C_6H_4C_6F_{13}]_3$ prepared by Hope and co – workers [Bhattacharyya *et al.*, 1997]. The reactions were carried out at 60 – 80 °C and 20 bar $CO/H_2$ (1:1) using perfluorodimethylcyclohexane as fluorous solvent for the phosphites and PFMC for the phosphine and toluene as the organic solvent. Initial phase behaviour screening of the system showed that 1 – octene was fully miscible with PFMC at temperatures ≥ *ca.* 60 °C under typical hydroformylation conditions but nonanal phase separated even at 80 °C [Foster *et al.*, 2002, b].

Phosphites $P[O3-C_6H_4C_6F_{13}]_3$ and $P[O4-C_6H_4C_6F_{13}]_3$ showed much better l:b ratios and higher initial rates than $PPh_3$. These reaction were generally carried out at a [Rh] of 10 mmol/l and even at ligand concentrations of only 30 mmol/l the l:b ratios were as high as 8.4. One disadvantage of these phosphite ligands was that significantly higher isomerisation was observed than when using $PPh_3$. These results are easily explained. Electron withdrawing groups attached to the aryl ring of phosphites or phosphines afford less basic ligands, resulting in more facile CO dissociation in the catalytic cycle and increased rates in hydroformylation. However, the concomitant increase in the electrophilicity of the metal centre leads to increased amounts of isomerisation, which in part accounts for the high l:b ratio observed [Trzeciak and Ziolkowski, 1999; Kamer *et al.*, 2000]. Using $P[O2-C_6H_4C_6F_{13}]_3$ as

ligand gave poor selectivity, presumably because the *ortho* – substituent results in significant steric crowding on coordination [Adams *et al*, 2003]. In respect to the catalyst leaching, when $P[O4-C_6H_4C_6F_{13}]_3$ was used, ICPMS analysis showed that at 60 °C 9.7% of Rh leached to the organic phase. This value was a lot higher for higher temperatures indicating that the catalyst and/or the ligand were decomposing. The mode of the catalyst decomposition involved decomposition of the phosphite ligand in presence of the product aldehyde [Foster *et al.*, 2002, b].

Based on the fact that nonanal has higher polarity than toluene/aldehyde mixture and that a reduced volume of the organic phase might also reduce the level of rhodium leaching, reactions were carried out in the absence of organic solvent. In these experiments the volume of toluene was replaced by PFMC. The reaction rates observed were significantly increased by a factor of 1.5 and l:b ratio was dramatically improved as well, from 4.8 to 7.8. The extent of leaching of rhodium (6%) and phosphorus (9.6 at 60 °C) were greatly reduced and there was much less of a temperature effect, suggesting that the catalyst was more stable in this system [Foster *et al.*, 2002].

In order to find a more stable system, phosphine $P[4-C_6H_4C_6F_{13}]_3$ ligand was investigated in great detail. Under dilute conditions. [Rh] at 2.0 mmol/l and P/Rh = 3, these reactions showed zero order (saturation) kinetics expected for low concentrations of phosphine [Horvath *et al.*, 1998]. The l:b ratios were modest at *ca.* 3.5, but the much lower levels of isomerisation ( 2%) meant that selectivity to the linear aldehyde, in absolute amounts, was almost as good as for the reactions using the phosphite. Both rhodium (0.5 – 2.5%) and phosphorus (6.2 – 9.2%) leaching were low and varied little with reaction temperature. Increasing the phosphine concentration to 20 mmol/l with [Rh] at 2 mmol/l (10:1 ratio) considerably improved

the l:b ratio and increased the selectivity to linear aldehyde (80.9%). The reactions in the presence of this excess of ligand were first order, presumably because the phosphine competed with the alkene for the rhodium, but the rate was still acceptable. The rhodium leaching was dramatically reduced. The best results were obtained for Rh (2 mmol/l)/ $P[4-C_6H_4C_6F_{13}]_3$ (20 mmol/l) ligand, in the absence of organic solvent. This gave a linear aldehyde selectivity of 80.9% and an initial productivity of 8.8 mmol $l^{-1}$ $h^{-1}$. Rhodium leaching into the organic phase was 0.05% [0.08 mg Rh per mol aldehyde] and phosphorus leaching was 3.3% [Foster *et al.*, 2002, b]. These values were a lot better than those reported by Horvath [Horvath *et al.*, 1998] and were well compared with the known industrial processes [Foster *et al.*, 2002, b].

The results described in the previous paragraph showed the possibility for a development of a process which is nearing the rigorous retention of the rhodium in the system that would be required for commercial application, whilst retaining a high rate and good selectivity to the linear aldehyde product. In order to evaluate the long term reactivity and stability of this system we developed a continuous process that incorporates a pressurised reactor, where liquids and gases can be continuously fed and products removed. The fluids coming out of the reactor phase separate in a gravity decanter and the catalyst phase is recycled to the reactor. A somewhat similar concept has been used for aqueous biphasic systems, but only limited details have been published [Herrmann *et al.*, 1992]. Another such reactor that has been developed for the Lewis acid – catalysed reactions under fluorous biphasic conditions did not involve any gaseous reactants [Yoshida *et al.*, 2003].

# Chapter 3:

# Theoretical work for phase separation

## 3.1 INTRODUCTION TO LIQUID – LIQUID EQUILIBRIUM

Many liquids are only partially miscible. Liquid – liquid equilibrium of these systems for constant pressure is usually described by the coexistence curve shown in Figure 3.1, where $T_c$ is the upper critical solution temperature below which the one phase mixture can be separated into two phases [Gupta *et al.*, 1999].

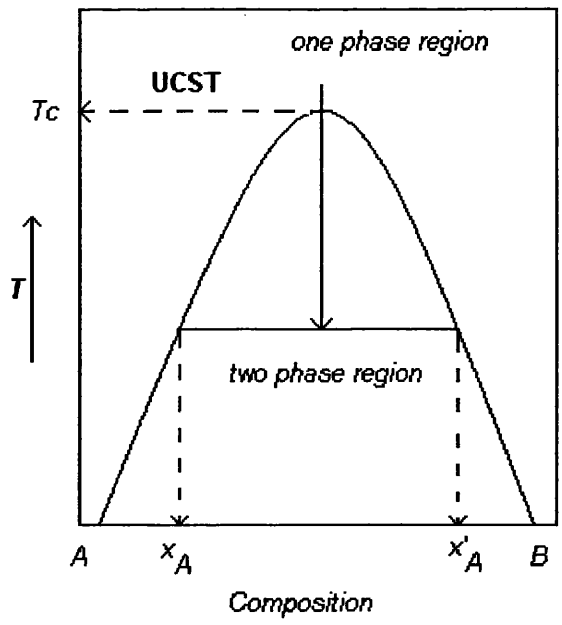


**Figure 3.1:** Typical phase diagram of partially miscible mixtures.

When an initially single – phase partially miscible binary mixture is brought across its miscibility curve into the two – phase region at temperature $T$, lower than the critical temperature, $T_c$, it phase separates. According to thermodynamic stability analysis a liquid mixture splits into two separate liquid phases if upon doing so it can lower its Gibbs energy. For a mixture of two partially miscible liquids, 1 and 2, with composition $x_1$ and $x_2$ respectively, the calculated Gibbs energy of mixing, $\Delta g_{mix}$, at constant temperature and pressure is given by line (1) in Figure 3.2. If the composition of the mixture is that corresponding to point **a**, then the molar Gibbs energy of the mixture is given by Equation 3.1 [Prausnitz and Lichtenthaler, 1986]

$$g_{mixture_{at\ a}} = x_1 g_{pure\ 1} + x_2 g_{pure\ 2} + \Delta g_a \qquad \text{(Eq.3.1)}$$

where, $\Delta g_a$, is the Gibbs energy of mixing at point **a**.

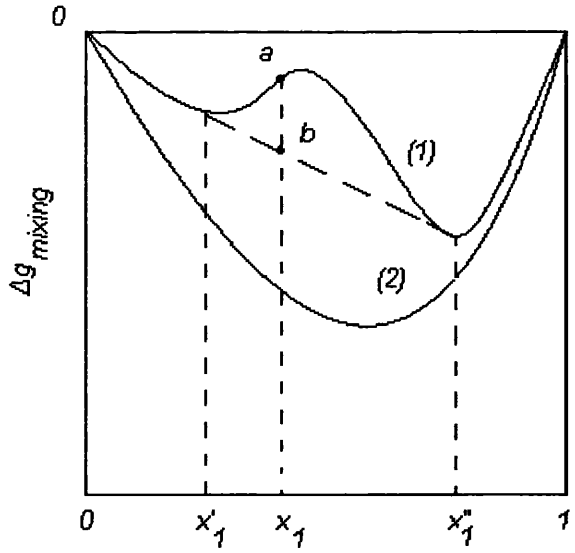


**Figure 3.2:** Molar Gibbs energy of mixing (at constant temperature and pressure) of a binary mixture: (1) partially miscible (2) totally miscible [Prausnitz and Lichtenthaler, 1986].

When the mixture splits into two separate phases, with the mole fraction of liquid 1 in the two phases being $x'_1$ and $x''_1$ respectively, then the Gibbs energy change upon mixing is given by point *b* and the molar Gibbs energy of the two – phase mixture is given by Equation 3.2,

$$g_{mixture_{at\ b}} = x_1 g_{pure\ 1} + x_2 g_{pure\ 2} + \Delta g_b \qquad \text{(Eq.3.2)}$$

where, $\Delta g_b$ is the Gibbs energy of mixing at point *b*.

Mole fractions $x_1$ and $x_2$ in Equation 3.2 represent the overall composition and they are the same as those in Equation 3.1 [Prausnitz and Lichtenthaler, 1986]. Point *b*, in Figure 3.2, represents a lower Gibbs energy of the mixture than point *a* does. Consequently, the liquid mixture having overall composition $x_1$ splits into two liquid phases having mole fractions $x'_1$ and $x''_1$. Point *b* represents the lowest possible Gibbs energy that the mixture may have at fixed temperature, pressure and overall composition $x_1$ [Prausnitz and Lichtenthaler, 1986].

A decrease in the Gibbs energy of a binary liquid mixture due to the formation of another liquid phase can occur only if a plot of change of Gibbs energy of mixing against mole fraction is, in part, concave downward, Figure 3.2. Therefore, the condition for instability of a binary liquid mixture is [Prausnitz and Lichtenthaler, 1986]:

$$\left(\frac{\partial^2 g_{mixture}}{\partial x^2}\right)_{T,P} < 0 \qquad \text{(Eq.3.3)}$$

or

$$\left(\frac{\partial^2 \Delta g_{mixing}}{\partial x^2}\right)_{T,P} < 0. \qquad \text{(Eq.3.4)}$$

The excess Gibbs energy of a mixture relative to the Gibbs energy of an ideal mixture in the sense of Raoult's law can be defined as

$$g^E \equiv g_{mixture} - RT[x_1 \ln x_1 + x_2 \ln x_2] - x_1 g_{pure\ 1} - x_1 g_{pure\ 2} \qquad \text{(Eq.3.5)}$$

Substituting into Equation 3.3, the inequality for instability becomes

$$\left(\frac{\partial^2 g^E}{\partial x_1^2}\right)_{T,P} + RT\left(\frac{1}{x_1} + \frac{1}{x_2}\right) < 0 \qquad \text{(Eq.3.6)}$$

For an ideal solution, $g^E = 0$ for all $x$. In that event, inequality is never obeyed for any values of $x_1$ and $x_2$ in the interval zero to one. Consequently, an ideal solution is always stable and cannot phase separate.

Supposing that the excess Gibbs energy is not zero but is given by the simple two suffix Margules equation

$$g^E = A x_1 x_2 \qquad \text{(Eq.3.7)}$$

where, $A$ is a constant dependent only on temperature and is generally derived by considering either the molecular interactions between nearest neighbours or summing all pair-wise interactions throughout the whole system, then

$$\left(\frac{\partial^2 g^E}{\partial x_1^2}\right)_{T,P} = -2A \qquad \text{(Eq.3.8)}$$

Substituting in Equation 3.6 it gives

$$RT\left(\frac{1}{x_1} + \frac{1}{x_2}\right) < 2A \qquad \text{(Eq.3.9)}$$

The smallest value of $A$ that satisfies the above inequality is

$$A_{\min} = 2RT \qquad \text{(Eq.3.10)}$$

Therefore, instability occurs whenever

$$\frac{A}{RT} > 2. \qquad \text{(Eq.3.11)}$$

The border line between stability and instability of a liquid mixture is called incipient instability. The condition corresponds to a critical state and it occurs when the two

points of inflection shown in Figure 3.2 merge into a single point [Prausnitz and Lichtenthaler, 1986]. Thus, incipient instability is characterised by the two Equations 3.12 and 3.13

$$\left(\frac{\partial^2 g_{mixture}}{\partial x^2}\right)_{T,P} = 0 \qquad \text{(Eq.3.12)}$$

and

$$\left(\frac{\partial^3 g_{mixture}}{\partial x^3}\right)_{T,P} = 0 \qquad \text{(Eq.3.13)}$$

For calculating purposes, it is more useful to express the excess Gibbs energy as a function of the components activity

$$g_{mixture} = RT[x_1 \ln \alpha_1 + x_2 \ln \alpha_2] + x_1 g_{pure1} + x_2 g_{pure2} \qquad \text{(Eq.3.14)}$$

In this case, incipient instability occurs when

$$\left(\frac{\partial \ln \alpha_1}{\partial x_1}\right)_{T,P} = 0 \qquad \text{(Eq.3.15)}$$

and

$$\left(\frac{\partial \ln \alpha_2}{\partial x_2}\right)_{T,P} = 0 \qquad \text{(Eq.3.16)}$$

where, activity $\alpha$ is given by [Prausnitz and Lichtenthaler, 1986]

$$\ln \alpha_1 = \ln \gamma_1 + \ln x_1 = \frac{A}{RT} x_2^2 + \ln x_1 \qquad \text{(Eq.3.17)}$$

According to Equation 3.10, the temperature $T_c$ at which instability occurs, when the excess Gibbs energy is given by a one parameter equation, is

$$T_c = \frac{A}{2R} \qquad \text{(Eq.3.18)}$$

Temperature $T_c$ is called consolute temperature or critical solution temperature. Critical temperature, $T_c$, may either be a maximum (Upper Critical Solution Temperature, UCST) or a minimum (Lower Critical Solution Temperature, LCST).

Some binary systems have both upper and lower critical temperatures [Prausnitz and Lichtenthaler, 1986].

When the excess Gibbs energy is given by Equation 3.7, the composition corresponding to the critical temperature is $x_1 = x_2 = 1/2$. However, when the excess Gibbs energy is given by a function which is not symmetric with respect to $x_1$ and $x_2$, the coordinates of the critical point are not at the composition midpoint. A more accurate description of many real mixtures is given when, the excess Gibbs energy is expressed by the three – parameter Redlich – Kister series

$$g^E = x_1 x_2 [A + B(x_1 x_2) + C(x_1 - x_2)^2] \qquad \text{(Eq.3.19)}$$

In this equation, coefficient B reflects the asymmetry of Gibbs energy function, while coefficient C affects the flatness or steepness of the excess Gibbs energy curve [Prausnitz and Lichtenthaler, 1986].

## 3.2 SPINODAL DECOMPOSITION

Phase separation of an initially single – phase binary mixture can occur either by nucleation (homogeneous or heterogeneous) or by spinodal decomposition. The former process describes relaxation to equilibrium of metastable systems and is an activated process: a free energy barrier must be overcome in order to form embryos of a critical size, beyond which the new phase grows spontaneously. Unstable systems relax via the latter process. Spinodal decomposition will occur, for example, when a binary mixture of near critical composition is rapidly cooled to a subcritical temperature, Figure 3.3. This mechanism of phase separation occurs spontaneously – no free energy barriers must be overcome – through the growth of fluctuations of

small amplitude that exceed a critical wavelength. The relevant fluctuating property is density of pure substances and composition for mixtures. Thus, metastable systems relax by the activated growth of localized fluctuations of large amplitude, whereas, unstable mixtures do so by spontaneous growth of long – wavelength fluctuations of small amplitude [Debenedetti, 1996].

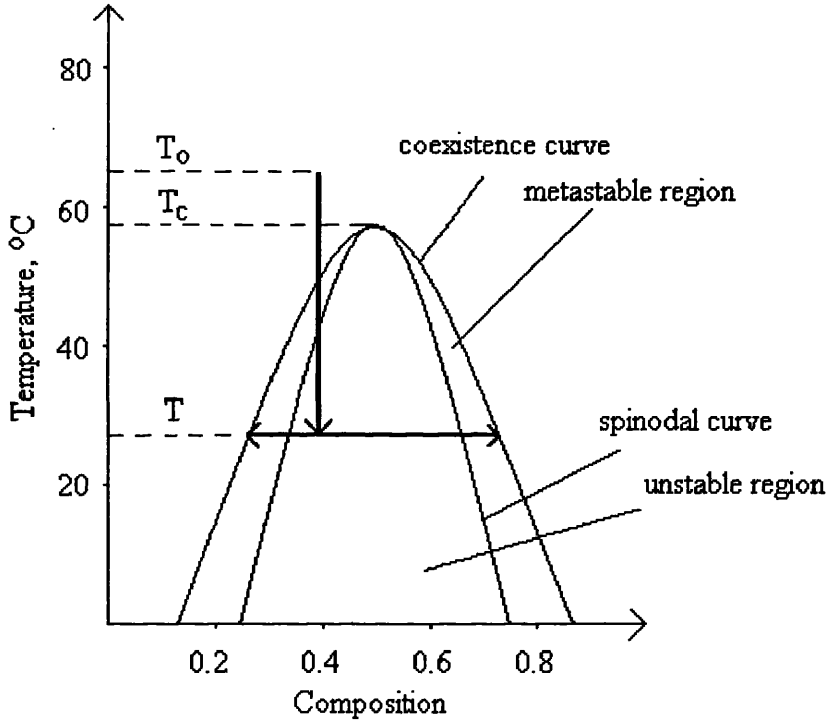


**Figure 3.3:** Temperature quench into the unstable region of a Critical Solution Temperature forming mixture [Ullmann *et al.*, 1995].

According to the previous description, nucleation and spinodal decomposition are fundamentally different from each other. However, for deep quenches the distinction between the two processes is not clear, because both the critical nucleus size and critical fluctuation wavelength decrease as the temperature quench increases [Gupta *et al.*, 1999].

Studies on spinodal decomposition have shown that at the end of a very fast separation process, small microdomains appear which later grow by diffusion and coalescence until they become large enough to sediment [Mauri *et al.*, 1996; Vladimirova *et al.*, 1998]. As the early stages of spinodal decomposition in fluids tend to be extremely rapid, in most of the experimental studies the process is retarded by considering very shallow quenches $\Delta T$ below the critical temperature, $T_C$. At these conditions fluid mixtures start to separate by diffusion only, leading to the formation of well – defined patches separated from one another by sharp interfaces [Vladimirova *et al.*, 1999].

Experimentally, the typical domain size is described by a power – law time dependence

$$r(t) \propto t^n \qquad \text{(Eq.3.20)}$$

where, $r$ is the domain size, $t$ is time and $n \approx 1/3$, when diffusion is the dominant mechanism of material transport. This initial diffusion – driven stage is followed by a convection – driven stage during which a linear growth, $n = 1$, is observed [Mauri *et al.*, 1996; Vladimirova *et al.*, 1999].

According to dimensional analysis studies that take into account hydrodynamic forces, the growth laws

$$r(t) \approx (\sigma / \eta)t \qquad \text{(Eq.3.21)}$$

and

$$r(t) \approx (\sigma / \rho)^{1/3} t^{2/3} \qquad \text{(Eq.3.22)}$$

can be obtained, depending on whether the surface tension $\sigma$ is balanced by viscous or inertia forces, with $\eta$ and $\rho$ being the typical mixture viscosity and density respectively [Mauri *et al.*, 1996; Vladimirova *et al.*, 1999].

Similar results were obtained when large scale molecular dynamics simulation were employed, showing that late time dynamics of spinodal decomposition reaches a

viscous scaling regime with a growth exponent $n=1$ [Laradji *et al.*, 1996], while $n=2/3$ is obtained at the inertia regime [Ma *et al.*, 1992; Leptoukh *et al.*, 1995]. Boltzmann lattice simulations produced the same growth exponents [Alexander *et al.*, 1993].

In order to study the behaviour of phase separation at later times when the typical domain size is of the order of magnitude, $O(1\mu m)$, the model $H$ has been used [Vladimirova *et al.*, 1998; Vladimirova *et al.*, 1999]. In this model, the equations of conservation of mass and momentum are coupled via the convective term of the convection – diffusion equation, which is driven by a composition depended body force [Hohenberg, 1977]. According to model $H$, during the early stages of phase separation, initial instabilities grow exponentially, forming at the end single – phase microdomains whose size corresponds to the fastest – growing mode $\lambda_0$ of the linear regime [Mauri *et al.*, 1996]. During the late stages of the process, for times $t > \tau_0 = \lambda_0 / D$, where $D$ is the molecular diffusivity, the system consists of well – defined patches, in which the average concentration is not too far from its equilibrium value [Vladimirova *et al.*, 1998].

Body force, $F$, inducing the separation equals the free energy gradient and is therefore driven by concentration gradients within the mixture:

$$F = \frac{\rho}{Mw}\nabla g = \left(\frac{\rho RT}{Mw}\right)\overline{\mu}\nabla x_i \qquad \text{(Eq.3.23)}$$

where, $\rho$ is the density of the system, $Mw$ is the molecular weight, $g$ is Gibbs free energy, $\overline{\mu} = \mu_A - \mu_B$ is the difference of chemical potential and $x_i$ is the mole fraction of component $i$ in the system. Physically, $F$, tends to minimise the energy stored at the interface driving for example A – rich drops towards A – rich region. Thus, it is an attractive force, enhancing coalescence of droplets. In addition, being

proportional to $\bar{\mu} = \mu_A - \mu_B$, the body force is driven by the surface energy and therefore it can be interpreted as a capillary force, which induces a bulk convection of the fluid mixture [Gupta *et al.*, 1999].

Spinodal decomposition is described by the non – dimensional number $\alpha$, Equation 3.24, which is the ratio between thermal and viscous forces and can be interpreted as the Peclet number that is the ratio between the convective and diffusive mass fluxes of the separating process [Vladimirova *et al.*, 1998; Vladimirova *et al.*, 2000]. A similar "fluidity" parameter was also defined [Tanaka and Araki, 1998]:

$$\alpha = \frac{a^2}{D}\frac{\rho}{\eta}\frac{RT}{M_W} \qquad \text{(Eq.3.24)}$$

where, $a$ is the microscopic length, $D$ is a composition independent diffusion coefficient, $\rho$ is the mixture mass density, $\eta$ is the mixture viscosity, $R$ is the gas constant and $M_W$ is the mixture molecular weight. Typical value of $a$ for a liquid mixture near its miscibility curve is $a \approx 0.1$ $\mu m$ [Vladimirova *et al.*, 1999].

For systems with very large viscosity, $\alpha$ is small, describing the diffusion separation process of polymer melts and alloys [Mauri *et al.*, 1996]. For most liquids, though, $\alpha$ is very large with typical values ranging from $10^3$ to $10^5$. Therefore, it appears that diffusion is important only at the very beginning of the process, in that it creates a non uniform concentration field. Then, the concentration gradient dependent capillary force induces the convective material flux which is the dominant mechanism for mass transport. At no time however, can diffusion be neglected as it stabilises the interface and saturates the initial exponential growth [Vladimirova *et al.*, 1999; Vladimirova *et al.*, 2000].

Figure 3.4 shows snapshots of the microdomains appearance of a critical binary mixture after a temperature quench for different Peclet numbers, $\alpha$, and at different times, $\tau$. Time, $\tau$, is non dimensional, and is defined through Equation 3.25

$$t = (10^5 a^2 / D)\tau \qquad \text{(Eq.3.25)}$$

Since typical values of $D$ and $a$ are $10^{-5}$cm$^2$/s and $10^{-5}$cm respectively, $\tau \approx t(1s)$ [Vladimirova *et al.*, 1999].

The first row of images represents the separation for $\alpha = 0$, the case when diffusion is the only mechanism of mass transfer, showing that, soon after the first drops appear, they coalesce into dendroidlike structures. The mean composition within these structures changes rapidly, as at time $\tau = 0.05$ there are already two clearly distinguishable phases. After this early stage, the structures start to grow, increasing their thickness and reducing their surface area, while at the same time composition within the domains approaches its equilibrium value. This, however, is a slow process, driven only by diffusion and at time $\tau = 0.1$ the phase domains still have a dendroidlike geometry with its characteristic width twice as large as its initial value [Vladimirova *et al.*, 1999; Vladimirova *et al.*, 2000].

For nonzero convection, $\alpha \neq 0$, dendric structures thicken faster, but up to $\alpha \approx 10^2$ domain growth still follows the same pattern as for $\alpha = 0$. Nevertheless, when $\alpha > 0$ phase separation occurs simultaneously with the growth process.

As shown in Figure 3.4, for $\alpha = 10^4$, isolated drops of each phase are formed, surrounded by the bulk of the fluid mixture, which is still not separated. These drops appear to move fast and randomly while they grow, absorbing material from the bulk,

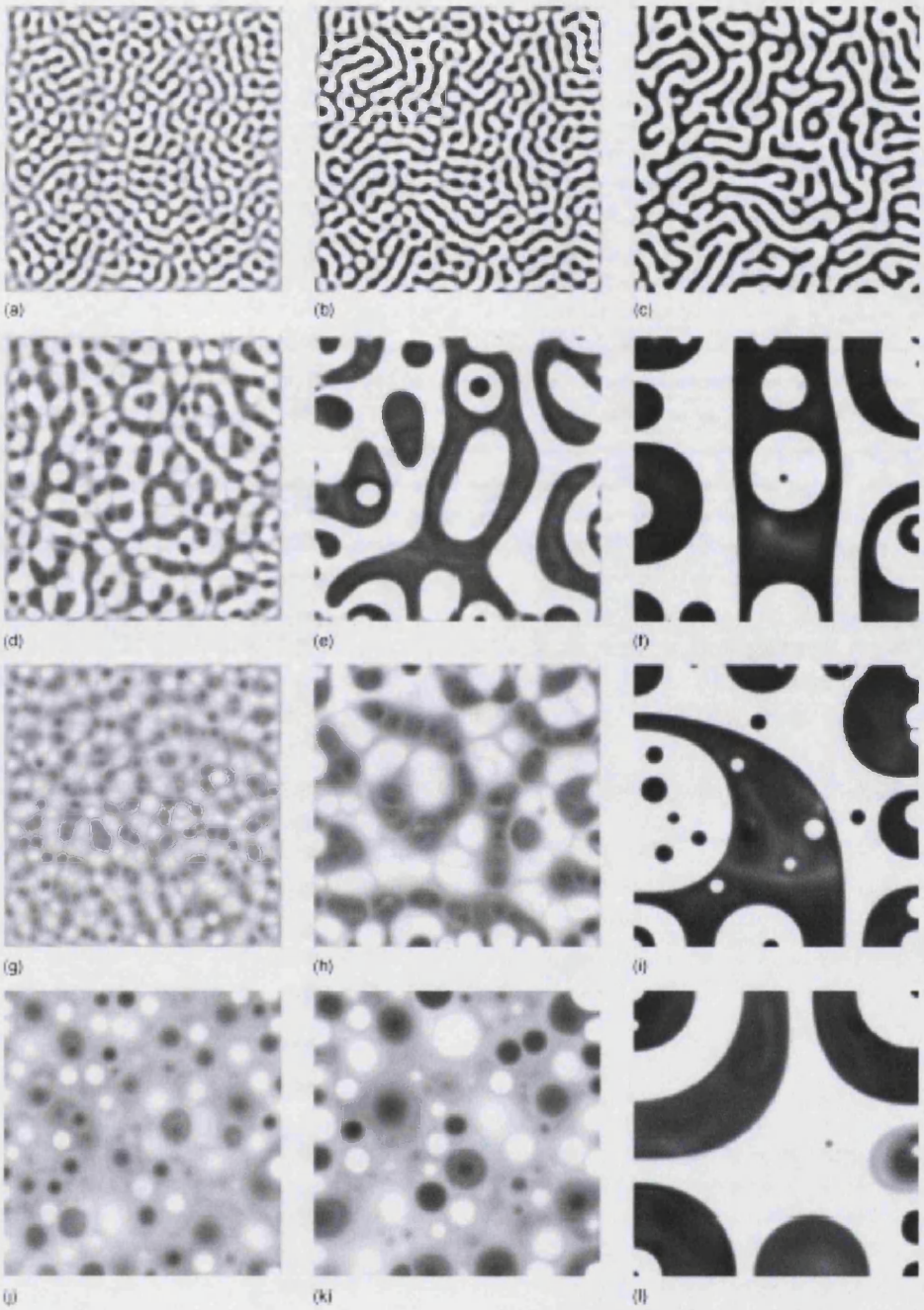

**Figure 3.4:** Composition of a critical binary mixture at different times $\tau$ after an instantaneous temperature quenching, when the Peclet number $\alpha$ is 0, $10^2$, $10^3$ and $10^4$. The snapshots correspond to $\tau = 0.04$, 0.05 and 0.10, expressed in $10^5 a^2 / D$ units [Vladimirova *et al.*, 1999].

colliding with each other and coalescing, so that single phase domains grow faster than when molecular diffusion is the only transport mechanism. It is interesting to compare the morphology of the systems at $\tau = 0.1$, for $\alpha = 10^4$ and $\alpha = 0$. In the first case, single phase domains have already reached a size comparable to that of the container's, while in the absence of convection the dendroilike domains have an approximate width of $20a$. For $\alpha = 10^4$, since the motion of the interface is too quick for concentration diffusion to establish a metastable state within the microdomains, double or multiple phase separation is observed [Tanaka and Araki, 1998; Vladimirova *et al.*, 1999].

Similar behaviour is observed for non – critical mixtures, as shown in Figure 3.5. As in the critical mixtures, the system tends to form larger single – phase domains as the Peclet number, $\alpha$, increases. Again, while for smaller $\alpha$ the process of separation and growth occur successively in time, for larger $\alpha$ they occur simultaneously. Nevertheless, while for critical mixtures the separating phases tend to form interconnected domains, for non critical mixtures we observe the formation of isolated, mostly circular drops [Tanaka and Araki, 1998; Vladimirova *et al.*, 1999]. .

Although the dynamics of phase separation in fluids is mostly driven by convection, for very short times, after the temperature quench, the convective driving force is negligible, as composition gradients have not developed yet, and therefore diffusion is the only mechanism of mass transport. As shown in Figure 3.6, at time $\tau = 0.02$, the concentration fields for $\alpha = 0$ and $10^4$ are almost the same, with patterns having a characteristic period $\lambda$ equal to the fastest growing mode in the linear regime for a diffusion process [Mauri *et al.*, 1996].

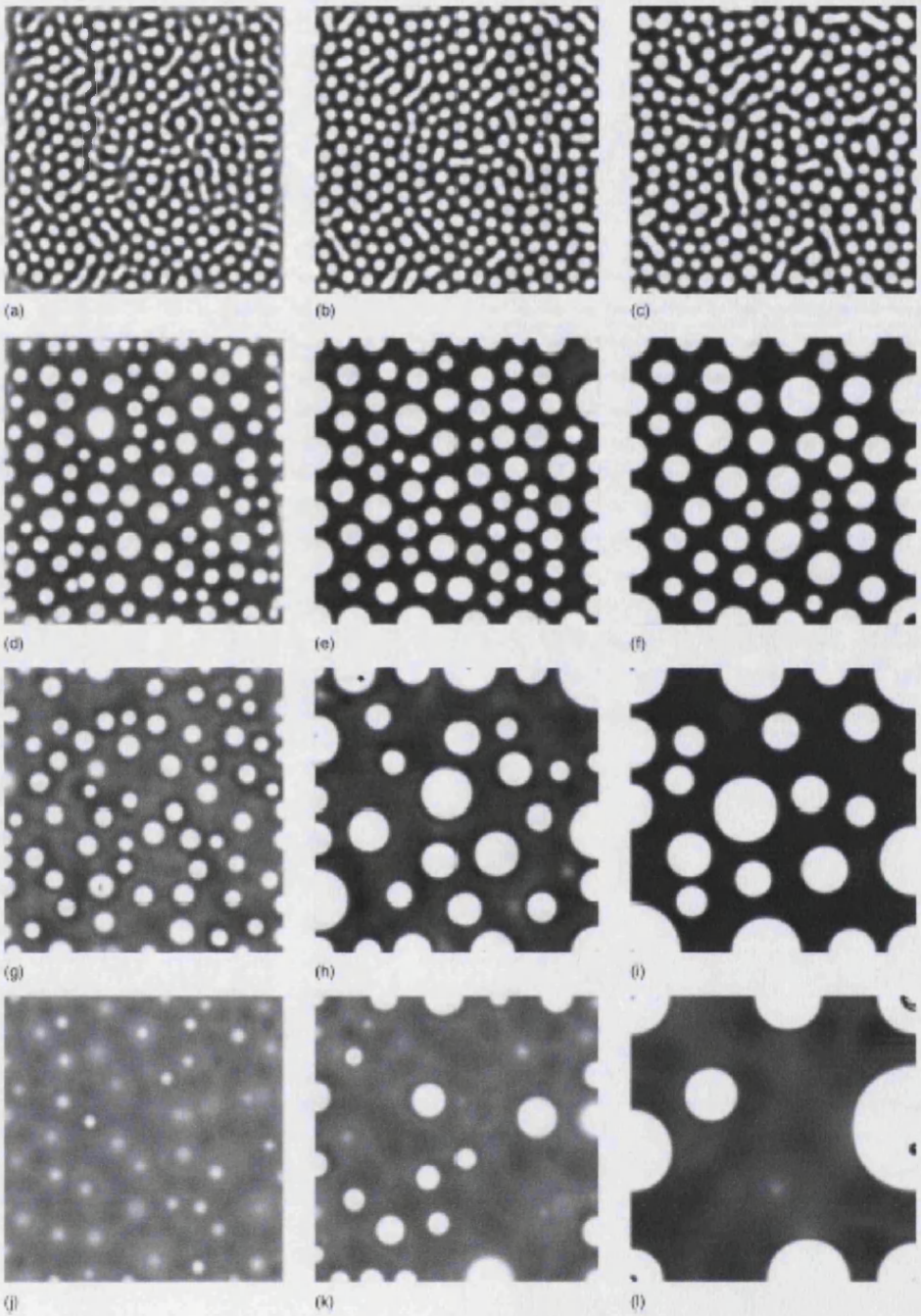


**Figure 3.5:** Composition of a non – critical binary mixture at different times $\tau$ after an instantaneous temperature quenching, when the Peclet number $\alpha$ is 0, $10^2$, $10^3$ and $10^4$. The snapshots correspond to $\tau = 0.04$, 0.05 and 0.10, expressed in $10^5 a^2 / D$ units [Vladimirova *et al.*, 1999].

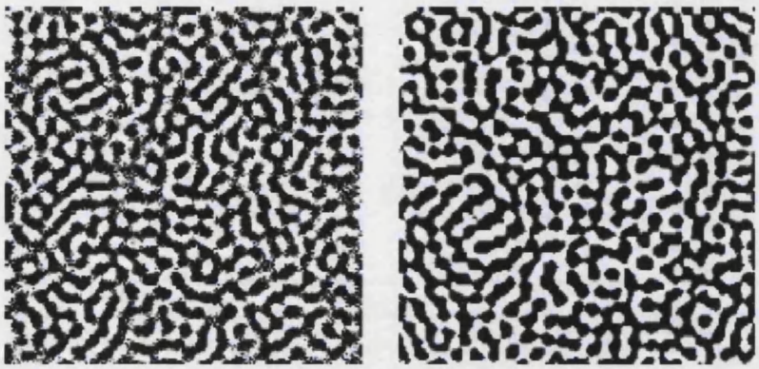


**Figure 3.6:** Concentration field after an instantaneous quenching for a critical mixture at time $t = 0.02 \times 10^5 a^2 / D$, when a) $\alpha = 0$ and b) $\alpha = 10^4$ [Mauri *et al.*, 1996].

During convection driven phase separation and before the formation of sharp interfaces, the equivalent average radius, $r$, grows linearly with time, $r(t) \approx t$, for all $\alpha$. This linear growth regime ends when sharp interfaces are formed and the system reaches values of a metastable state, where diffusion again is the dominant mechanism of mass transport. As Peclet number increases, transition from a convection driven to a diffusion driven process occurs at later times and larger sizes of nucleating domains. Practically, however, for large $\alpha$, the diffusion driven regime might never be reached, as the nucleating drops continue to grow linearly until they become large enough that buoyancy dominates and the mixture separates under gravity. This occurs when the size of the domains becomes equal to the capillary length, $r_{max}{}^2 = O(\sigma / g\Delta\rho)$, where $\sigma$ is the surface tension, $g$ is the gravity field and $\Delta\rho$ is the density difference between the two separating phases [Vladimirova *et al.*, 1999; Vladimirova *et al.*, 2000].

## 3.3 SEPARATION OF A FLUOROUS – ORGANIC MIXTURE

Figure 3.7 shows the phase diagram of the perfluoromethylcyclohexane – toluene mixture for atmospheric pressure [Stephen, 1963]. This mixture has an upper critical solution temperature of 88.9 °C and a critical composition of 26.7% mol PFMC.

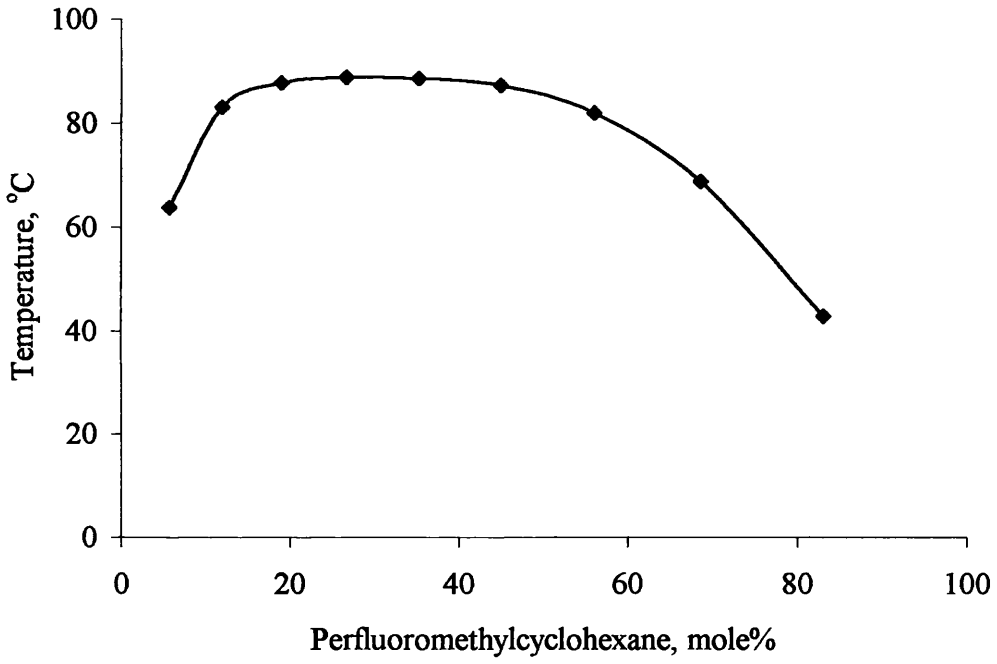


**Figure 3.7:** Phase coexistence curve for a mixture of perfluoromethylcyclohexane and toluene at atmospheric pressure [Stephen, 1963].

As experimental studies have showed [Ullmann *et al.*, 1995], such systems phase separate very quickly. At room temperature, the domain size for which transition from the convective dominated stage to buoyancy dominated stage happens is $r = O(1mm)$ [calculations of $r$ in Appendix 2]. This size is very small and domains of this magnitude are formed very quickly. From that moment on the system settles under gravity.

Thus, combining the phase separation theory with the fluorous catalytic systems discussed in Chapter 2, the system toluene – PFMC can be used as a fluorous biphasic reaction system. PFMC would be the fluorous solvent, where the fluorous modified catalyst would be dissolved, while toluene would be the organic solvent containing the reagents and the products of the reaction. The reaction should take place at temperature higher than 89 °C, the upper critical temperature, where the system would be homogeneous. The separation of the products after the end of the reaction would be easy and would be achieved just by lowering the temperature of the FBS below critical temperature. In a continuous reacting – separating system, by the time the mixture would enter the separator, the only mechanism affecting separation would be gravity, as the earlier stages of separation would occur in the pipes connecting the equipment.

# Chapter 4:

# Experimental Set Up

## 4.1 INTRODUCTION

Based on the Fluorous Biphasic Catalysis concept, a continuous homogeneous catalytic system for the long term testing of hydroformylation has been developed. The system includes a reactor in which all reagents can be fed continuously and from which the reaction mixture can be continuously removed to a gravity separator. The product is continuously removed from the separator, while the catalyst phase is recycled to the reactor.

We choose to study the hydroformylation reaction as it was the first catalytic reaction to be reported in fluorous biphasic system [Horvath and Rabai, 1994; Horvath *et al.*, 1998], it has been extensively studied since [Fish, 1999; Osuna *et al.*, 2000; Bonafoux *et al.*, 2001; Mathivet *et al.*, 2002, a; Mathivet *et al.*, 2002, b; Foster *et al.*, 2002, a; Foster *et al.*, 2002, b;] and the only long term testing of the reaction in FBS was performed in a series of batch experiments [Horvath *et al.*, 1998]

In order to test the system we performed three kinds of studies, phase equilibrium studies, which will be further discussed in Chapter 5, phase separation studies discussed in Chapter 6 and reaction studies, which will be discussed in Chapter 7. In phase separation experiments the efficiency of separation of the fluorous system was tested in the absence of catalyst and modifying ligand. Both batch experiments in separating vials and continuous experiments on the developed set up were performed, giving useful insight for the continuous reaction experiments.

## 4.2 MATERIALS

### *4.2 1. Phase equilibrium and separation experiments*

The materials used in separation experiments are perfluoromethylcyclohexane, (PFMCH, 90% pure, Aldrich), used as the fluorous solvent, 1 – octene, (98% pure, Aldrich), as the organic reactant and *n*-nonanal (95% pure, Aldrich) as the organic product. The substances were used as received without any further purification.

### *4.2.2. Reaction experiments*

The materials used in reaction experiments are perfluoromethylcyclohexane (PFMC, 90% pure, Aldrich), used as the fluorous solvent and 1 - octene (98% pure, Aldrich) as the organic reactant. Complex $[Rh(acac)(CO)_2]$ (Strem) and fluorous triphenylphosphine modifying ligand $P(-C_6H_4-4-C_6F_{13})_3$, Figure 4.1, were used for the formation of the active catalytic species.

The main concern when handling those materials is that the modified catalyst is very easily oxidized. The fact that the fluorous solvent dissolves considerable amounts of atmospheric oxygen makes its handling even more complicated. In order to avoid the decomposition of the catalyst through oxidation all liquids were treated before use. Perfluoromethylcyclohexane was thoroughly degassed before use by freeze-pump-thawing under argon at least three times. 1 – Octene (98% pure, Aldrich) was shaken with an aqueous solution of ferrous ammonium sulphate and filtered through an alumina column under anaerobic conditions to remove any peroxides. Complex $[Rh(acac)(CO)_2]$ (Strem) and fluorous ligand $P(C_6H_4\text{-}4\text{-}C_6F_{13})_3$ , which was prepared according to the method described previously [Bhattacharyya *et al.*, 1997] by our collaborators in Leicester University and St. Andrews University, were used as received. The fluorous catalyst solution was prepared by dissolving the rhodium complex, $[Rh(acac)(CO)_2]$, and the fluorous modified ligand, $P(C_6H_4\text{-}4\text{-}C_6F_{13})$, (Rh:P = 1:10 or 1:5) in PFMC (150 $cm^3$) (a concentration of 2 mmol/l [Rh]) with stirring. The mixing of the brown catalyst powder and the white ligand powder was done in a glove-box.

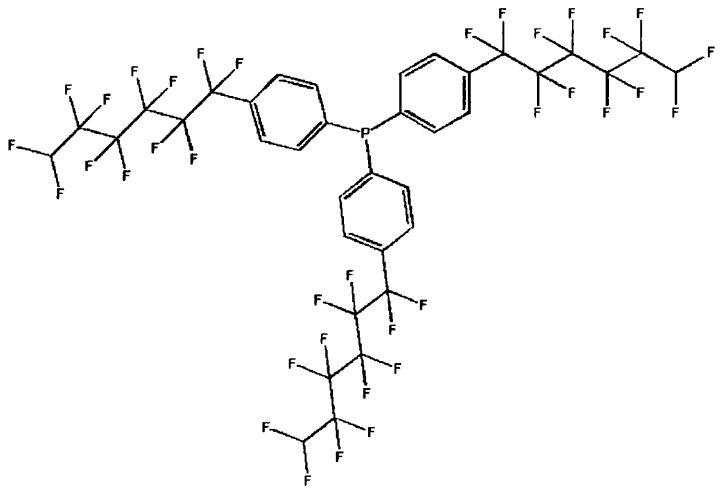

**Figure 4.1:** *p* – perfluorohexyl triphenylphosphine used for the modification of the Rh catalyst.

All liquid mixtures were carefully syringed in their feeding bottles in the experimental set up and were kept under argon atmosphere during the experiment. The whole experimental set up was also flushed with argon before the beginning of the experiment.

## 4.3 EQUIPMENT DESIGN

All continuous experiments were performed in the system shown schematically in Figure 4.2. The continuous flow system comprises of a continuous stirred tank reactor (CSTR), a glass separator, a heat exchanger, two HPLC pumps, a pressure controller, two mass flow controllers for gases and a mass flow meter for liquids. Figure 4.3 is a photograph of the experimental set – up.

*Reactor*: The CSTR (S.S. 100 $cm^3$, Parr) was fitted with an outside heating mantle, a thermocouple, a pressure gauge, a stirrer (1200rpm), a gas/liquid inlet, an outlet port and a bursting disc.

*Separator*: The separator (glass, 100 ml) was a gravity decanter of cylindrical shape where the top organic phase overflowed through the top outlet, while the bottom fluorous phase, containing the fluorous modified catalyst was removed from the bottom outlet. The separator was also fitted with a gas vent and a sampling port.

*Heat exchanger*: The heat exchanger (S.S) was a simple 1 – 1 tube-shell type, designed according to standard procedures [Sinnott, 1996].

*Pressure controller*: The pressure controller (Brooks Instrument) was used for down stream pressure regulation, keeping the pressure in the reactor constant independent of the gas inlet stream pressure variations.

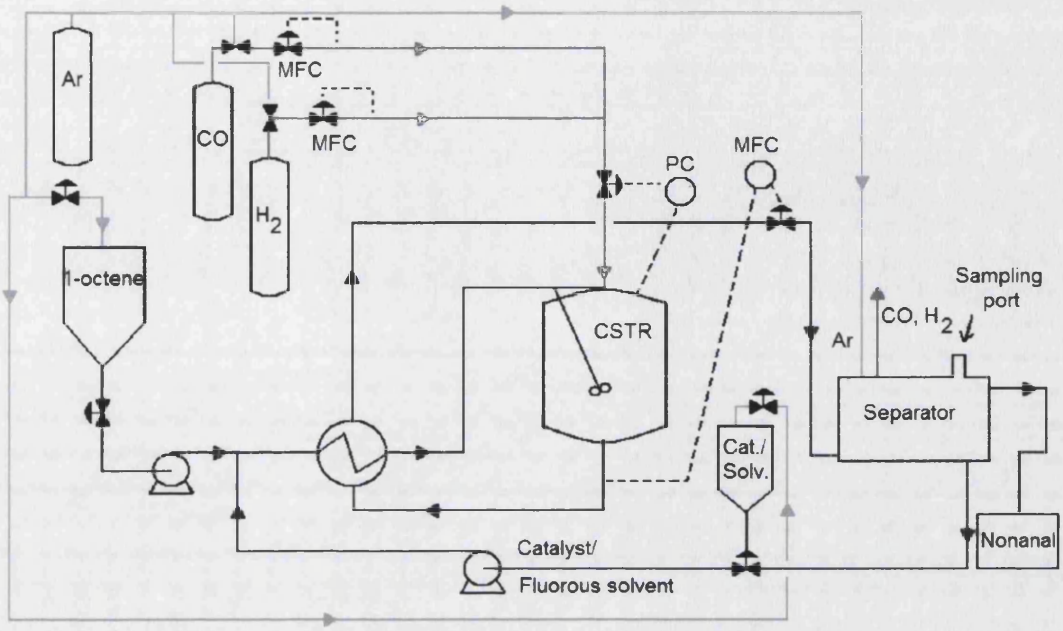


**Figure 4.2:** Flow diagram of the continuous flow fluorous biphasic experimental set-up.

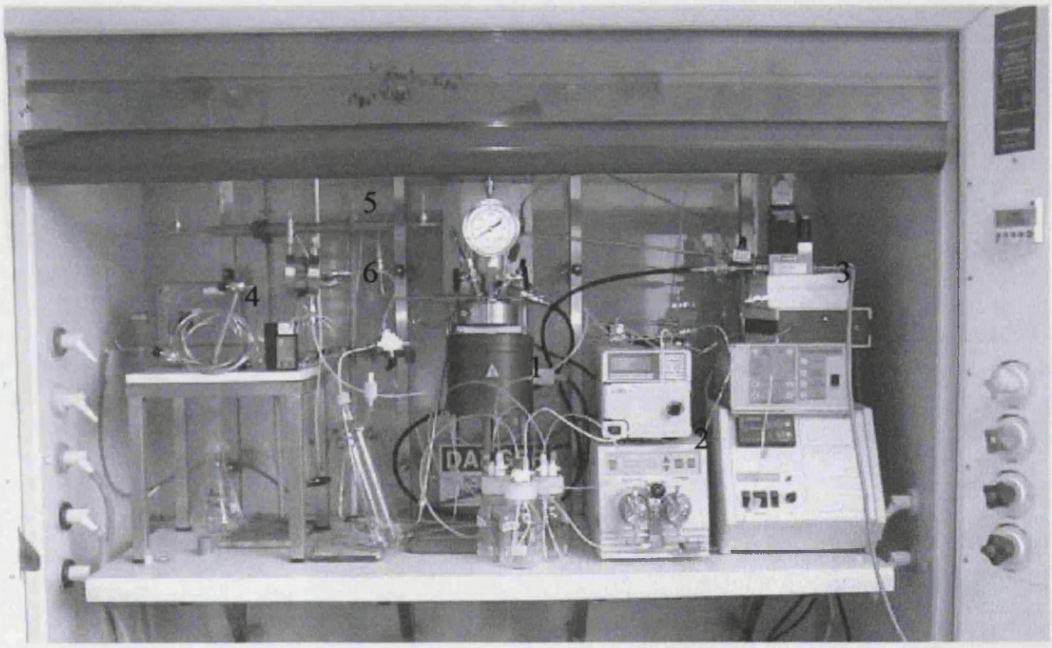


**Figure 4.3:** Photo of the experimental set – up (1: CSTR, 2: HPLC pumps, 3: pressure controller, 4: MFC for liquids, 5: heat exchanger, 6: separator).

### *4.3.1 Reactor*

The CSTR used in the project was a stainless steel reactor of 100 ml total volume. An outside heating mantle was used to provide a uniform temperature profile within the reactor. An internal thermocouple allowed the reactor temperature to be monitored. The stirrer, which could reach speeds up to 1200 rpm, ensured that the components were homogeneously mixed and enhanced the dissolution of the gas reactants in the liquids. The reactor was designed to withstand pressures up to 100 bar and temperatures up to 300 °C. These conditions were much higher than the conditions used at the experiments, 70 °C and 20 bar, and ensured the safe operation of the reactor. The reactor was also equipped with an additional safety burst disk.

As hydroformylation is a first order reaction regarding the alkene concentration (Foster *et al.*, 2002, b) the reaction rate is given by Equation 4.1 [Fogler, 2002]:

$$r_A = -kC_A(1-x_A) \qquad \text{(Eq.4.1)}$$

where, $k$ is the reaction rate constant, $s^{-1}$, $C_A$ is the alkene concentration and $x_A$ is the alkene conversion.

The reaction time in a batch reactor, as well as the residence time in a CSTR are given by the following equations (Fogler S.H., 2002):

Batch Reactor: $$t = -\frac{1}{k}\ln(1-x_A) \qquad \text{(Eq.4.2)}$$

CSTR: $$\tau = \frac{1}{k}\frac{x_A}{(1-x_A)} \qquad \text{(Eq.4.3)}$$

From Equations 4.2 and 4.3 it is obvious that for a first order reaction in a CSTR a much longer residence time is needed, in order to achieve the same conversion level than the reaction time needed in a batch reactor under the same reaction conditions.

Experiments of hydroformylation in batch mode were performed at St. Andrews University in order to obtain a value for the reaction rate constant [Foster *et al.*, 2002, b]. Figure 4.4 shows the reaction residence time for the hydroformylation of 1 – octene in batch reactor and CSTR versus conversion. The reaction rate constant was considered to be $k = 1.9 * 10^{-3}\ s^{-1}$ [Foster *et al.*, 2002, b].

According to the results shown in Figure 4.4, we chose the residence time of the CSTR to be 60 min. This residence time was long enough for a satisfying conversion of 87% to be achieved and short enough for continuous run. Longer residence time would not have been of any benefit, as an extra 20 min were required to achieve 3% higher conversion (conversion level of 0.9 is achieve at 80 min). In order to achieve the desired residence time in the reactor during experiments, the flow of the inlet and outlet liquid streams were controlled by the pumps and the mass flow controller respectively.

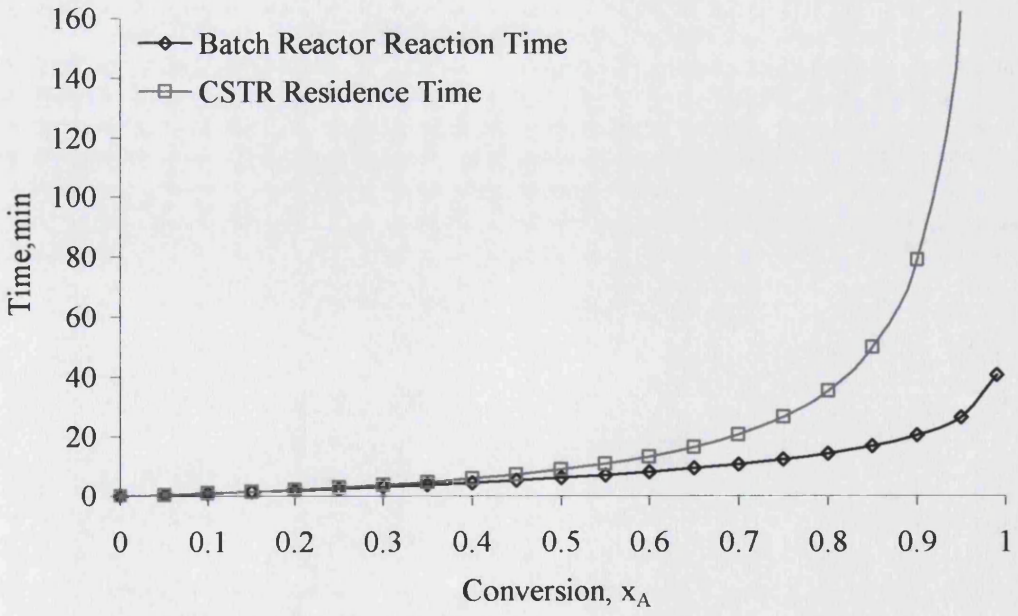


**Figure 4.4:** Reaction residence time versus conversion of 1 – octene for batch and CSTR.

### *4.3.2 Separator*

The separator designed for the set – up was a glass settler of cylindrical shape, which had a total volume of 100 ml. As shown in Figure 4.5, the top organic phase overflowed through the top outlet, while the fluorous organic phase, containing the catalyst was removed from the bottom of the settler and then recycled back to the reactor. On the top of the settler, the gas outlet allowed the released unreacted gasses to be vent while samples from both phases were taken with a syringe through the sampling port. Overflow was placed at such a position for the total liquid volume to be 60 ml and the residence time of the liquids was the same with the reactor residence time. As it will be shown below, this time was long enough for the two phases to separate.

When designing the separator two parameters had to be kept in mind. First, the time needed for the two phases to settle completely and second the inclusion of the separator in the experimental set – up.

According to the theory discussed in Chapter 3, the first stage of the phase separation and until the liquid drop radius becomes $O(1\text{mm})$, is very fast, $t \approx 1\text{sec}$. After this point, buoyancy dominates and the two phases separate under gravity [Vladimirova *et al.*, 1999].

The velocity with which a drop of PFMC travels through the bulk of liquid organic mixture, considered to be consisted in our case of 13% mol 1 – octene and 87% mol nonanal (87% conversion), due to gravity is given by Equation 4.4 [Bird *et al.*, 2002].

$$U = 2\sqrt{\frac{d * \Delta\rho * g}{3 * C_d * \rho_l}} \qquad \text{(Eq.4.4)}$$

where, $d$ is the drop radius, $\Delta\rho$ is the density difference of the two liquid mixtures, $\rho_l$ is the density of the liquid organic mixture, $C_d$ is the drag coefficient and $g$ is the gravitational constant. Obviously, for a drop of radius $d$ of the organic mixture travelling through the bulk of fluorous phase the same equation is valid, where $\rho_l$, in this case, is the density of the fluorous liquid.

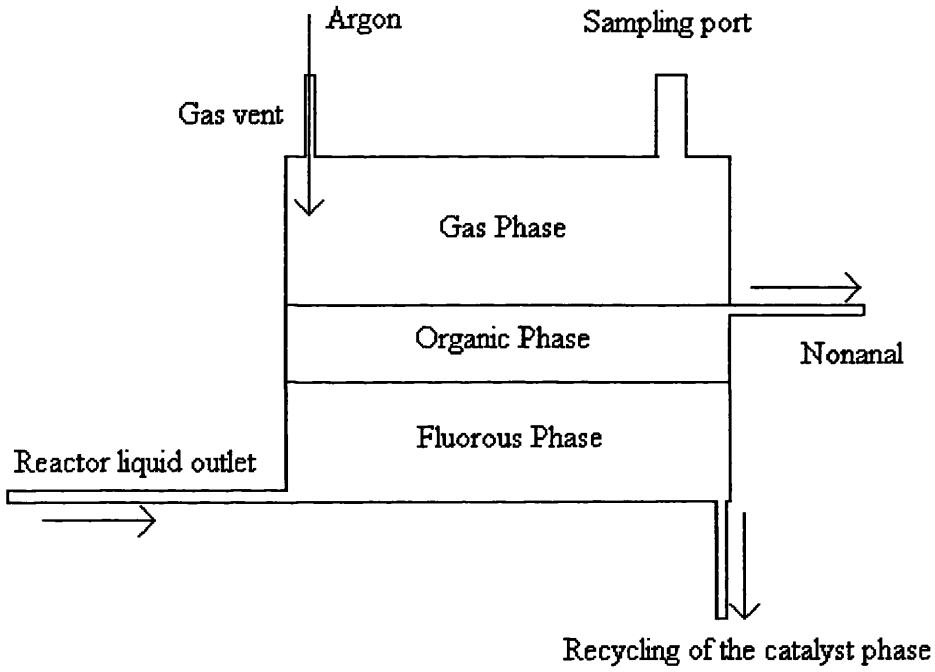


**Figure 4.5:** Separator of the fluorous biphasic system.

Figure 4.6 shows the dependence of settling velocity on the drop radius. For calculations we have assumed that a drop of pure PFMC moves through pure organic mixture (Ur fluorous 100%) and vice versa (Ur organic 100%). We have also assumed a worse case scenario where at the equilibrium the fluorous phase contains 20% mol of the organic mixture (Ur fluorous 80%) and the organic phase contains 20% mol PFMC (Ur organic 80%) [for calculations see Appendix 3].

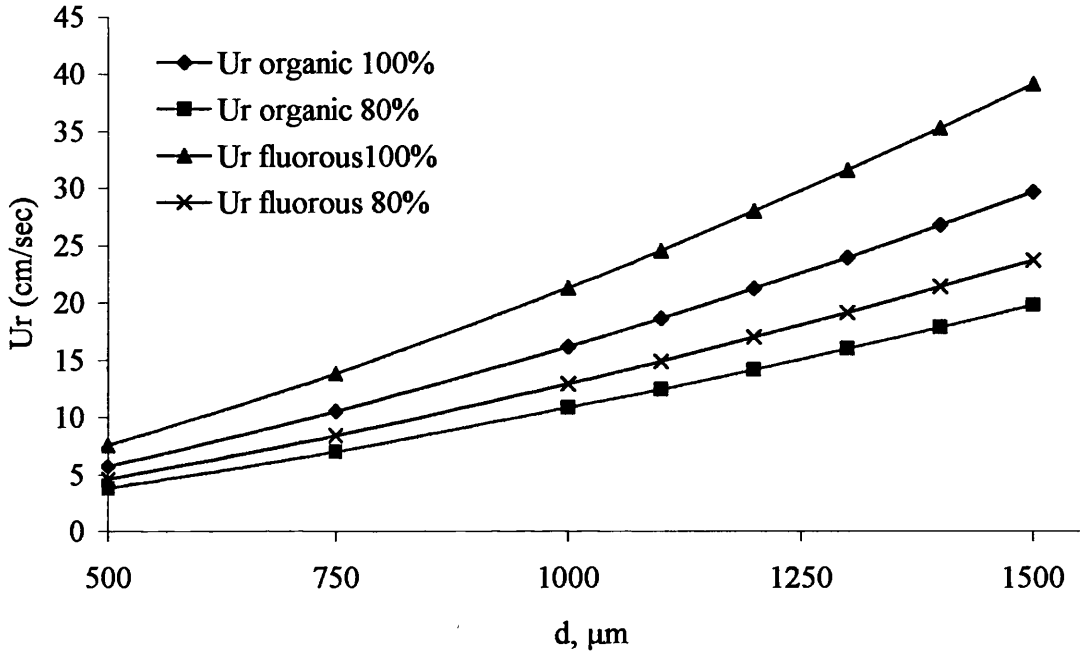


**Figure 4.6:** Dependence of settling velocity Ur on the drop radius (▲: drop of pure PFMC moving in pure organic mixture, ♦: drop of pure organic moving in pure PFMCH, x : drop of 80% mol PFMCH and 20% mol organic moving in the bulk of 80% mol organic and 20% mol PFMC, ■ : drop of 80% mol organic and 20% mol PFMC moving in the bulk of 80% mol PFMC and 20% mol organic).

According to Figure 4.6, a 500 μm radius drop of 80% mol organic moving through the bulk of 80% mol PFMC, the worse case, has a settling velocity of 3.8 cm/s. The height of liquid in the 100 ml cylindrical separator is 2.9 cm. This means that even these drops need only 0.76 s to travel from the bottom of the separator at the level of the overflow. Thus, the residence time of 60 min is long enough for the two phases to settle in equilibrium.

Knowing that separation of the two phases, once in room temperature, is very fast we decided the volume of the separator to be 100 ml so as to have a size comparable to that of the reactor that would allow visual observations of the separating system.

Photograph in Figure 4.7 shows the separator in real dimensions. The two liquid phases are well separated.

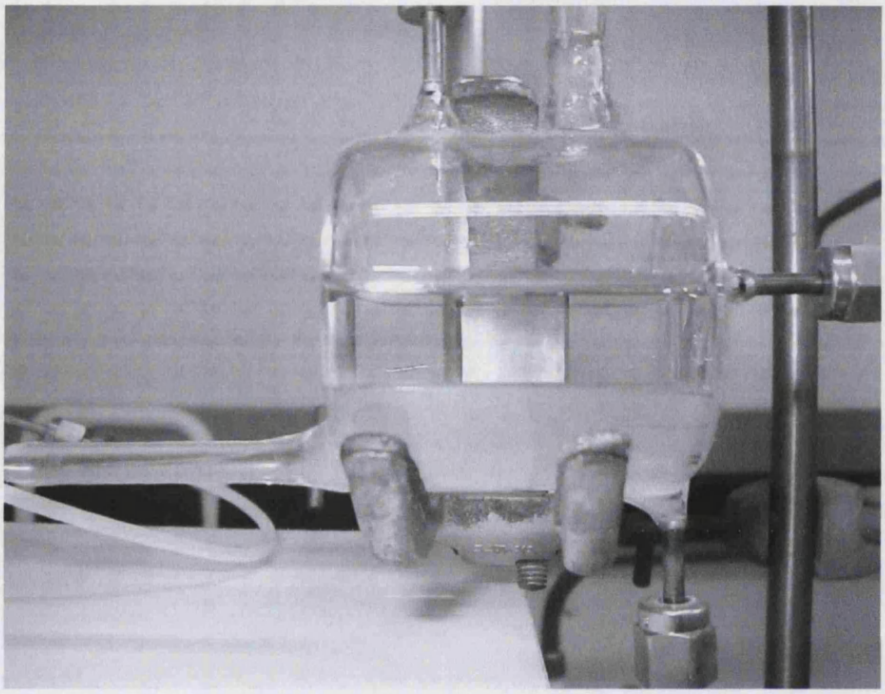

Figure 4.7: Photograph of the separator in real dimensions.

### *4.3.3 Heat exchanger*

A major research target of the design and operation of the system is to use the heat of the exothermic reaction to minimise the overall heat input. Thus, the feed stream to the reactor is preheated at the heat exchanger by the reactor outlet stream, which is at reactor temperature. This energy exchange has three main advantages. First, reduced energy demands to increase the temperature of the reaction liquid, second, homogenisation of fluorous and organic phase before they enter the reactor and third, lower temperature of the product mixture that allows for easier and faster separation.

The heat exchanger used in this experimental set up is a simple 1-1 tube-shell heat exchanger. This type was found to be the most appropriate for the small flows used at the experiment. All calculations were based on the shell liquid to be consisted of 50% mol 1 – octene and 50% mol PFMC and the tube side liquid being consisted of 40% mol nonanal, 10% mol 1-octene and 50% mol PFMC. The heat exchanger is made of stainless steel. The tube side has an internal diameter of 0.8 cm and an outer diameter of 1 cm, while the inner shell diameter is 1.5 cm. The length of the heat exchanger was calculated to be 30 cm [Sinnot, 1996].

## 4.4 DESCRIPTION OF THE FLOW DIAGRAM

The organic phase (pure 1 – octene, or mixture of 1 – octene and nonanal and the fluorous phase with the catalyst from the tank or the recycling stream are mixed and preheated at the heat exchanger before entering the CSTR. Two HPLC pumps (one for the organics, the other for the fluorous solvent) are used to deliver the liquid streams at a constant flow rate. CO and $H_2$ are delivered through two mass flow controllers at a 1:1 ratio, connected to the pressure controller keeping reactor pressure at high levels. The liquid stream leaving the reactor was cooled down at the heat exchanger in order to facilitate a faster phase separation and then entered the separator through a mass flow meter and a capillary. The pressure in the separator was atmospheric and the flow of the liquid stream due to the differential pressure between reactor and separator was controlled by the capillary length. Any gases not dissolved in the liquids were exhausted through the gas vent at the separator. The reaction mixture, products and unreacted reactants, were collected at the overflow outlet, while

the fluorous phase was recycled to the CSTR. In order to avoid oxidation of nonanal to nonanoic acid, argon stream was used to degas the set up before the beginning of the experiment and keep the liquid tanks and the separator under argon atmosphere during the experiment.

## 4.5 ANALYTICAL METHODS

### *4.5.1 Gas Chromatography, (GC)*

Gas Chromatography (GC) is used in this project for quantitative analysis. From the GC chromatogram the percentage of each component in the sample can be determined. Moreover, Gas Chromatography Mass Spectroscopy (GC-MS) analysis is used for the qualitative analysis of the samples. The results obtained from GC - MS lead to identification of the compounds present in the sample, by comparison of their retention time with those of authentic samples.

In gas chromatography the sample is volatilised and is driven by a stream of carrier gas, He, into a heated column. The column contains an absorbent support infused with an involatile liquid that acts as the stationary phase. The temperature of the injector is maintained at 180 °C, temperature at which all the components of the analysed samples are in the gaseous phase. The partition of the components of the mixture between the stationary phase and the carrier gas is due to a combination of volatility and the degree with which they interact with the stationary phase. The separated components are then eluted from the column and passed over to a detector, in this case a Flame Ionisation Detector (FID). The effluent components are ionised in

$H_2$/air flame and the ions are detected and translated into an electric current. The current produced is then directed into a high – impedance operational amplifier for measurement.

The lapsed time between injection in the column and the exit of each component is the retention time. The latter is diagnostically very useful, as once the compounds have been identified, retention times are used as means of labelling the peaks on each analysis.

Injections in a GC can be either split or split less. In a split less injection the entire sample goes through the column. In a split injection a needle valve vents most of the injected sample to the atmosphere and only a small portion of the sample passes into the column. The latter method gives better resolution and is used in this project.

Gas chromatographic analyses of both phase mixtures from the continuous separation experiments were carried out in a Perkin Elmer 8410 gas chromatograph equipped with a flame ionisation detector (GC/FID, split injection of 1:100). The column used was a J&W Scientific DB – Petro capillary column (100m × 0.25mm × 0.5 μm).

Gas chromatographic analyses of both phase samples from the equilibrium experiments and the organic phase of the continuous reaction experiments were carried out in Hewlett – Packard 5890 series gas chromatograph equipped with a flame ionisation detector (GC/FID, split injection 1:100). The column used was a Supelco MDN – 35 capillary column (30m × 0.25mm × 0.25 μm).

Two series of calibration mixtures containing all components were used to calibrate the FID signal. One series contained small quantities of the organic components in PFMCH and the second series contained small quantities of PFMCH in 1 – octene and/or nonanal.

The program used to ensure good separation of the components in all analyses is shown in Figure 4.8.

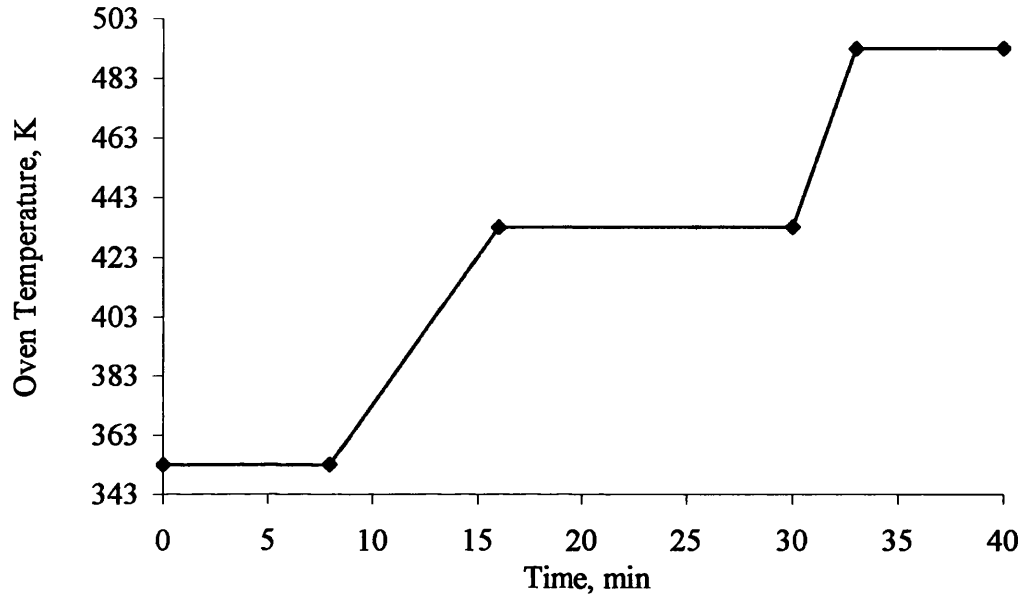


**Figure 4.8:** Temperature program of the GC oven.

### *4.5.2 ICPMS analysis*

ICPMS analysis is used in this project for quantitative determination of the Rhodium leaching in the organic phase. All Inductively Coupled Mass Spectrometry (ICPMS) analyses were done on an Agilent 7500a instrument at the Solid State Department of the School of Chemistry at St Andrews University. The instrument was modified for direct analyses of the organic fractions by using $O_2$ as a makeup gas to prevent carbon deposition on the sample and skimmer cones. Platinum cones were used together with a self-aspirating nebulizer held at -5 °C. Samples were diluted by a factor of 1000 in a mixture of xylene and toluene (50:50) and ion counts were referenced against calibration curves obtained from standard solutions of $[Rh(acac)(CO)_2]$ (acac is 2,4 – dimethylpentanedione) in xylene/toluene (50:50).

Standard solutions were run intermittently between samples to ensure that there were no drifts in instrument response and that the rate of aspiration was constant.

## 4.6 CALCULATIONS

The GC reports produce the GC peak area fractions of the main components of the reaction which if multiplied by a coefficient characteristic for each component are equal to the number of moles.

$$N_i = \lambda_i A_i \qquad \text{(Eq.4.5)}$$

where, $N_i$ is the number of moles of the component $i$, $A_i$ is the chromatogram area of the component $i$, and $\lambda_i$ is a coefficient characteristic for each component when absolute calibration is used for the GC.

In this work the GC is relatively calibrated and 1 – octene is used as the reference component. For this situation Equation 4.5 is transformed to Equation 4.6:

$$\left(\frac{N_i}{N_{ref}}\right) = \left(\frac{\lambda_i}{\lambda_{ref}}\right) \times \left(\frac{A_i}{A_{ref}}\right) = CF_{i/ref}\left(\frac{A_i}{A_{ref}}\right) \qquad \text{(Eq.4.6)}$$

where, $CF_{i/ref}$ is the calibration factor of the component $i$ to the reference component.

The only reactions happening in our system, shown in Figure 4.7, are hydroformylation of 1 – octene to linear and branched nonanal and isomerisation of 1 – octene. Hydrogenation of 1 – octene to octane was less than 0.5% and was not taken into account in the calculations.

The total number of moles of liquid compounds (1- and 2 - octene, *n* – and *iso*-nonanal) is conserved, so:

$$\overset{o}{N}_{total,out} = \overset{o}{N}_{1\text{-}C_8H_{16},in} = \overset{o}{N}_{1\text{-}C_8H_{16},out} + \overset{o}{N}_{n\text{-}C_9H_{18}O} + \overset{o}{N}_{iso\text{-}C_9H_{18}O} + \overset{o}{N}_{iso\text{-}C_8H_{16}} \quad \text{(Eq.4.7)}$$

where, $\overset{o}{N}_i$ is the flow rate of component *i* in the continuous system.

The mole fraction of 1 – octene in the mixture is:

$$y_{1\text{-}C_8H_{16}} = \frac{\overset{o}{N}_{1\text{-}C_8H_{16},out}}{\overset{o}{N}_{total}} = \frac{1}{1 + \sum_{i \neq 1\text{-}C_8H_{16},out} \left( CF_{i/1\text{-}C_8H_{16}} \left( \frac{A_i}{A_{1\text{-}C_8H_{16}}} \right) \right)} \quad \text{(Eq.4.8)}$$

$$1\text{-}C_8H_{16} + CO + H_2 \rightarrow n\text{-}C_9H_{18}O$$

$$1\text{-}C_8H_{16} + CO + H_2 \rightarrow iso\text{-}C_9H_{18}O$$

$$1\text{-}C_8H_{16} \rightarrow iso\text{-}C_8H_{16}$$

**Figure 4.7:** Possible reactions of 1 – octene in the studied fluorous biphasic system.

The mole fraction of the products is,

$$y_i = \frac{\overset{o}{N}_i}{\overset{o}{N}_{1\text{-}C_8H_{16}}} y_{1\text{-}C_8H_{16}} = CF_{i/_{1\text{-}C_8H_{16}}} \frac{A_i}{A_{1\text{-}C_8H_{16}}} y_{1\text{-}C_8H_{16}} \quad \text{(Eq.4.9)}$$

The olefin conversion is,

$$X_{1\text{-}C_8H_{16}} = \frac{\overset{o}{N}_{1\text{-}C_8H,in} - \overset{o}{N}_{1\text{-}C_8H_{16},out}}{\overset{o}{N}_{1\text{-}C_8H_{16},in}} = 1 - \frac{\overset{o}{N}_{1\text{-}C_8H_{16},out}}{\overset{o}{N}_{1\text{-}C_8H_{16},in}} = 1 - y_{1\text{-}C_8H_{16}} \quad \text{(Eq.4.10)}$$

while, the yield of each component is given by the Equation 4.11

$$Y_i = \frac{\overset{o}{N}_i}{\overset{o}{N}_{1\text{-}C_8H_{16},in}} = y_i \quad \text{(Eq.4.11)}$$

Finally, the rate of the hydroformylation reaction is calculated from Equation 4.12

$$r_{hydroformylation} = \frac{\overset{o}{N}_{C_9H_{18}O}}{V_R} = \frac{\overset{o}{N}_{1\text{-}C_8H_{16},in} * Y_{C_9H_{18}O}}{V_R} \qquad \text{(Eq.4.12)}$$

where $V_R$ is the reactor volume.

# Chapter 5:

# Phase Equilibrium Experiments

## 5.1 INTRODUCTION

Horvath *et al.* [Horvath *et al.*, 1998] have reported that PFMC/toluene/1 – octene (40:40:20 molar ratio) mixtures form a monophasic system under typical hydroformylation conditions (100°C, 10 bar, $CO/H_2$ = 1:1), while Cole – Hamilton and co – workers [Foster *et al.*, 2002, b] have reported that 1 – octene is totally miscible with PFMC at temperatures above 60 °C under 20 bar $CO/H_2$ (1:1), but nonanal is visually separated even at 80 °C. Nevertheless, not many studies have been published on the partition coefficients of the substrates and the products in the fluorous and the organic phase at the conditions of the separation process (room temperature, atmospheric pressure) [Barthel Rosa and Gladysz, 1999]. Such data are very useful for the design and optimisation of fluorous catalyst and reagents [Barthel Rosa and Gladysz, 1999].

In order to obtain these data we performed various phase equilibrium experiments, which can be divided into three groups. In the first group, the effect of temperature on PFMC/nonanal phase behaviour and on 1 – octene distribution for

equal volumes of PFMC and nonanal, was studied. The effect of simulated conversion on 1 – octene's distribution at reaction temperature (70 °C) was also investigated in order to obtain data for the computational modelling of the reaction kinetics in batch reactions. In the second group, the liquid – liquid equilibrium of PFMC/1 – octene/nonanal mixture at room temperature was studied in graduated cylinders. Finally, in the third group of experiments we examined in continuous mode the separation efficiency of the PFMC/1 – octene/nonanal system for different reaction conversions, using the developed experimental set – up shown in Figure 4.2. Results from the final set of experiments are reported in the next chapter.

In phase equilibrium experiments, the mass balance of 1-octene partitioning between two phases, top and bottom, is obtained through the partition ratio, G, which is defined by Equation 5.1:

$$G = \frac{number\ of\ moles\ of\ 1-octene\ in\ top\ layer}{number\ of\ moles\ of\ 1-octene\ in\ bottom\ layer} \qquad \text{(Eq.5.1)}$$

Distribution of octene between the two bulk phases is characterised by the total percentage of octene in the top or bottom layer:

$$Distribution\ of\ 1-octene\ in\ top\ layer = \frac{moles\ of\ 1-octene\ in\ top\ layer}{total\ number\ of\ moles\ of\ 1-octene}$$

(Eq.5.2)

$$Distribution\ of\ 1-octene\ in\ bottom\ layer = \frac{moles\ of\ 1-octene\ in\ bottom\ layer}{total\ number\ of\ moles\ of\ 1-octene}$$

(Eq.5.3)

## 5.2 EXPERIMENTAL PROCEDURE

All phase equilibrium experiments were carried out in a pressurised round bottom flask under nitrogen atmosphere. Known quantities of PFMC, nonanal and 1 – octene were loaded in the flask which was heated in a temperature controlled water bath. The liquids in the flask were vigorously stirred for 90 min, so that perfect mixing could be assumed before phases were allowed to settle at the desired temperature. After 120 min, when all liquids came to equilibrium, samples from both phases were taken and analysed by GCMS.

During liquid – liquid equilibrium experiments, 5 ml of PFMC and 5 ml of the organic mixture were syringed in a sealed graduated glass test tube (25 ml), which was then heated at 70 °C for 40 min using an oil bath. During heating the tube was shaken well three times in order to ensure good mixing. Following the heating, the test tube was put in a temperature controlled oil bath set at 27 °C for 40 min to phase separate. This time was long enough for liquid – liquid equilibrium to be achieved, as analysis of samples taken after 40 min, 1h and 3h produced the same results. Samples were taken from both phases and analysed by GCMS.

In order to ensure that samples from different phases did not contaminate each other, fluorous layer samples were taken from the bottom of the phase, while product layer samples were taken from the top of the organic phases, using different syringes. The same technique was followed in all phase equilibrium experiments.

All experiments were performed in the absence of any catalyst or fluorous ligand, while conversion level was simulated by using organic mixtures of 1 – octene and nonanal of different molar composition – the mole fraction of nonanal in the mixture simulated the reaction conversion level. Five different organic mixtures of 1 – octene and nonanal were prepared:

1. 100% mole 1 – octene; simulated conversion 0%,
2. 60% mole 1 – octene; simulated conversion 40%,
3. 40% mole 1 – octene; simulated conversion 60%,
4. 20% mole 1 – octene; simulated conversion 80%,
5. 100% mole nonanal; simulated conversion 100%

## 5.3 RESULTS AND DISCUSSION

### *5.3.1 Phase performance of PFMCH and nonanal with increasing temperature in the absence of 1-octene*

Although perfluoromethylcyclohexane and nonanal are immiscible even at 80 °C as stated previously [Foster *et al.*, 2002, b] and shown in Figures 5.1 and 5.2, mole fractions of each component in the other phase, nonanal content in PFMCH and PFMCH content in nonanal, increased linearly with temperature. However, the amounts of PFMCH and nonanal in the other phase were kept below certain limits. Nonanal in PFMCH was ≤12.5mol% even at 80 °C and PFMCH in nonanal was ≤3.8 mol %. In bottom fluorous layer the molar ratio of PFMCH/nonanal was 6.0 while in top nonanal layer the molar ratio of nonanal/PFMCH was 21. These results indicated that, at typical hydroformylation temperature (70 °C) even during the process of nonanal formation hydroformylation product nonanal was mostly separated from the fluorous phase. This surprising phase behaviour could have further implications in the reaction kinetics.

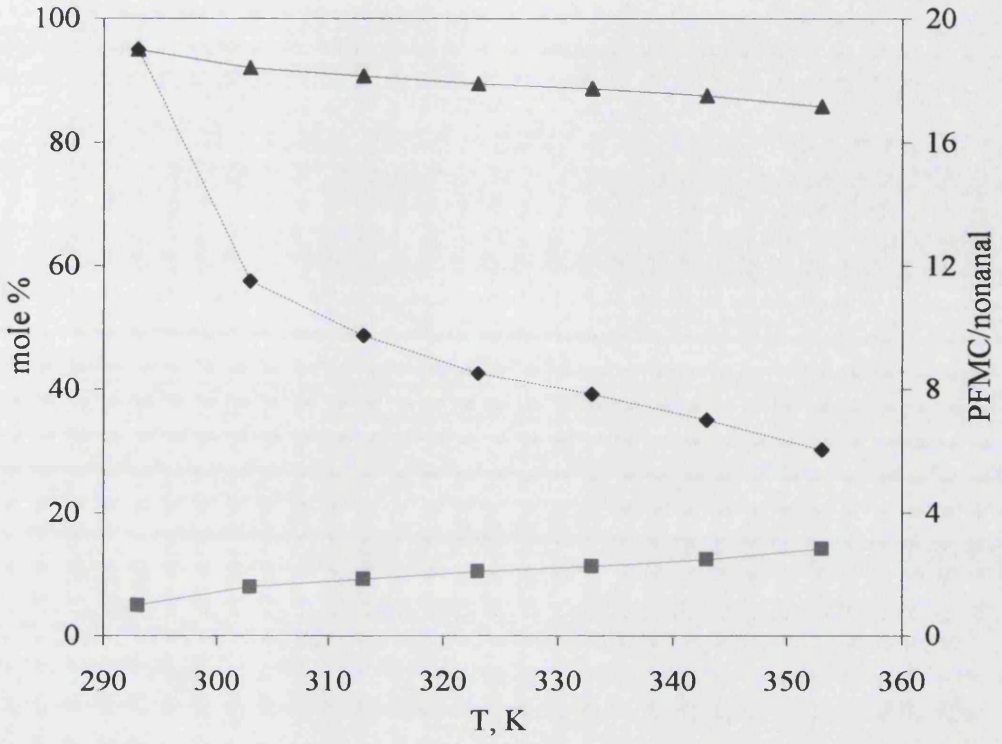


**Figure 5.1:** Effect of temperature on composition of bottom layer in the absence of 1 – octene (■: nonanal; ▲: PFMCH; ♦: molar ratio of PFMCH to nonanal).

Because of its immiscibility with perfluoromethylcyclohexane, nonanal should form another immiscible phase in the hydroformylation reaction system just after it was formed from 1-octene in the original single phase containing the catalyst, 1-octene and PFMCH. Because of the miscibility of 1-octene and nonanal, it was expected that some octene would be drawn out of the fluorous phase by nonanal. Due to the decrease of 1 – octene's concentration in the fluorous phase where the catalyst was retained hydroformylation rate might had been reduced. In order to understand hydroformylation process better, we studied the distribution of 1-octene in fluorous biphasic system ($V_{PFMCH}/V_{nonanal}$ = 1.0). In all these experimental runs, the volume ratio of nonanal to octene was kept at 5.0 corresponding to a conversion of *ca.* 80%.

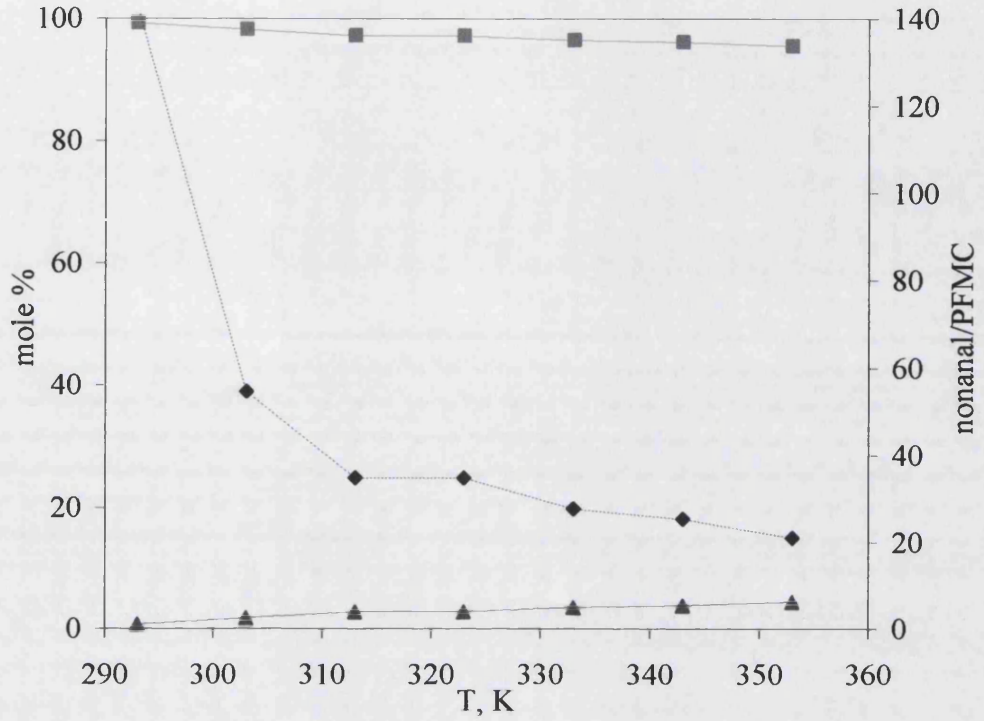


**Figure 5.2:** Effect of temperature on composition of top layer in the absence of 1 – octene (■: nonanal; ▲: PFMCH; ♦: molar ratio of PFMCH to nonanal).

### *5.3.2. Effect of temperature on 1-octene distribution in the PFMCH / nonanal biphasic system*

As shown in Figure 5.3, concentration of 1-octene in the fluorous phase increased with temperature while it decreased in the organic phase. Distribution of 1-octene between the two layers changed dramatically up to 70 °C (343K) above which it levelled off. These results suggested that 1-octene had its most favourable distribution in PFMCH in a hydroformylation reaction mixture at 70 °C (343K) or above. They confirmed that 70 °C is an ideal temperature for this fluorous biphasic system [Horvath *et al.*, 1998; Foster et al, 2002, b]. However, even under these conditions, the majority of 1-octene (> 82 %) resided in the organic phase, so that reaction rates were expected to be lower than if a monophasic system existed within

the reactor. The problem was even more pronounced at lower temperatures, as unreacted 1-octene would be removed with the aldehyde rather than be recycled with the fluorous phase.

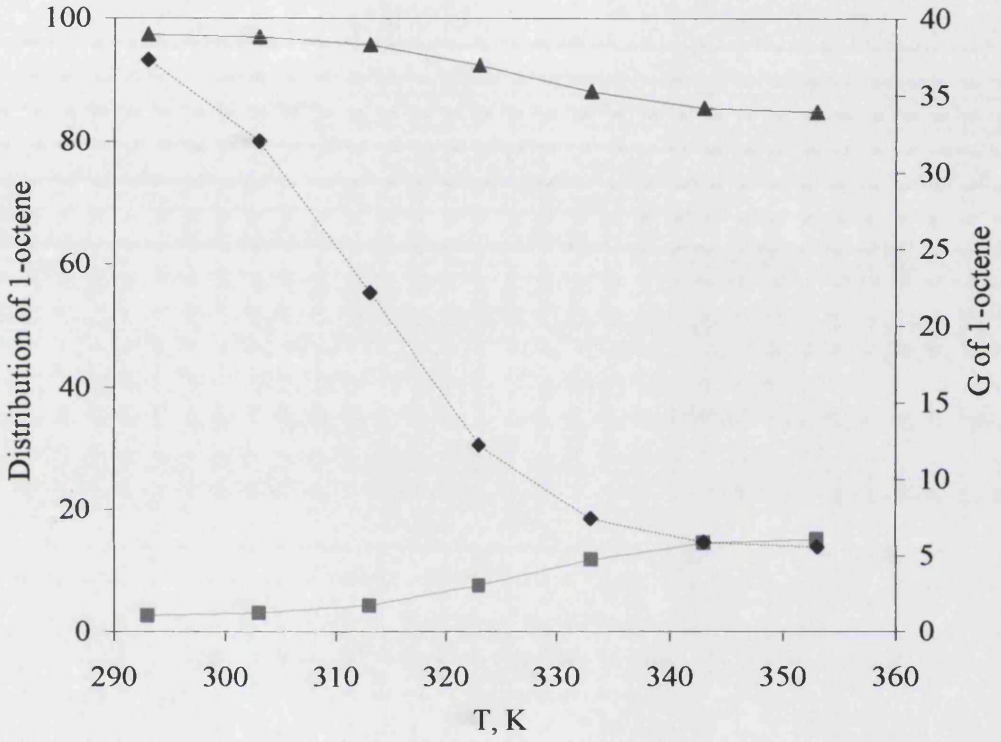


**Figure 5.3:** Effect of temperature on partitioning of octene in PFMCH/Nonanal (▲: in the top layer; ■: in the bottom layer; ×: G of octene).

### *5.3.3 Effect of conversion on partition of octene at systems with equal volumes of PFMCH and organic components, $V_{PFMCH}/(V_{nonanal}+V_{octene}) = 1.0$*

As typical reaction temperature was 70 °C (343K) [Foster *et al.*, 2002, b] (this temperature was also used at continuous reaction experiments) it was of great use to study the effect of reaction conversion on 1 – octene's phase distribution between the organic, top, and the fluorous, bottom, layer at this temperature.

During these experiments it was observed that for conversion levels of 5%, 10% and 13% only one liquid phase was present in the flask. Even after 24h, no other phase had been formed. For conversion level of 15%, during stirring of the mixture, one haze phase was present. The haziness was probably caused by very fine droplets of organic phase being dispersed in the bulk of the fluorous phase. Immediately after stirring was stopped one haze phase was present in the flask for a couple of minutes, before it phase separated in two clear phases of approximately the same volume. For higher conversion levels, two distinct phases were present even during stirring. The phases had approximately the same volume, though accurate measurements of the volume at 70 °C could not be made.

As shown in Figure 5.4, as soon as two phases were formed, 15% conversion, the majority of 1 – octene was present in the fluorous phase, 55%. Nevertheless, this picture was quickly reversed and for 17% conversion the majority of 1 – octene, 74%, was present in the organic phase. From there onwards, there was almost a linear increase in the distribution of 1 – octene in the top phase that reached asymptotically the value of 85%.

In accordance with the previous observations, as it is shown in Figure 5.5, the total amount of 1 – octene in the organic and fluorous phase decreased with approximately the same rate as the conversion increased from 17% to 70%. For conversion levels higher than 70% decrease of the absolute amount of 1- octene in the organic phase was even more profound. Nevertheless, at no time for conversion higher than 17% was the total amount in the fluorous phase higher than that in the organic phase.

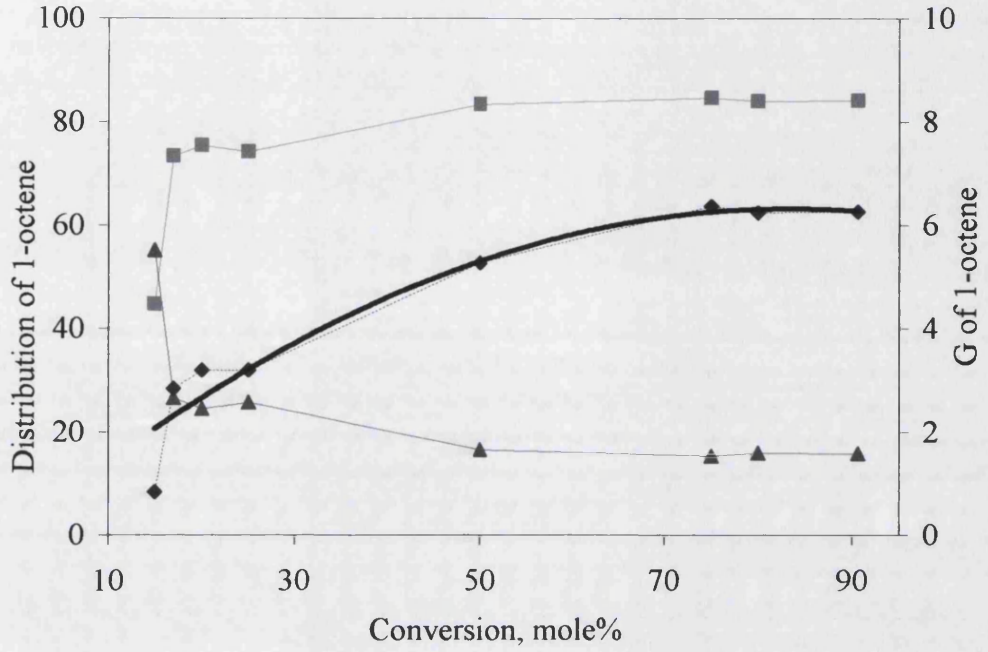


**Figure 5.4:** Effect of conversion on partitioning of 1 – octene at 343K ( ■ : distribution at top phase, ▲: distribution at the bottom phase, ♦ : G of octene ).

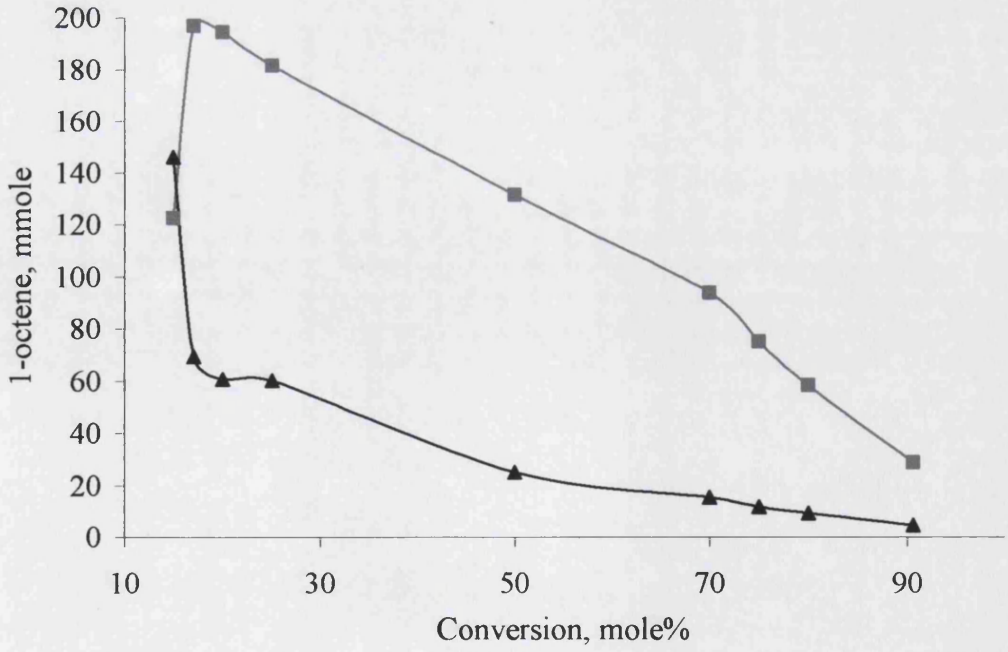


**Figure 5.5:** Effect of conversion on partitioning of absolute amount of 1 – octene at 343K ( ■ : absolute amount of 1 – octene at the top phase, ▲: absolute amount of 1 – octene at the bottom phase ).

To summarise the results obtained so far, it was shown that an increase in temperature caused an increase in nonanal's partition in the fluorous phase and vice versa. Moreover, at reaction temperature 70 °C only one phase was present up to 15% conversion. For higher conversion levels distribution of 1 – octene in the organic phase reached a maximum of 85% for conversion up 90.6%. As most 1 – octene was present in the organic phase it would be expected that longer reaction times would be needed to achieve full conversion in this biphasic system.

### *5.3.4 Liquid – liquid equilibrium of PFMC/1 – octene/nonanal mixture at room temperature*

An important issue on the successful implementation of fluorous biphasic systems is efficient separation of primary the product and secondly the reactant from the fluorous phase. As separation in the developed continuous system happened at room temperature, liquid – liquid equilibrium of PFMC/1 – octene/nonanal mixture at room temperature for different conversion levels was studied. These results were later used for comparison with separation results from the settler of the continuous set – up.

Tables 5.1 and 5.2 list the equilibrium values of composition of the fluorous and organic phase respectively, showing the effect of conversion level. The values presented are the averaged values of the three times repeated experiments.

Examining the composition of fluorous phase we note that 17.5% of pure 1 – octene partitioned into the fluorous phase, while only 1.9 mol% of pure nonanal partitioned in the same phase under the same conditions. As simulated conversion level increased from 40% to 60% to 80%, the total amount of organics in the fluorous phase decreased from 10.4 to 7 to 4.8 mol%. Consequently, the higher the conversion

**Table 5.1:** Composition of the fluorous phase at equilibrium at room temperature, in mol%.

| *Simulate conversion level* | *0%* | *40%* | *60%* | *80%* | *100%* |
|---|---|---|---|---|---|
| PFMC, mol% | 82.5 | 89.5 | 93.0 | 95.2 | 98.1 |
| 1 – octene, mol% | 17.5 | 9.1 | 5.5 | 3.2 | - |
| Nonanal, mol% | - | 1.3 | 1.5 | 1.6 | 1.9 |

**Table 5.2:** Composition of the organic phase at equilibrium at room temperature, in mol%.

| *Simulate conversion level* | *0%* | *40%* | *60%* | *80%* | *100%* |
|---|---|---|---|---|---|
| PFMC, mol% | 11.2 | 5.5 | 4.1 | 3.3 | 2.8 |
| 1 – octene, mol% | 88.8 | 58.6 | 40.2 | 22.1 | - |
| Nonanal, mol% | - | 35.9 | 55.8 | 74.6 | 97.2 |

level the less the leaching of the organics. However, since in a continuous system fluorous phase would be recycled, quantities of the organics within it should not be considered as loss.

Similar behaviour was observed in organic phase composition. When organic phase was composed only by pure 1 – octene, 11.2 mol% of PFMC was found in the organic phase, while for pure nonanal it dropped to 2.8 mol%. Again, an increase in conversion level resulted in less leaching of fluorous solvent in the organic phase.

## 5.4 MODELLING OF HYDROFORMYLATION REACTION KINETICS

### *5.4.1 Introduction*

Phase equilibrium experiments at elevated temperature (70 °C) proved the peculiar behaviour of PFMC/1 – octene/nonanal system. Formation of a separate organic phase

at simulated conversions higher than 15% and change of distribution of 1 – octene in between the two phases with increasing conversion is expected to affect the reaction kinetics, as it results in reduced concentration of the reactant in the catalyst phase. In order to investigate this effect further, a mathematical model was developed using first order reaction kinetics (we assume hydroformylation to be first order reaction in respect to the substrate concentration under fluorous biphasic conditions [Foster *et al.*, 2002, b]), taking in account the change in 1 – octene's distribution with change in conversion. The estimated results were compared with those of reaction kinetics of an ideal first order reaction occurring in a homogeneous catalytic system. Furthermore, a batch hydroformylation experiment performed under fluorous biphasic conditions provided experimental data for comparison with the developed model and standard batch reactor model without phase separation. Incentive for this comparison was deviation of the experimental reaction kinetics from the typical first order reaction kinetics in a batch reactor.

### *5.4.2 Description of batch experiment*

To obtain experimental values of kinetics of a batch hydroformylation reaction, an experiment in an autoclave under fluorous biphasic conditions was performed by our co – workers at St. Andrews University according to the experimental procedure described elsewhere by Foster *et al.* [Foster *et al.*, 2002, b]. PFMC, 2.5 ml, and 1 – octene, 2.5 ml, were degassed and treated for removal of peroxides before being injected in the batch autoclave. The fluorous modified catalyst was formed in situ with addition of $Rh(acac)(CO)_2$ (2mmol/l) as catalyst precursor modified with P(4-$C_6H_4C_6F_{13}$) ligand (P:Rh=5). Reaction was performed at 70 °C and 15 bar. The

pressure of the ballast vessel from which gases were fed into the autoclave through a mass flow controller to keep pressure within the autoclave constant was monitored and recorder every 5 sec. This pressure change was used to obtain experimental reaction kinetics. According to ideal gas equation, Equation 5.4

$$P \cdot V = n \cdot R \cdot T \qquad \text{(Eq.5.4)}$$

for a constant ballast volume, $V$, and temperature, $T$, the moles of gases consumed, $n$, were calculated using the change in pressure, $P$. Moles of product were half the moles of gases, as two moles of gases reacted for production of one mole of aldehyde.

### *5.4.3 Description of mathematical model*

The design equation of a batch for a first order reaction is given by Equation 5.5

$$\frac{dN_i}{dt} = -k \cdot C_i \cdot V_R \qquad \text{(Eq.5.5)}$$

where, $N_i$ is moles of substrate $i$, k is the initial reaction rate constant and $C_i$ is the concentration of component $i$ in the volume of the reaction mixture $V_R$.

First assumption made for the development of the model was that the only reaction happening in the autoclave was hydroformylation. Isomerisation of 1-octene was found to be less than 4%, thus not having a great effect on the obtained results. Consequently, Equation 5.5 was rewritten as:

$$\frac{dN_{C_8H_{16}}}{dt} = -k \cdot C_{C_8H_{16},fl} \cdot V_{fl} \qquad \text{(Eq.5.6)}$$

where, subscript $C_8H_{16}$ denoted 1-octene and $fl$ the fluorous phase.

Total conversion of used alkene was

$$x_{C_8H_{16}} = \frac{N^o{}_{C_8H_{16}} - N^f{}_{C_8H_{16}}}{N^o{}_{C_8H_{16}}} = 1 - \frac{N^f{}_{C_8H_{16}}}{N^o{}_{C_8H_{16}}} \qquad \text{(Eq.5.7)}$$

where, $x$ is conversion, $N$, is number of moles and superscripts, $o$ and $f$, denote initial and final states.

Two more assumptions were made: the first was that no fluorous solvent partitioned in the newly formed organic phase, thus all catalyst remained in fluorous phase, and second was that reaction was taking place only in the bulk of fluorous phase, $V_f$. Thus, change in volume of the reacting mixture would be:

$$V_{fl} = V^o{}_{fl} - V_{org} \qquad \text{(Eq.5.8)}$$

with $$V^o{}_{fl} = V^o{}_{PFMC} + V^o{}_{C_8H_{16}} \qquad \text{(Eq.5.9)}$$

Initially all alkene was present in the fluorous phase. The formation of nonanal and of a second organic phase lead to some reactant being drawn in the newly formed phase. The amount of alkene being present in the organic phase was calculated through partition coefficient, $G$, Equation 5.1. According to phase equilibrium experiments, partition coefficient $G$ was expressed as a second order polynomial function of conversion of 1 – octene, Figure 5.4.

$$G = A{x_{C_8H_{16}}}^2 + Bx_{C_8H_{16}} \qquad \text{(Eq.5.10)}$$

where, $A$= -0.0009068259 and $B$=0.1514387874.

Knowing the distribution of reactant in the two phases, thus the change in volume and concentration of the two phases, the developed algorithm was:

- At time $t$=0, initial number of moles of alkene, $N^o{}_{C_8H_{16}}$, and fluorous solvent, $N^o{}_{PFMC}$, were present in one liquid phase and Equation 5.6 was applied, while initial number of moles of nonanal, $N^o{}_{C_9H_{18}O}$, was zero.

- At time t= 0+dt, the moles of alkene present in the system were the initial moles minus those that have reacted for the production of nonanal

$$N_{C_8H_{16},0+dt} = N^o{}_{C_8H_{16}} - k \cdot N^o{}_{C_8H_{16}} \cdot \Delta t \qquad \text{(Eq.5.11)}$$

produced nonanal was

$$N_{C_9H_{86}O,0+dt} = k \cdot N_{C_8H_{16},0+dt} \cdot \Delta t \qquad \text{(Eq.5.12)}$$

and conversion

$$x_{C_8H_{16},0+dt} = \frac{N_{C_9H_{86}O,0+dt}}{N^o{}_{C_8H_{16}}} \qquad \text{(Eq.5.13)}$$

According to the definition of partition coefficient some alkene remained in the fluorous phase, while the rest partitioned in the organic phase

$$G_{C_8H_{16},0+dt} = \frac{N_{C_8H_{16},org,0+dt}}{N_{C_8H_{16},fl,0+dt}} \qquad \text{(Eq.5.14)}$$

Furthermore, conservation of moles for the liquid reactants was

$$N^o{}_{C_8H_{16}} = N_{C_8H_{16},fl,0+dt} + N_{C_8H_{16}.org,0+dt} + N_{C_9H_{86}O,0+dt} \qquad \text{(Eq.5.15)}$$

Combining Equations 5.14 and 5.15 the amount of octene in each phase was calculated

$$N_{C_8H_{16},fl,0+dt} = \frac{N^o{}_{C_8H_{16}} - N_{C_9H_{18}O,0+dt}}{1+G_{C_8H_{16},0+dt}} \qquad \text{(Eq.5.16)}$$

and

$$N_{C_8H_{16},org,0+dt} = \frac{G_{0+dt}}{1+G_{0+dt}}(N^o{}_{C_8H_{16}} - N_{C_9H_{18}O,0+dt}) \qquad \text{(Eq.5.17)}$$

As the volume of fluorous phase decreased with the production of nonanal due to partition of the alkene in both phases, the concentration of the catalyst increased, thus causing an increase in reaction rate constant, *k*, which for the next time interval *dt* would be:

$$k_{0+dt} = k_0 \frac{V_{fl,0}}{V_{fl,0+dt}} \qquad \text{(Eq.5.18)}$$

- At time, t = t + dt, the remaining alkene in the system was:

$$N_{C_9H_{86}O,t+dt} = N_{C_9H_{86}O,t} - k \cdot N_{C_8H_{16},fl,t} \cdot \Delta t \qquad \text{(Eq.5.19)}$$

where, it should be noted that only alkene present in the fluorous phase reacted for the production of nonanal

$$N_{C_9H_{86}O,t+dt} = k \cdot N_{C_8H_{16},fl,t} \cdot \Delta t + N_{C_9H_{18}O,t} \qquad \text{(Eq.5.20)}$$

Total conversion was

$$x_{C_8H_{16},t+dt} = \frac{N_{C_9H_{86}O,t+dt}}{N^o{}_{C_8H_{16}}} \qquad \text{(Eq.5.21)}$$

and for this conversion level, using Equation 5.10 for calculation of $G$, the number of moles of alkene present in each phase were

$$N_{C_8H_{16},fl,t+dt} = \frac{N^o{}_{C_8H_{16}} - N_{C_9H_{18}O,t+dt}}{1+G_{C_8H_{16},t+dt}} \qquad \text{(Eq.5.22)}$$

$$N_{C_8H_{16},org,t+dt} = \frac{G_{t+dt}}{1+G_{t+dt}}(N^o{}_{C_8H_{16}} - N_{C_9H_{18}O,t+dt}) \qquad \text{(Eq.5.23)}$$

The new reaction rate constant was calculate as

$$k_{t+dt} = k_t \frac{V_{fl,t}}{V_{fl,t+dt}} \qquad \text{(Eq.5.24)}$$

The above described equations were used for development of an algorithm on an Excel file. The time interval, $\Delta t$, used for integration was 5 sec, the same as the recording of pressure of the ballast vessel in the autoclave experiment.

### *5.4.4 Results*

The effect of distribution of the reacting olefin on reaction kinetics was studied for three different values of rate constant: 0.001 $s^{-1}$, 0.005 $s^{-1}$, and 0.01 $s^{-1}$, covering reaction times of 25 min to 4h. Kinetics of an ideal first order reaction, model 1, occurring in a homogeneous system was used to compare the divergence of the developed model, model 2. In model 1 reaction rate constant does not change for the duration of the reaction.

Figure 5.6 shows the results obtained for different reaction rate constants for models 1 and 2. Graphs a) to c) show the change of reaction conversion for the three values of k, while graph d) is the plot of ln(1-x) vs. reaction time for k = 0.005 $s^{-1}$. Plots of ln(1-x) vs. time are used for estimation of the reaction rate constant from experimental results. In all cases, results from model 2 converged with those of model 1 for conversions up to 15%. As formation of the second organic phase occurred for conversions higher than 15%, the effect of partition coefficient in developed model 2 was significant for conversions higher than this value. In all different values of rate constant the reaction time for complete conversion (99.99%) in model 2 was 4.4 times the reaction time of model 1. Thus, for a first order reaction, formation of a second phase containing products and the biggest portion of reactant (the absolute amount of reactant in organic phase could be up to 6 times the amount of reactant in fluorous phase, Figure 5.5), caused a dramatic increase in the reaction time. As expected, increase of reaction rate constant from 0.001 $s^{-1}$ to 0.005 $s^{-1}$ to 0.01 $s^{-1}$ decreased the reaction time for complete conversion by a factor of 5 and 2 respectively, both in models 1 and 2.

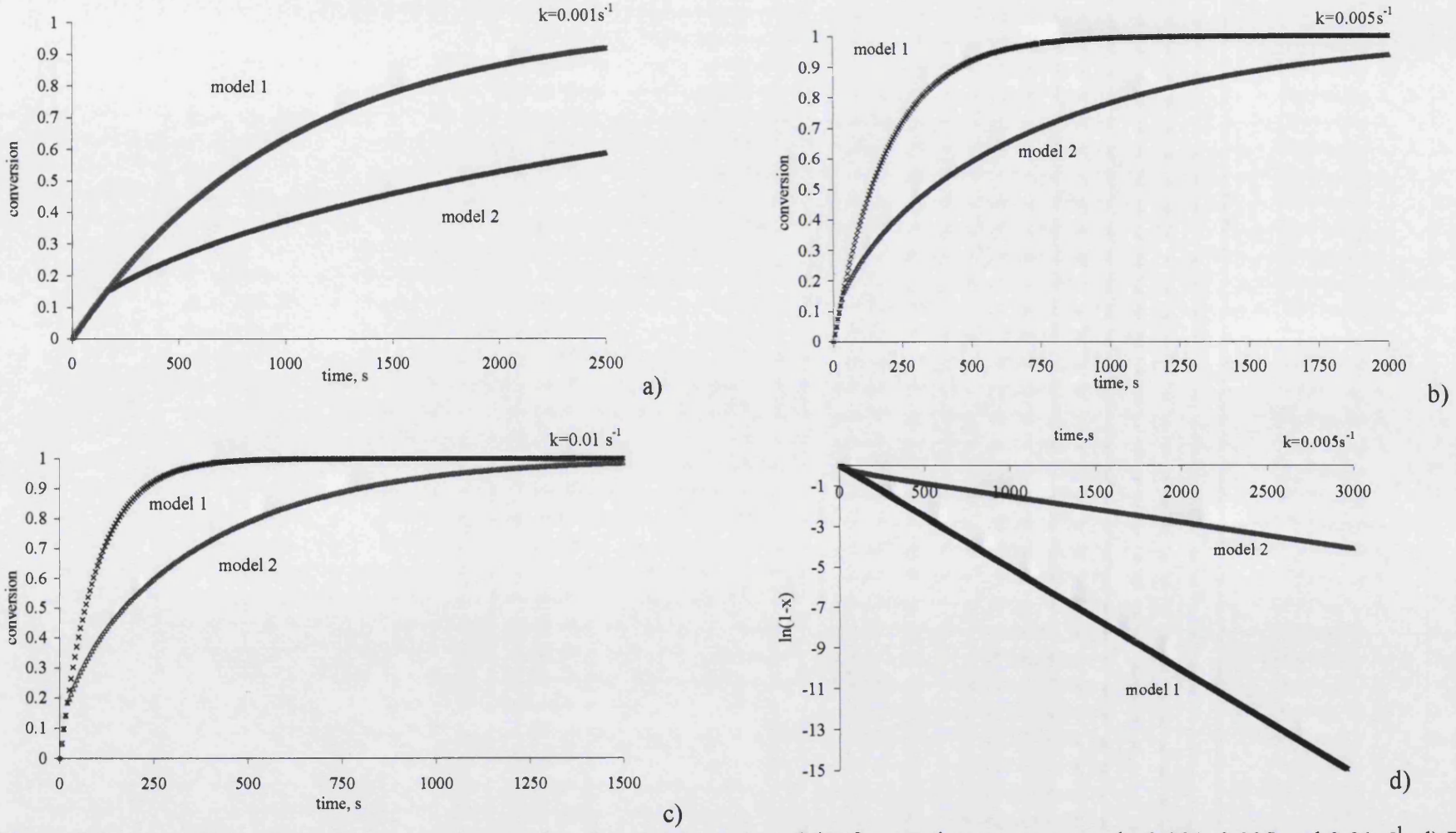


**Figure 5.6:** a) – c) Plots of reaction conversion vs. time for model 1 and model 2 for reaction rate constant k=0.001, 0.005 and 0.01 $s^{-1}$; d) Plot of ln(1-x) vs. time for k=0.005 $s^{-1}$.

In order to compare the results of models 1 and 2 with experimental results, we estimated the reaction rate constant values for which the plots of ln(1-x) vs. reaction time of model 1 and model 2 best converged with that of the experimental values. Model 1 best fitting was for k = $0.0025s^{-1}$, while best convergence of model 2 was achieved for k= $0.007s^{-1}$.

Comparing the results obtained from models 1 and 2 with experimental data, Figure 5.7, it is evident that the experimental reaction kinetics did not describe a standard first order reaction happening in a batch reactor. Model 1 was in good agreement for conversion levels up to 0.6, but deviated considerably from experimental results for higher conversion levels, where the effect of formation of the second phase was stronger. Model 2 was in better agreement with experimental values for higher conversion levels as it took into account the partition of reactant in between

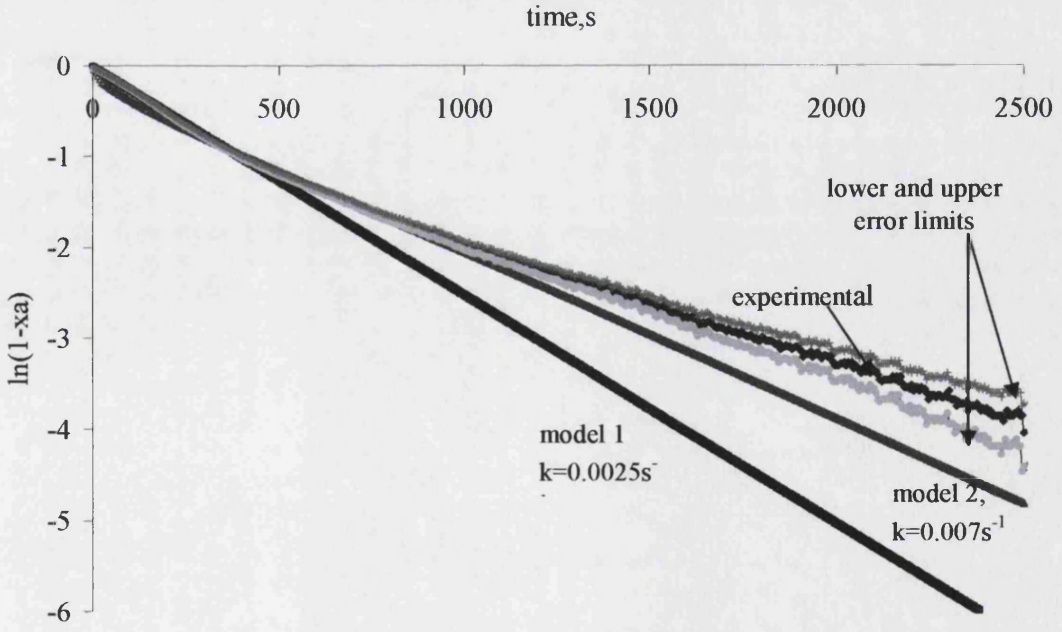


**Figure 5.7:** Plot of ln(1-x) vs. reaction time of model 1 (k = 0.0025 $s^{-1}$), model 2 (k = 0.007 $s^{-1}$) and experimental data. The experimental data are plotted together with the lower and upper error limits.

the two phases. What was surprising was the somewhat high value of conversion (0.6) up to which model 1 converged with the experimental results. According to our observations in phase separation experiments, a second phase was formed at 0.15 conversion level, thus divergence of the experimental values was expected to happen around this value of conversion. Nevertheless, reaction was taking place in a pressurised, rapidly stirred autoclave, where the two phases were well dispersed one into the other, thus formation of the second phase started obviously to affect conversion at longer times.

Divergence of model 2 from the experimental values for conversion levels lower than 0.5 was also surprising. However, no chemical parameters, i.e. saturation kinetics observed for hydroformylation reactions happening under fluorous biphasic conditions at low Rh/P ratios [Horvath *et al.*, 1998; Foster *et al.*, 2002, b], were taken into account when the model was developed.

Model 2 is a very simple model studying the effect of only one parameter, that of phase separation at reaction temperature with increasing conversion. Divergence of the model from experimental values could be attributed to the simple approach made according to which all catalyst remained in the fluorous phase, thus reaction happened only in this phase. Nonetheless, it became evident that formation of a second phase and partition of the reactant in between two phases during reaction did affect the reaction kinetics.

# Chapter 6:

# Separation Experiments Using the Continuous Experimental Set-Up

## 6.1 INTRODUCTION

As phase equilibrium experiments verified the separation principle of the studied system in batch mode, the need to study the separation efficiency under continuous flow mode was generated. In order to investigate that effect, separation experiments using the developed continuous system were performed in the absence of any catalyst. These experiments provided useful information on the operation of the continuous system and confirmed the separation efficiency of the designed gravity settler. Results of these experiments are studied in this chapter.

## 6.2 EXPERIMENTAL PROCEDURE

In a typical separation experiment on the continuous set – up, a mixture of PFMC, 1 – octene and nonanal (1:1 volume ratio of organics:fluorous) was prepared and

injected into the reactor. The system was then sealed and heated with rapid stirring (1000 rpm) to 70 °C. CO and $H_2$ were added slowly to the reactor to the desired pressure of 10 bar. The mixture in the reactor was left to equilibrate for 30 min before the reactor outlet valve was opened and liquid started entering the separator. At the same time the pumps started to deliver new fluorous and organic liquids into the reactor. As soon as the separator was filled with liquids and the organic phase started to overflow, the fluorous phase was recycled to the reactor in place of the fresh fluorous solvent. The system was run continuously with the two phases in the separator being sampled every 30 min for a total duration of 2.5 h. The same procedure was followed in experimental runs with increased reactor pressure of 15 and 20 bar. Samples were analysed by GCMS as previously described.

In order to ensure that samples from different phases did not contaminate each other, fluorous layer samples were taken from the bottom of the phase, while product layer samples were taken from the top of the organic phases, using different syringes.

All experiments were performed in the absence of any catalyst or fluorous ligand, while conversion level was simulated by using organic mixtures of 1 – octene and nonanal of different molar composition – the mole fraction of nonanal in the mixture simulated the conversion level of the reaction. Five different organic mixtures of 1 – octene and nonanal were prepared:

1. 100% mole 1 – octene; simulated conversion 0%,
2. 60% mole 1 – octene; simulated conversion 40%,
3. 40% mole 1 – octene; simulated conversion 60%,
4. 20% mole 1 – octene; simulated conversion 80%,
5. 100% mole nonanal; simulated conversion 100%

and used at the continuous separation experiments.

## 6.3 RESULTS AND DISCUSSION

### *6.3.1 Efficiency of the separation principle*

During these experimental runs and after the system had reached a steady state, the fluorous phase was recycled to the reactor, photographs of the two phases in the separator were taken which gave useful information about the separation process. As shown in Figure 6.1, the liquid entering the separator at steady state was already separated into two phases, the top organic and the bottom fluorous phase. Drops of organic phase appeared distinct in the bulk of fluorous phase in the transparent tube at the inlet of the separator. As soon as these drops entered the separator they quickly ascended and were added to the organic phase, Figure 6.2. Any fluorous solvent that had been dragged to the top layer, due to motion of the drop, quickly coagulated to drops that fell back to the bottom layer, Figure 6.3. In Figure 6.4 the system was highly disrupted. Because of malfunction of the liquid flow control there was too high flow of liquids and gases in the separator causing the agitation observed. Nevertheless, looking closely at the separator, at the side of overflow and recycling outlets, the two liquid phases were well separated and the interface was unaffected. Thus, not only separation was fast, but also the design of separator was appropriate for this system.

In all photographs of the separator at steady state the organic phase was clear while the fluorous phase was haze. This haziness was caused by fine droplets of organic phase in the fluorous. It was always observed during experiment and it cleared up about 15 min after inlet flow in the separator was stopped. The total amount of organic droplets causing haziness was too small and it did not affect the

separation process. Samples of fluorous and organic phase, taken both when the phase was haze and after it cleared up, produced the same results. As the system was not agitated it is believed that this haziness was caused by late nucleation of the organic phase in the fluorous phase in accordance to what has been observed by Ullmann and co-workers (Ullmann *et al.*, 1995) during phase transition extraction of partially immiscible mixtures.

The organic phase used when photographs were taken was pure nonanal. Similar observations were made when different conversion levels were studied.

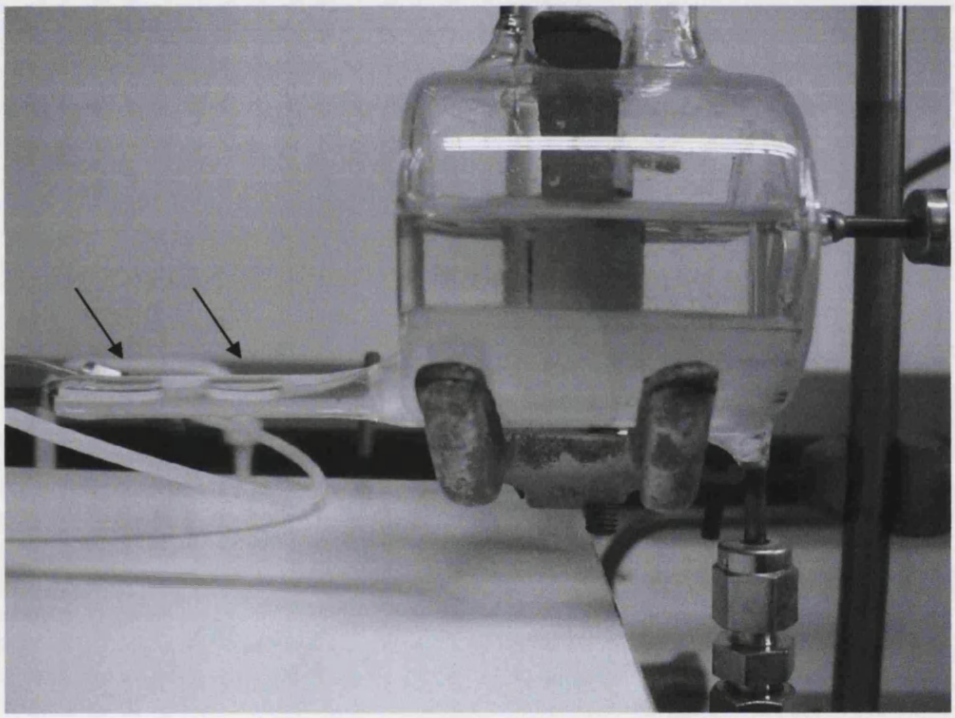

**Figure 6.1:** Separator at steady state. Arrows point at separated drops of organic phase moving in the bulk of fluorous phase.

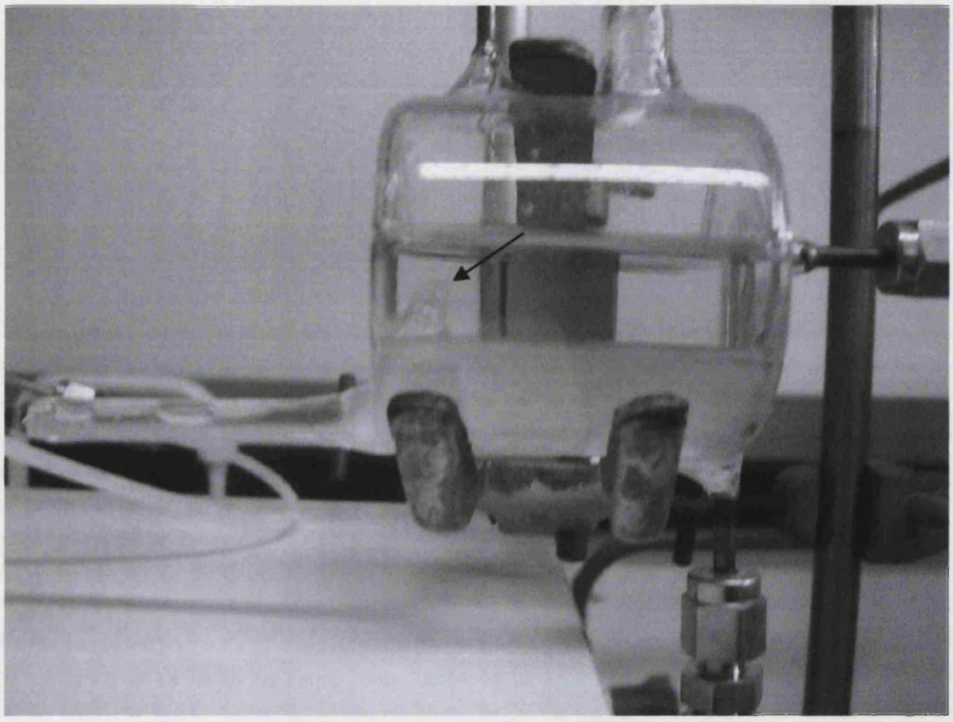

**Figure 6.2:** Ascending of organic phase in the separator. Arrow points at a drop of nonanal entering the separator and ascending to the organic phase.

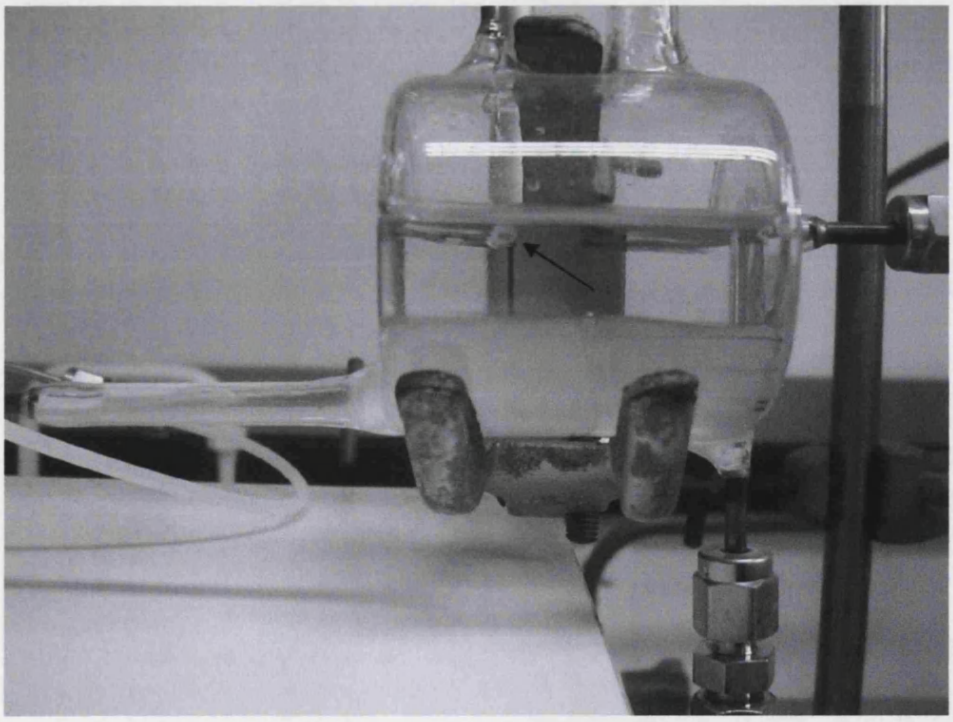

**Figure 6.3:** Descending of fluorous phase in the separator. Arrow points at a drop of fluorous phase ready to fall back at bottom of the separator.

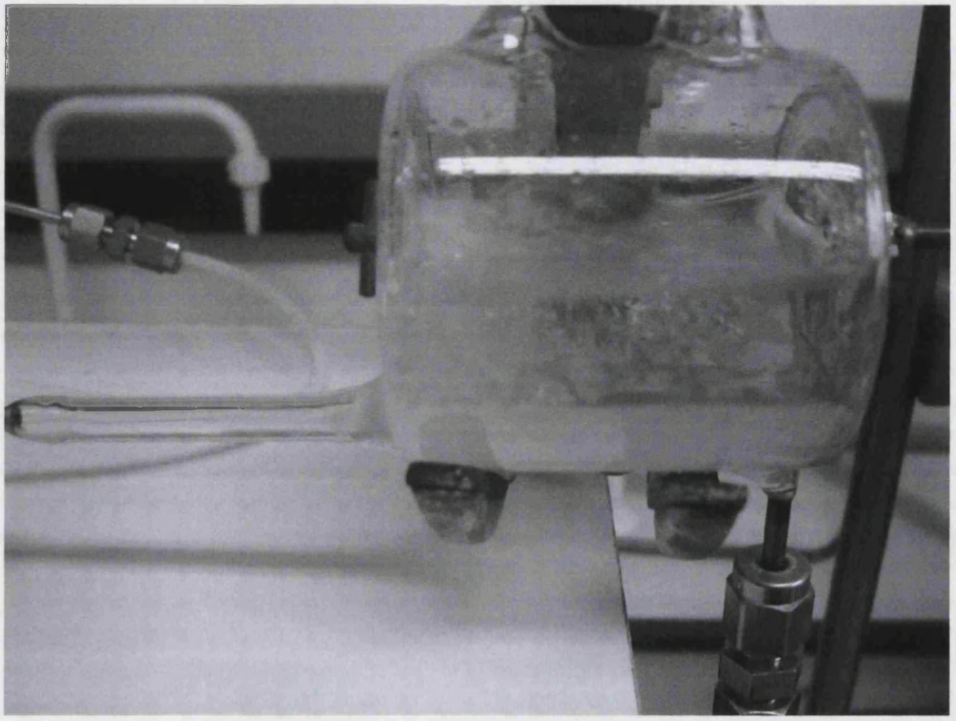

**Figure 6.4:** System under high flow conditions.

### *6.3.2 Effect of reactor pressure*

Figures 6.5 and 6.6 show the composition of the fluorous and the organic phase respectively. Each column corresponds to different conditions (different conversion level and different reactor pressure) with vertical lines in between the columns grouping conversion levels. Comparing results for the same composition of organic feed and for the three reactor pressures it is obvious that reactor pressure had no effect on the separation process. This was expected since separation was carried out at the same temperature and pressure for all feed mixtures and reactor pressures, achieving the same equilibrium values. Small deviations in the values were due to experimental scatter in the GC analysis.

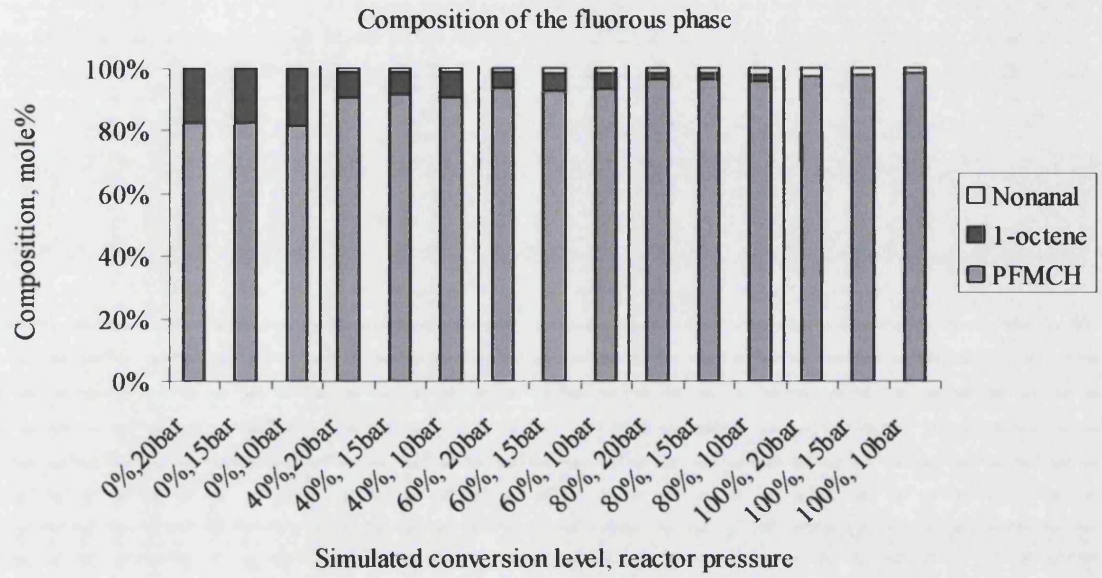


**Figure 6.5:** Composition of the fluorous phase, effect of reactor pressure.

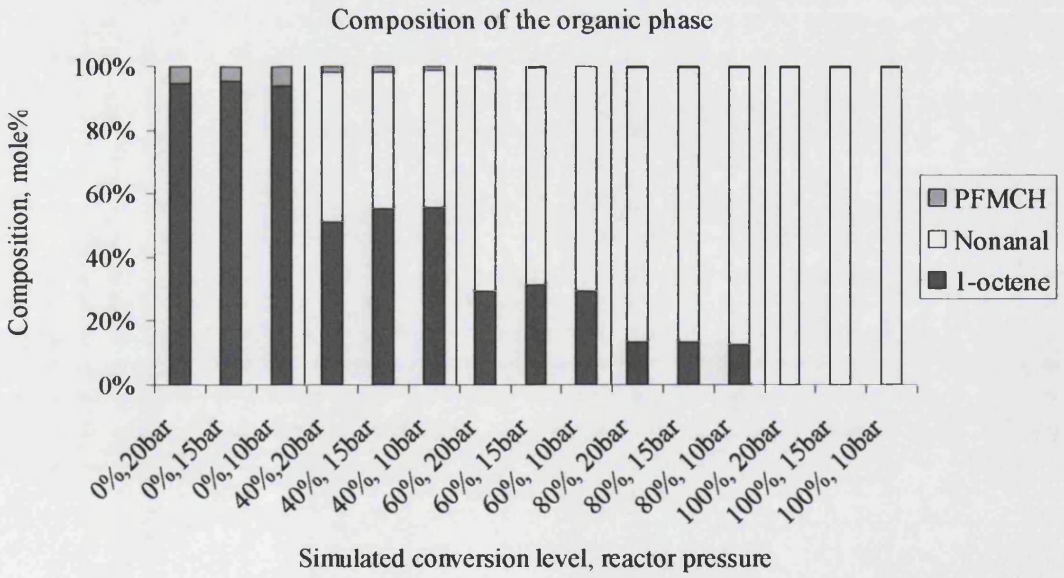


**Figure 6.6:** Composition of the organic phase, effect of reactor pressure.

### *6.3.3 Composition of the fluorous and organic phase at equilibrium in the separator*

Tables 6.1 and 6.2 list the composition of the fluorous and the organic phases, respectively. The values presented are the averaged values of the three pressures. Composition is expressed in mol%. Examining the composition of fluorous phase, we note that 17.3 mol% of pure 1 – octene partitioned in the fluorous phase, while only 2 mol% of pure nonanal partitioned in the same phase under the same conditions. As the simulated conversion level increased from 40% to 60% to 80%, the total amount of organics in the fluorous phase decreased from 8.7 to 6.3 to 4 mol%.

**Table 6.1:** Composition of fluorous phase, in mol%.

| *Simulate conversion level* | *0%* | *40%* | *60%* | *80%* | *100%* |
|---|---|---|---|---|---|
| PFMC, mol% | 82.7 | 91.3 | 93.7 | 96 | 98 |
| 1 – octene, mol% | 17.3 | 7.7 | 5 | 2 | - |
| nonanal, mol% | - | 1.0 | 1.3 | 2 | 2 |

Similar behaviour was observed in organic phase composition. When pure 1 – octene was fed in the system, 5.3 mol% of PFMC was found in the organic phase, while for pure nonanal it dropped to less than 1%. Again, an increase in conversion level resulted in less leaching of the fluorous solvent in the organics. It is important to keep this leaching to minimum since not only would the fluorous solvent be removed continuously from the system, but the fluorous solvent would also carry the expensive modified Rh catalyst out of the system. Thus, it is desirable to keep conversion level at a maximum.

**Table 6.2:** Composition of organic phase, in mol%.

| *Simulate conversion level* | *0%* | *40%* | *60%* | *80%* | *100%* |
|---|---|---|---|---|---|
| PFMC, mol% | 5.3 | 1.3 | 0.5 | 0.3 | 0.2 |
| 1 – octene, mol% | 95.7 | 53.7 | 30 | 13.3 | - |
| nonanal, mol% | - | 45 | 69.5 | 86.4 | 99.8 |

Comparing the results of the continuous run with equilibrium values, Tables 5.1 and 5.2, we see that composition of the fluorous phase was in good agreement with the equilibrium experiments. Thus, equilibrium conditions were achieved in the separator. Nevertheless, composition of the organic phase in continuous runs seemed to contain less fluorous solvent than the equilibrium values. This is not as paradox as it might seem. The separator, in contrast to the graduated cylinder, was an open system with large quantities of CO and $H_2$ flowing through both phases. Moreover, a constant Ar stream flowed over the top of organic phase causing to some extent vaporisation of its components. As PFMC is much more volatile than 1 – octene and nonanal, it evaporated more, resulting in concentrations lower than the equilibrium values[a].

In order to investigate this further, the gas phase being vented from the separator was collected for some time during one of the reaction experiments using a dry ice trap. The gases were liquefied and two distinct phases were formed, with the volume of the bottom fluorous rich phase being three times as large as volume of organic phase.

Moreover, in order to examine the effect of catalyst and modifying ligand present in the reaction on the separation efficiency of the system, during one of the reaction experiments samples were taken and analysed from both the fluorous and the organic

[a] Vapour pressure of PFMC, 1 – octene and nonanal at room temperature, 25 °C, is 141 mbar, 23.2 mbar and 0.75 mbar respectively.

phases. Conversion for this sample was 50% and the composition of each phase is shown in Table 6.3.

**Table 6.3:** Composition of fluorous and organic phases in separator during a reaction experiment. Effect of the presence of catalyst and fluorous ligand on separation efficiency at 50% conversion[b].

| | *Composition of the fluorous phase* | *Composition of the organic phase* |
|---|---|---|
| PFMC, mol% | 93.55 | 2.87 |
| 1 – octene, mol%[c] | 5.17 | 48.87 |
| nonanal, mol%[d] | 1.29 | 48.26 |

Comparing these results with composition of the two phases, both from phase equilibrium experiments and continuous separation experiments, we see that they are well compared, see also Figure 6.7. Thus, it is proved that the presence of catalyst and/or fluorous ligand did not affect the separation efficiency of the system.

The results listed in Tables 5.1 and 5.2 can be used to form the phase diagram for the PFMC + 1 – octene + nonanal ternary mixture at 300K, Figure 6.7. The system exhibits type II phase behaviour [Sorensen, 1979], having two pairs of partially miscible solvents ( PFMC + 1-octene and PFMC + nonanal ) and one pair of completely miscible solvents (1 – octene + nonanal), over the temperature investigated. Equilibrium values are those represented by open squares, while points represented by filled squares are composition of the fluorous and organic phase from the continuous runs.

[b] The conversion was calculated from the GCMS report.
[c] 1 – octene includes the amount of unreacted 1 – octene plus the isomers formed during the reaction.
[d] nonanal includes the linear and branched aldehydes formed during the reaction.

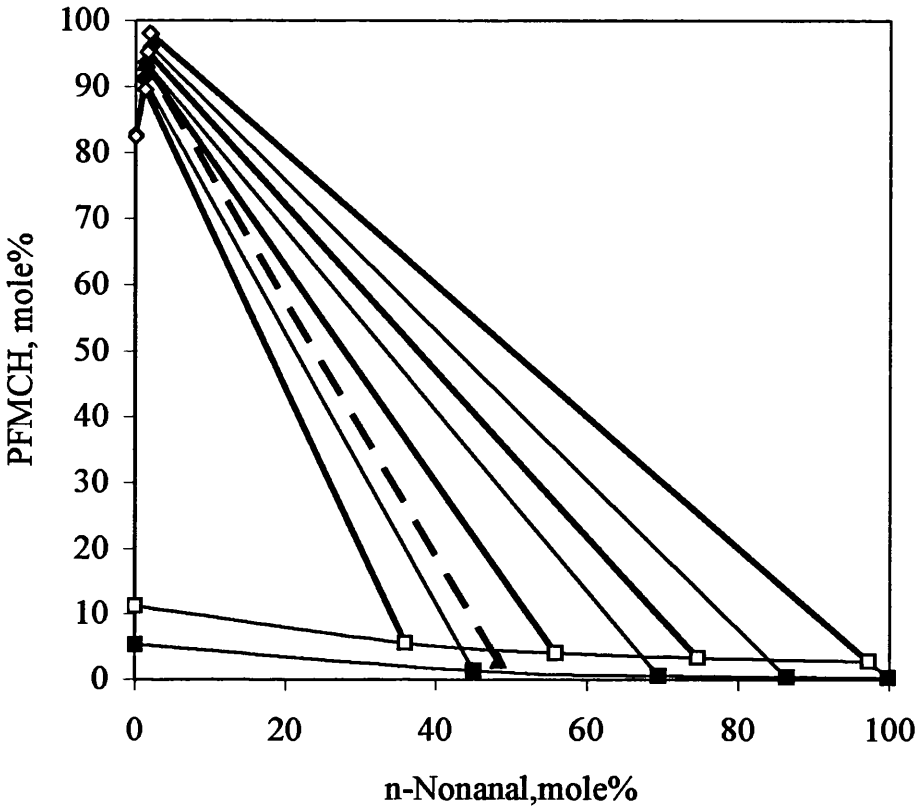


**Figure 6.7:** Right triangle three – component phase diagram for the system PFMC + 1 – octene + nonanal, at 27 °C and atmospheric pressure (□: organic phase at equilibrium, ◊: fluorous phase at equilibrium, ■: organic phase at continuous experiments, ♦: fluorous phase at continuous experiments, —▲—: continuous flow under reaction conditions).

## 6.4 CONCLUSIONS

Overall, we conclude that:

- Initial tests in the absence of chemical reaction verified the efficient separation of the system. The two well distinct phases settled quickly in the separator. The organic phase ascended through the fluorous phase creating a top organic – rich phase

while the fluorous phase descended through the organic phase creating a bottom fluorous – rich phase.

- Partition of nonanal in the fluorous phase and of PFMC in the organic phase was kept at low levels provided that conversion was high (60%). With reference to the simulated conversion levels, the higher the conversion (more polar products present in the organic phase) the less the leaching of the expensive fluorous solvent in the product phase.
- The reactor pressure had no effect on the efficiency of separation.
- The composition of both phases in the separator reached equilibrium values. However, a method should be developed to recover the fluorous solvent from the exhaust gas stream.

# Chapter 7:

# Reaction Experiments

## 7.1 INTRODUCTION

In this section we describe the results obtained for the hydroformylation reaction of 1 – octene using the continuous flow apparatus. The amount of information upon the effect of flow on the fluorous biphasic reacting system that can be gleaned in a short time from such a system is significant. Engineering factors, such as stirrer type, as well as, chemical factors, such as ligand oxidation, affect the productivity of the system and are discussed in detail in the following paragraphs.

As it has been reported earlier, during hydroformylation of 1 – octene under fluorous biphasic conditions using $Rh(acac)(CO)_2$ as catalyst precursor and $P(\text{-}C_6H_4\text{-}4\text{-}C_6F_{13})_3$ as modifying ligand the only products formed are *n* – nonanal, *iso* – nonanal and *cis*- and *trans*- 2 – octene [Foster *et al.*, 2002, b]. Thus, the following equations can be written:

$$S_{aldehydes} = y_{n-nonanal} + y_{iso-nonanal} \qquad \text{(Eq.7.1)}$$

$$S_{2-octene} = y_{2-octene} \quad \text{(Eq.7.2)}$$

$$l:b = \frac{y_{n-nonanal}}{y_{iso-nonanal}} \quad \text{(Eq.7.3)}$$

and $$S_{\text{int}\,rinsic} = \frac{y_{n-nonanal}}{y_{iso-nonanal} + y_{2-octene}} \quad \text{(Eq.7.4)}$$

where, $S_{aldehydes}$ and $S_{2-octene}$ is the selectivity to aldehydes and to isomerised octenes respectively and $y_i$ is the mole fraction of component *i* in the analysed sample. The linear to branch ratio, $l:b$, is an indication of reaction selectivity to the linear over the branched product, while the intrinsic selectivity, $S_{intrinsic}$, is an indication of the overall reaction selectivity to the linear aldehyde.

Morover, the TurnOver Number, TON, and TurnOver Frequency, TOF, reported are calculated according to the following equations:

$$TON = \frac{(total\ moles\ of\ substrate\ used) \times (conversion\ to\ aldehydes)}{(total\ moles\ of\ catalyst\ used)} \quad \text{(Eq.7.5)}$$

$$TOF = \frac{TON}{(total\ duration\ of\ the\ experiment)} \quad \text{(Eq.7.6)}$$

According to Equation 7.6 the TOF reported is the average value for the experiment. TON expresses the productivity of the catalyst, i.e how active the catalyst is, while the TOF expresses how quick is the reaction under used conditions.

The performed experiments could be categorised as following:

i. Preliminary experiments, which only lasted for a few hours

ii. Experiments which had to be stopped due to equipment malfunction while there was still catalyst activity. These experiments lasted for longer times and some useful information could be obtained for the further improvement of the system.

iii. Experiments which were stopped only after the catalyst activity was lost. These long experiments lasted for more than 20 h and since they showed the full effect of the flow on the reactivity of the system they are discussed in great detail.

## 7.2 EXPERIMENTAL PROCEDURE

In a typical reaction experiment the fluorous solution containing the fluorous modified rhodium catalyst and 1 – octene (1:1 volume ratio of organics:fluorous) were pumped rapidly into the degassed reactor up to a volume of 60 ml. The pumping was then stopped and the system was heated with rapid stirring (1000 rpm) to 70 °C. CO and $H_2$ were then added slowly into the reactor to a pressure of 20 or 15 bar. The homogeneous mixture in the reactor was left to react in batch mode for 60 min or 120 min before the reactor outlet valve was opened. The reaction was first run in batch mode to ensure that the organic phase was as polar as possible, since catalyst leaching is known to be higher at low conversion. As soon as the liquid mixture started entering the separator, the reactor outlet valve and the gas feed valve were closed and the stirring was stopped. Simultaneously, the pumps were started, feeding liquids in the reactor at high flow rates to compensate for the dead volume of liquids in the heat exchanger and the tubing connections from the reactor to the separator. When the pressure in the reactor was again at the desired level, the pumps were stopped and the system was left to react for another 60 or 120 min. Then, the reactor outlet valve was

Table 7.1: Experimental conditions of hydroformylation of 1 – octene using the continuous apparatus.

| | $Rh(acac)(CO)_2$ gr[a] | $P(-C_6H_4-4-C_6F_{13})_3$, gr | [Rh], $mmoledm^{-3}$[b] | [P], $mmoldm^{-3}$ | Rh:P | T,°C | P, bar | Stirrer type | Duration, hr[c] |
|---|---|---|---|---|---|---|---|---|---|
| 1 | 0.0775 | 3.6504 | 1 | 10 | 1:10 | 70 | 20 | Simple | 9 |
| 2 | 0.1549 | 7.2984 | 2 | 20 | 1:10 | 70 | 15 | Simple | 3.5 |
| 3 | 0.1552 | 3.6494 | 2 | 10 | 1:5 | 70 | 15 | Simple | 5 |
| 4 | 0.0843 | 3.676 | 1 | 10 | 1:10 | 70 | 15 | Simple | 14 |
| 5 | 0.1549 | 3.5825 | 2 | 10 | 1:5 | 70 | 15 | Simple | 12 |
| 6 | 0.0773 | 3.6489 | 1 | 10 | 1:10 | 70 | 15 | Simple | 18.5 |
| 7 | 0.1546 | 3.7191 | 2 | 10 | 1:5 | 70 | 15 | Simple | 30 |
| 8 | 0.1551 | 3.6494 | 2 | 10 | 1:5 | 70 | 15 | Spurger | 45.5 |

[a] Catalyst and the fluorous ligand are dissolve in 150 ml of PFMC
[b] This is the concentration in the total reaction mixture, half of the concentration in the fluorous solvent
[c] Duration of continuous mode operation of the experiment

opened and at the same time the pumps started to deliver new fluorous and organic liquids into the reactor. As soon as the separator was filled and the organic phase started to overflow, the fluorous phase and consequently the catalyst were recycled to the reactor in place of the fresh fluorous mixture. The system was run continuously with the organic phase being sampled every 15 min for the first two hours and every 30 min thereafter. Table 7.1 shows the exact experimental conditions for all the reaction experiments performed.

## 7.3 RESULTS AND DISCUSSION

### *7.3.1 Preliminary experiments*

The very first continuous hydroformylation experiment lasted for the total of 9 h, from the time the continuous flow operation started. Initially for 60 min the reactor was operated as batch. The experiment was run over two days, 3 h 30 min the first day and 5 h 30 min in the second day. Overnight, the stirring in the reactor was stopped, the temperature was lowered and the reactor pressure was reduced to 2 bar. Thus, no reaction was taking place overnight. The results obtained during this run are shown in Figure 7.1, where the conversion to nonanals (linear and branched), the extent of isomerisation and the linear over the branched aldehydes ratio (l:b) are plotted vs. time. The first five samples were taken the first day, while the rest were taken during the second day.

Conversion to nonanals of up to 56 % was observed in the first day. This was the high conversion achieved during the batch operation of the system and was expected to decrease during the continuous operation. Indeed, conversion was much lower the

second day, starting at 21.3% and interestingly increasing up to 46%. This increase, as it will be explained in detail in the next experiments, was due to ligand leaching.

Isomerisation of 1-octene was kept at low levels, with an average value of 4.3%, the highest value reached 8%, at the beginning of the experiment. Moreover, very good linear to branched aldehydes ratios were achieved, 5.5 average value - 6.1 at the maximum and 4.1 at the minimum.

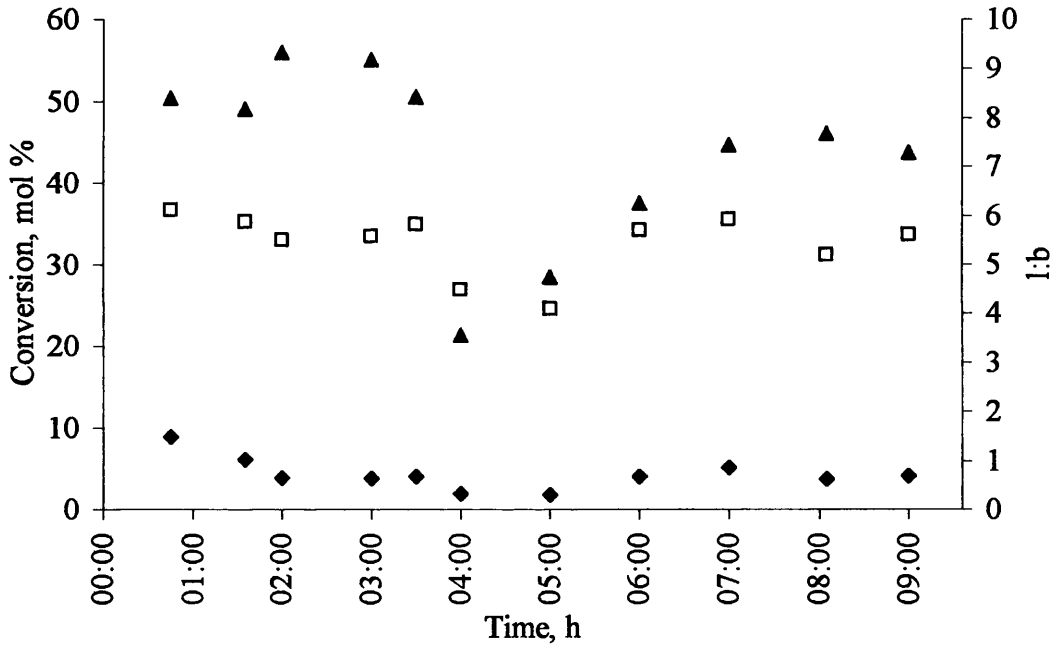


**Figure 7.1:** Results of hydroformylation experiment No.1 (▲: conversion to aldehydes, ♦: isomerised octenes □: linear to branched aldehydes ratio).

Results of the very first experiment, No. 1, were very encouraging, but they were followed by two unsuccessful experiments, No.2 and No.3, the results of which are shown in Figures 7.2 and 7.3. In an attempt to increase the conversion to aldehydes, lower reactor pressures were employed, 15 bar instead of 20 bar. As the flow of the liquid stream coming out of the reactor depends on the differential pressure, for

constant capillary length, higher residence times were achieved for lower reactor pressures. Moreover, double the catalyst concentration was used for both experiments, while the Rh:P was 10 and 5 in experiments No.2 and No.3, respectively.

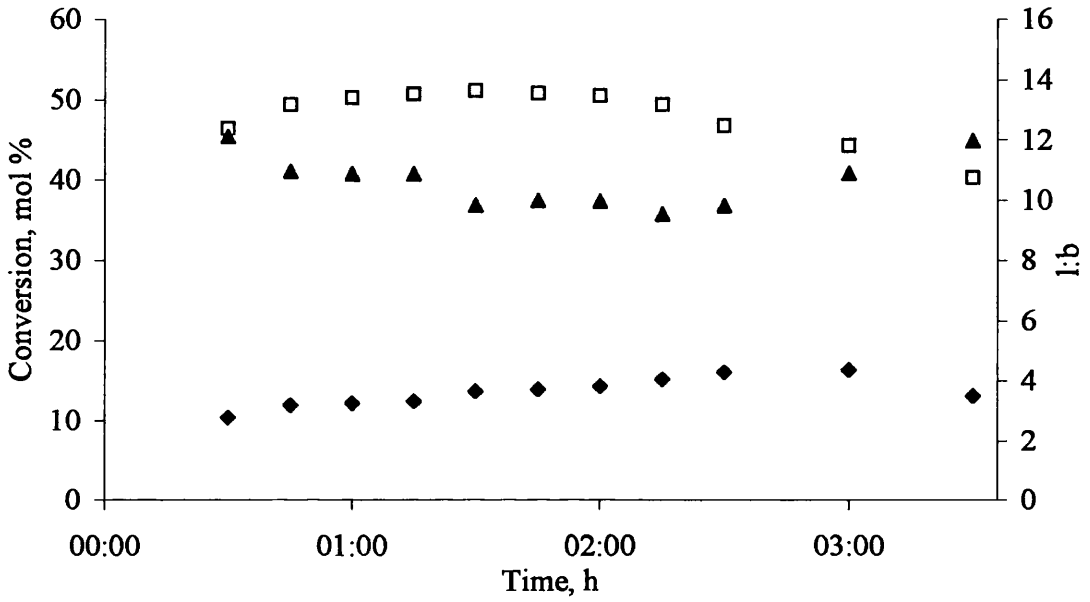


**Figure 7.2:** Results of hydroformylation experiment No.2 (▲: conversion to aldehydes, ♦: isomerised octenes, □: linear to branched aldehydes ratio).

In experiment No.2, Figure 7.2, initial conversion of 45% was achieved which decreased to 35%, transition from batch mode to continuous steady state, and then started increasing again to 45% as the fluorous ligand started leaching in the fluorous phase. Much higher linear to branch ratios were obtained, average value of 12.8, which were accompanied by higher isomerisation, average value 10.4%. As isomerisation products and branched aldehydes are produced by the same intermediate, Figure 7.4, increased isomerisation results in the production of less branched products, giving thus higher l:b ratios. Unfortunately, the experiment had to be stopped early due to malfunction of one of the pumps.

The results of experiment No.3 were quite surprising, Figure 7.3. The conversion to aldehydes was very low, lower than 15%, even at the beginning of the experiments when the reactor was operated as batch. The increased catalyst concentration in comparison to experiment No.1 did not seem to affect the conversion. At the same time the quite low isomerisation, reaching 5% at the maximum, implied that there was an overall lower reactivity. The experiment was stopped as the conversion was too low and a sample of the fluorous phase was analysed by P NMR to see if the ligand was oxidised. The analysis however did not show that the catalyst was oxidised.

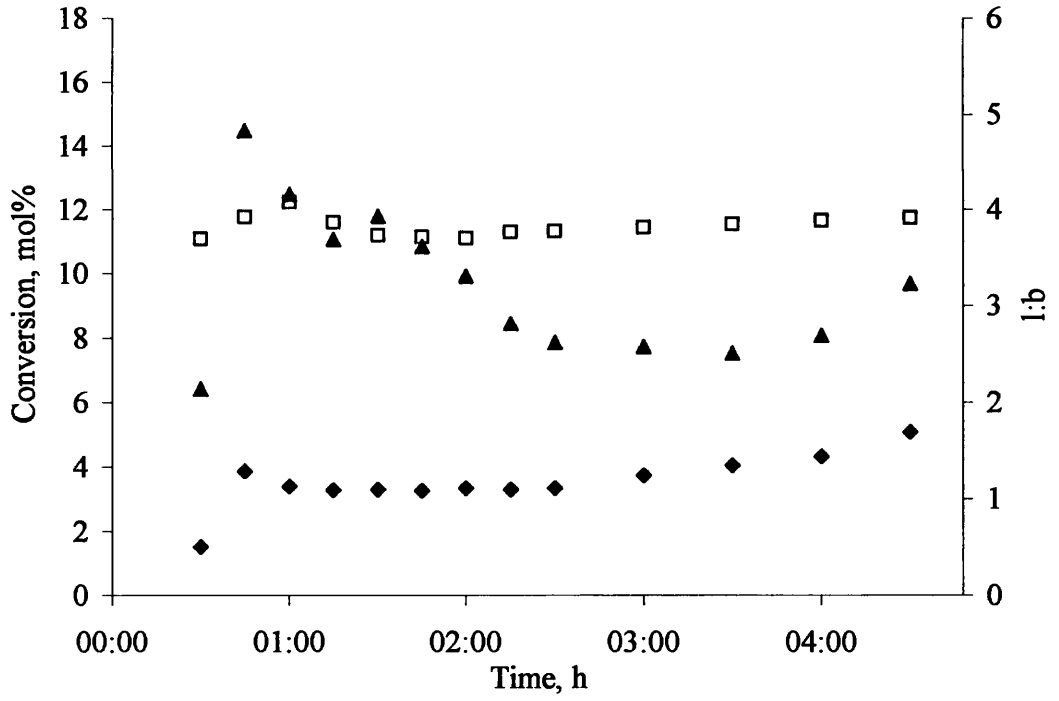


**Figure 7.3:** Results of hydroformylation experiment No.3 (▲: conversion to aldehydes, ♦: isomerised octenes □: linear to branched aldehydes ratio).

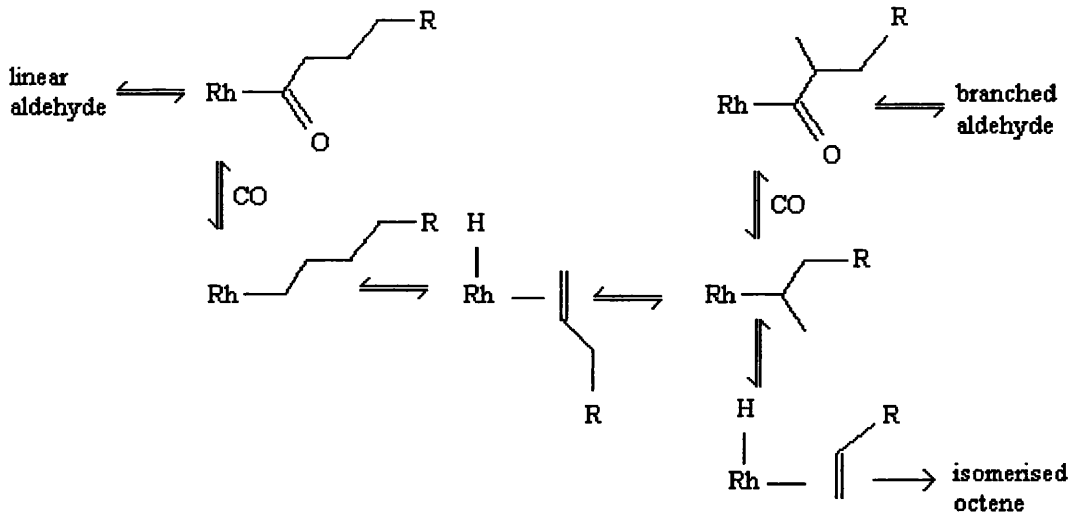


**Figure 7.4:** Catalyst intermediates during hydroformylation of 1 – octene.

### *7.3.2 Longer experiments*

Figure 7.5 shows the conversion to nonanals, the extent of isomerisation and the l:b ratio of hydroformylation experiment No.4. Many different factors contributed to the unusual shape of the conversion curve. Initially, the conversion was at high levels, around 35%. This was the conversion of the batch operation of the reactor. As the system was operated continuously, the conversion dropped and it would have reached the steady state at the conversion level of approximately 15%. Nevertheless, the conversion started to increase again, reaching the level of 55 %, as the excess of the modifying phosphine was leaching to the organic phase taken away from the system. The reaction rate is inversely proportional to the ligand concentration, but some excess of ligand is needed in order to have good l:b ratios [Divekar *et al.*, 1993; Horvath *et al.*, 1998]. The experiment had to be stopped at 8:30 h as the $CO/H_2$ gas cylinder was empty and it was continued the following day. The system did not react any further overnight, as the stirring in the reactor was stopped, and the temperature

and pressure lowered to ambient conditions. The peak in the isomerisation results at the beginning of the second day was due to the CO deficiency in the system from the previous day. As the liquid outlet stream flow rate was 1.3 ml/min and the volume of liquids between the reactor and the separator outlet was 80 ml, approximately 60 min were needed before any change in the reactor composition could be observed in the separator sample. That is why the peak was observed 60 min after the experiment started.

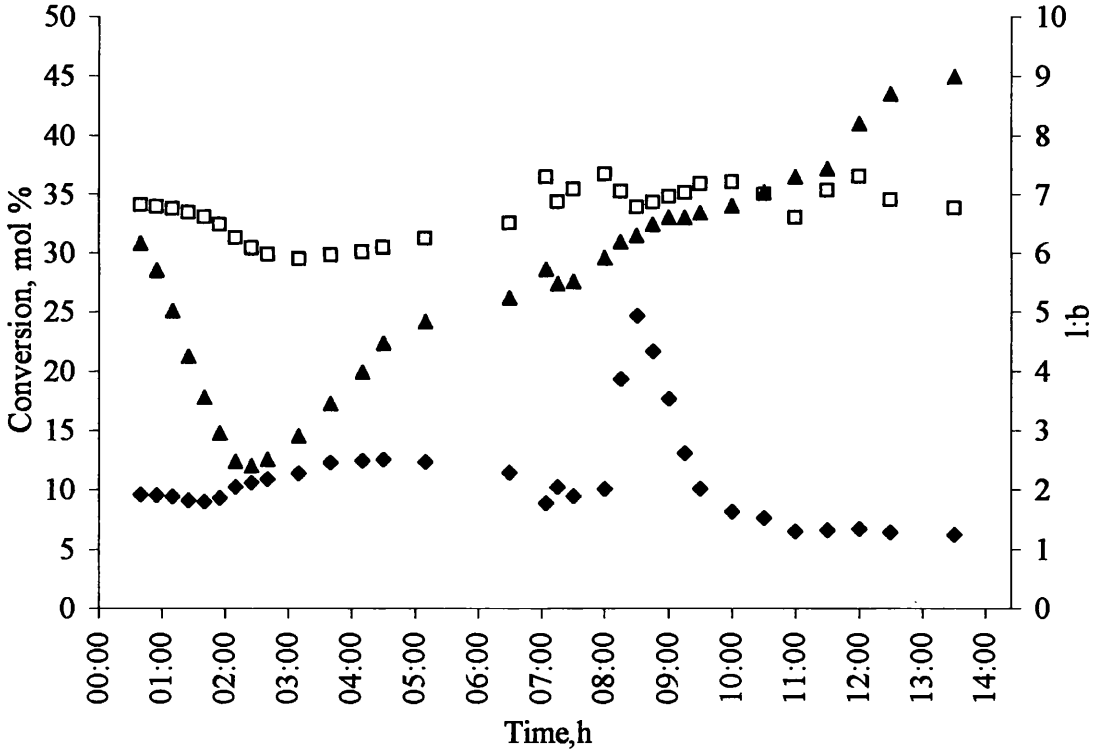


**Figure 7.5:** Results of hydroformylation experiment No.4 (▲: conversion to aldehydes, ♦: isomerised octenes, □: linear to branched aldehydes ratio).

Isomerisation was around 10%, reaching 24% at the peak and dropping to less than 6% towards the end of the experiment. The l:b ratio was almost constant during the whole experiment at the value of 6. The system looked like it had reached the steady state but the experiment had to be stopped 14:00 h after the beginning of the

continuous flow operation because there was a blockage in one of the tubing. Though the experiment was not completed, satisfactory TON of 7230 was achieved at an average rate of 452 $h^{-1}$ (TOF).

Figure 7.6 shows the conversion to nonanals, the extent of isomerisation and the l:b ratio of hydroformylation experiment No.5. Initially, the conversion corresponding to batch operation of the reactor was 58% dropping to 40% at what would be the steady state of the continuous operation of the system and then started increasing again up to 60% as the ligand was leaching to the organic phase. Comparing the achieved conversion levels in experiments No. 4 and No. 5, it is obvious that the increase in catalyst concentration from 1 mmol/l to 2 mmol/l did influence positively the reactivity of the system. The effect of the catalyst concentration was clearly indicated by the higher conversion achieved in the batch operation of the reactor, 35% in experiment No.4 and 58% in experiment No.5. The higher conversion at the continuous operation was also due to the higher residence time in experiment No.5. The flow rate of the reactor liquid stream was 1ml/min, thus the residence time was 60 min in comparison to 45 min in experiment No.4.

Initially isomerisation was about 10%, about the same level with experiment No.4 as the ligand concentration was the same [Foster *et al.*, 2002, b]. The sudden peak reaching 25% was due to problems with the $CO/H_2$ feed during the experimental run. These problems were also responsible for the second peak in the isomerisation curve at about 13%. As isomerisation and formation of the branched aldehyde are competing reactions, Figure 7.4, the l:b ratio followed the same trend with the isomerisation curve. Initial l:b ratios of 6 were achieved peaking at 14 and then at 10.8, while being around 8 towards the end of the experiment. Though the catalytic

system was active the experiment was stopped due to malfunction of one of the pumps.

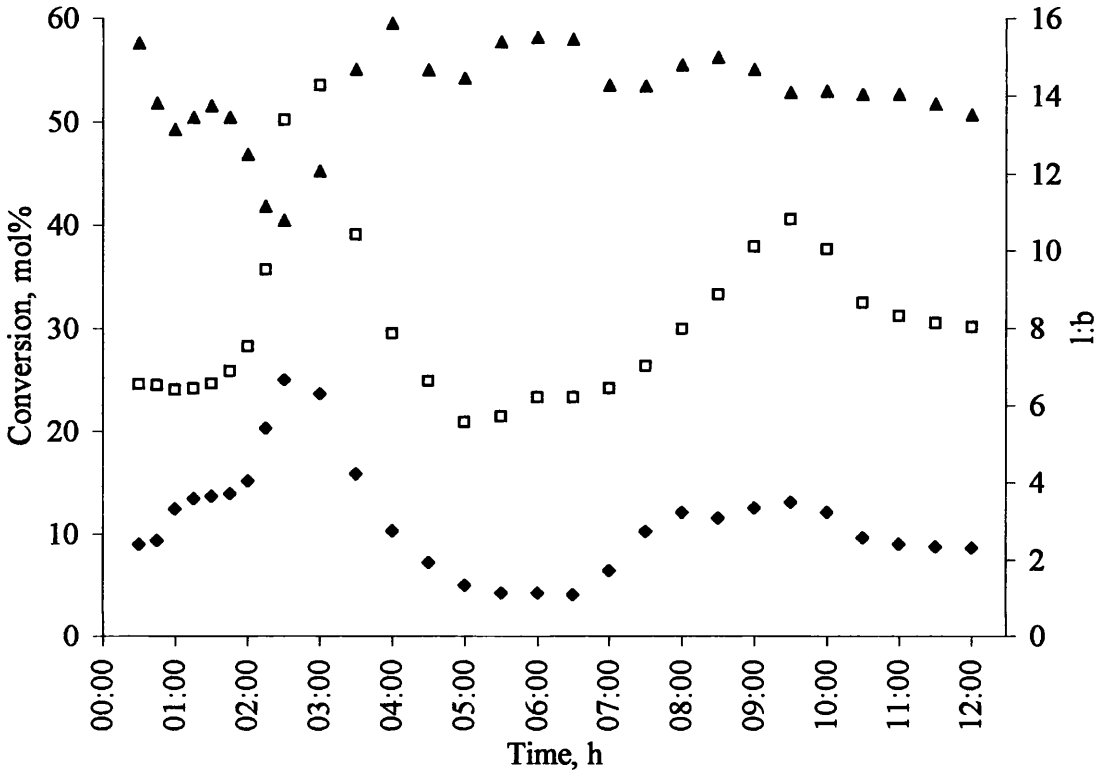


**Figure 7.6:** Results of hydroformylation experiment No.5 (▲: conversion to aldehydes, ♦: isomerised octenes, □: linear to branched aldehydes ratio).

### *7.3.3 Experiments where full catalytic activity of the system is investigated*

In the following experiments the full catalytic activity of the system was investigated allowing thus for better explanation of the effect of the different parameters. Moreover, comparison with batch experiments allowed for better understanding of the change in the catalyst activity in the continuous system.

Figure 7.7 shows the results obtained during experimental run No.6. To start the experiment, the reactor was run in batch mode for 60 min where the conversion was

*ca.* 30%, which is much lower than that obtained under optimised conditions in a simple static reactor [Foster et al, 2002, b]. This conversion dropped in continuous flow mode, which was expected since the residence time was shorter, 45 min, and it would be expected that a steady state would be reached once the composition of the separator became the same as that in the reactor. This steady state was observed after 60 min of continuous flow, but only remained for a short time (2 – 3 h) before the conversion started to rise. Although it has been reported that leaching of the catalyst (0.05%) and the phosphine (3.3%) into the organic phase is minimal in single batch reactions where the conversion is close to 100% [Foster *et al.*, 2002, b], partition studies, see Table 7.2, showed that the phosphine is more soluble in 1 – octene than in nonanal. This means that phosphine leaching is significant when the conversion is low, as in this experiment, and indeed, a white precipitate of $(4\text{-}C_6F_{13}C_6H_4)_3PO$ accumulated in the collected organic fraction as the experiment proceeded. This loss of phosphine to the organic phase accounted for the rise in conversion observed over the period 5 – 12 h after the start of the continuous flow operation, since this type of reaction is known to be negative order in phosphine concentration [van Leeuwen *et al.*, 2000]. After 15 h of continuous flow operation, the rate started to drop again. At this point, the collected organic fractions were yellow, having been colourless earlier, suggesting that the amount of phosphine lost was so great that there was insufficient to keep the rhodium as $[RhH(CO)\{P(4\text{-}C_6H_4C_6F_{13})_3\}_3]$. Spectroscopic studies suggested that this was the form present within the separator[a]. Since it contained the most fluorine, this complex would be the least soluble in the organic phase of the possible monomeric rhodium species present. Once complexes containing two or only one phosphine ligand started to form, significant rhodium leaching would occur,

[a] Unpublished data from studies performed at St. Andrews University.

leading to a yellow colour in the collected organic fractions, reduced catalyst concentration and lower reaction rates. The drop in rate would be especially marked when the dominant species was $[RhH(CO)_3\{P(4\text{-}C_6H_4C_6F_{13})_3\}]$, because the intrinsic rate of reactions catalysed by monophosphine complexes is much less than when using bis-phosphine species [van Leeuwen *et al.*, 2000].

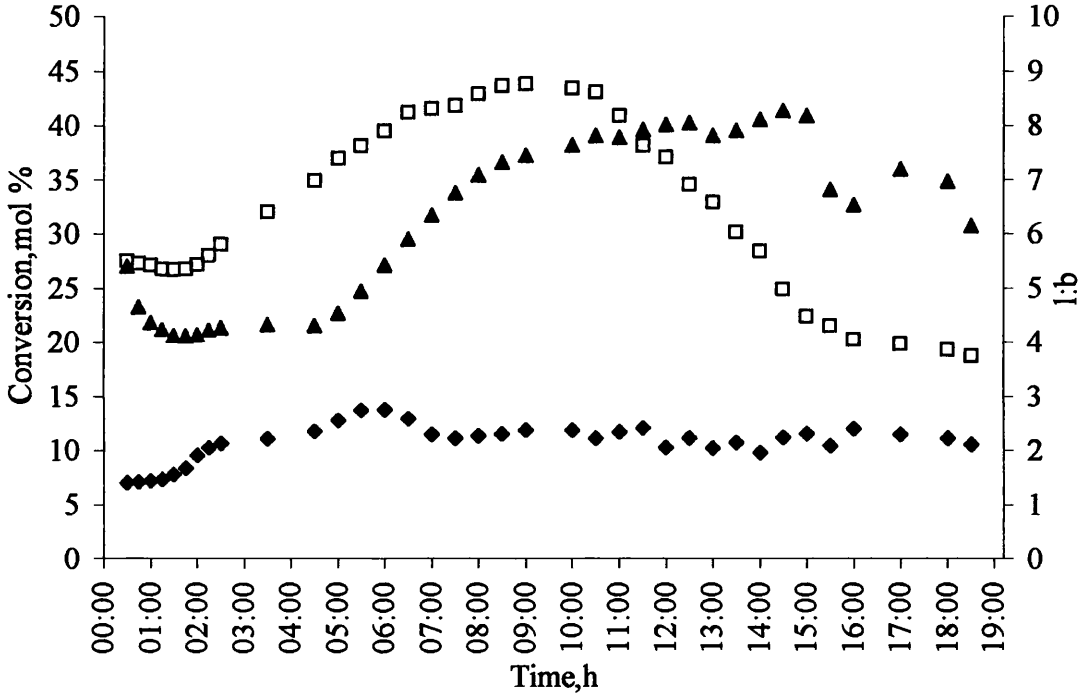


**Figure 7.7:** Results of hydroformylation experiment No.6 (▲: conversion to aldehydes, ♦: isomerised octenes, □: linear to branched aldehydes ratio).

Presumably, the approximate steady state that was reached between 11 and 15 h arose because the increased reaction rate attributable to the reduced phosphine concentration was balanced by a reduced rate arising from the decreasing catalyst concentration. The amount of isomerised alkene generated in this reaction (*ca.* 10%) was higher than that observed in batch reaction runs at high conversion (4%) [Foster *et al.* 2002, a; Foster *et al.*, 2002, b], perhaps because of the lower CO pressure and lower catalyst concentration. Isomerisation and carbonylation to give the branched

product both occur from the same intermediate, but carbonylation is bimolecular, whilst isomerisation is unimolecular; hence, isomerisation is expected to be favoured at lower partial pressures of CO.

**Table 7.2:** Partition of $[RhH(CO)_3\{P(4\text{-}C_6H_4C_6F_{13})_3\}]$ between PFMC and organic liquids[b].

| *Organic Solvent* | *Partition* |
|---|---|
| Toluene | 89:11 |
| 1 – octene | 92:8 |
| nonanal | 97:3[c] |

This would also account for the higher l:b ratio (up to 8.8) observed in this study compared with that obtained in the batch reactions (6.3) [Foster *et al.*, 2002, b] The intrinsic selectivity was only *ca.* 2 compared to 4.3 for a batch reaction carried out using double the concentration of ligand and rhodium [Foster *et al.*, 2002, b]. This was expected because the reaction selectivity is determined by the concentration of phosphine [Foster *et al.*, 2002, b]. The increase in l:b ratio during the period 4 – 9 h after the start of continuous flow operation was somewhat surprising, since it was associated with increased conversion and lower phosphine concentration, both of which generally lead to reduce l:b ratios. The drop after 8 h arose because complexes with <2 phosphine ligands, which are less selective to the linear aldehyde, contribute to catalysis. Overall, for the 19 h of continuous operation the catalyst underwent >15500 turnovers (TON) at an average rate in the region of 750 $h^{-1}$.

Figure 7.8 shows the results of experimental run No.7. In this run double the catalyst concentration was used compared to experiment No.6, while the Rh:P ratio

[b] Measured gravimetrically (Department of Chemistry, Leicester University, UK).
[c] Subject to significant error because of low volatility of nonanal. Values as high as 99:1 have been measured.

was reduced to 1:5, from 1:10. Moreover, in this run the liquid 1 – octene was pretreated in order for peroxides to be removed, procedure not used for experiment No.6. It is immediately obvious that the conversion in the initial batch reaction was higher (*ca.* 60%) than that in run No.6 (25%). This was caused both by the higher catalyst concentration, as well as, the higher residence, 85 min in this run compared to 45 min in run No.6. The conversion once again dropped when the reaction was in continuous flow mode to a low point of about 20 % from which it gradually rised over the next 12 h consistent with the gradual loss of phosphine from the system, the reaction being negative order in [phosphine]. More dramatic changes occurred later in the reaction, leading to the formation of unliganded rhodium which was then extracted from the system and accounted for the fall off in conversion at the end of the reaction. The overall low yield of the reaction can be attributed to the poor mixing of the organic and fluorous phases (as already showed in Chapter 5 they are phase separated at >15 % conversion at 70 °C), but the most dramatic effect of the poor mixing was the very high conversion to isomerised products (>20 %), which was as high as the conversion to nonanal throughout much of the reaction. Low CO availability lead to high isomerisation and the poor stirring, without gas entrainment, accounted for the high levels of isomerisation. When CO availability is low, the linear alkyl intermediate shown in Figure 7.4 is not trapped by CO to give linear aldehyde and reverts to the hydrido alkene complex. This means that the intrinsic selectivity can be greatly reduced as was observed in this reaction (<1).

In order to investigate the role of mass transport in the system, we carried out a reaction in which the stirring of the system was much better through replacing the simple paddle stirrer with a gas entrainment stirrer (spurger). The results of this

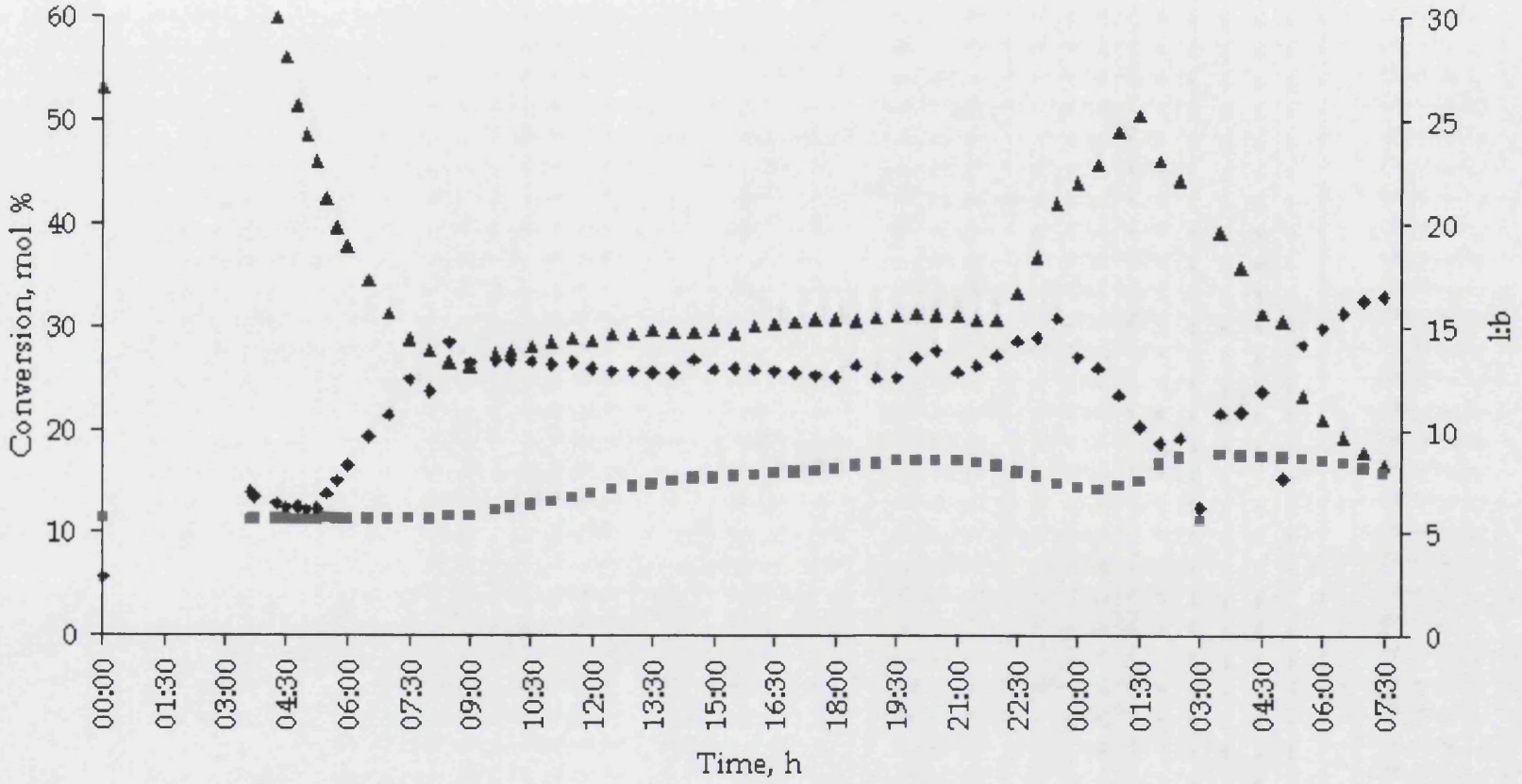


**Figure 7.8:** Results of hydroformylation experiment No. 7 (▲: conversion to aldehydes, ♦: isomerised octenes, ■: linear to branched aldehydes ratio).

experiment are shown in Figure 7.9. The initial reaction run for 2 h with the recirculating system turned off gave a conversion of 89%, much higher than that in the previous run. A similar conversion in an optimised batch system where mass transport limitations did not occur was obtained in 1 h under the same conditions. This suggests that the mixing in the continuous reactor, even when using a sparging stirrer was still not totally efficient. This could also be attributed to the shape of the reactor, as the internal diameter was 3.3 cm and the height 11.7 cm, leaving small interface for contact between the two phases and leading to positioning of the stirrer totally in the fluorous phase. Assuming that the reaction was first order in substrate [Foster *et al.*, 2002, b], it was possible to calculate that the steady state conversion expected in the continuous flow reactor when the residence time was 100 min (flow rate for 1 – octene and recycling solution of 0.3 ml/min, volume in the reactor is 60 ml) should have been *ca.* 64%.

After the initial batch reactions filling the entire system with a 1:1 organic: fluorous solvent mixture and again running with the recycling system turned off to ensure as polar an organic phase as possible, the reactor was switched to continuous flow operation with flow rates of 0.3 ml/min for the recycling catalyst solution and the fresh 1-octene. As expected, the conversion to aldehydes dropped from its initial high value over the first 7 hours of the continuous flow reaction. It started to level off at *ca.* 30 %, significantly lower than expected from the initial high value in the batch reaction. The product analysis indicated that some fluorous solvent (typically *ca.* 0.4 mole % of the organic phase) was present in the collected organic phase and this was also evident from a gradual drop in the level of the fluorous phase in the separator. In practice this would not be a serious problem because the fluorous solvent (b. pt. 76 °C) could readily be separated from the product (b. pt. 93 °C) by distillation, but it

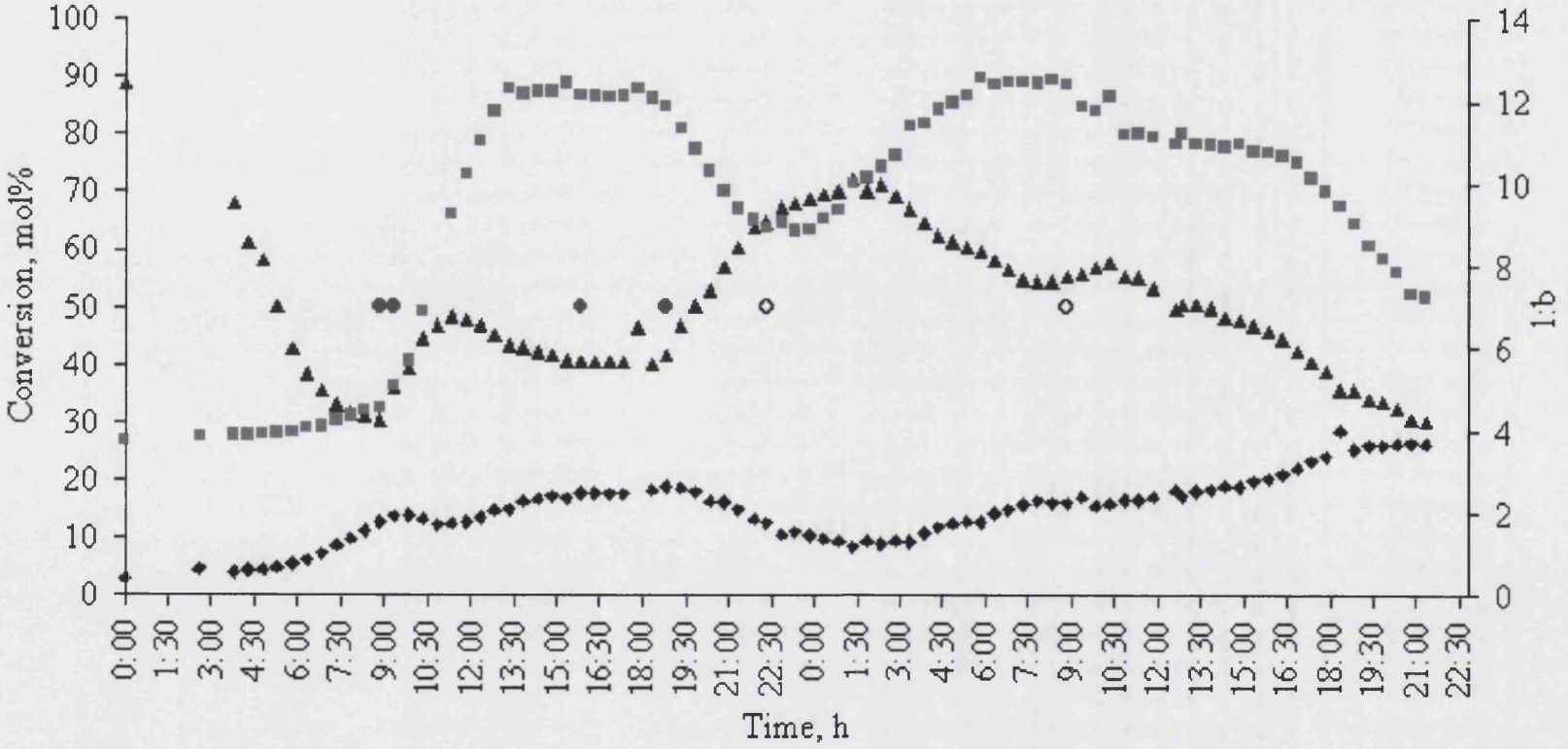


**Figure 7.9:** Results of hydroformylation experiment No. 8 (▲: conversion to aldehydes, ♦: isomerised octenes, ■: linear to branched aldehydes ratio, ●: time catalyst solution was added in the system, ○: time pure PFMC was added in the system).

was necessary to replenish the fluorous phase during the continuous flow run. Assuming that the lower than expected steady state rate might have arisen because of loss of catalyst into the product phase, the fluorous phase was replenished by adding more catalyst solution (ligand and $[Rh(CO)_2(acac)]$ (5:1) in PFMC) at 8 h 50 min of operation (5.1 ml) and again at 9 h 20 min (7.8 ml). This led to a rise in conversion as expected for the higher catalyst solution, a drop in isomerised products and a rise in l:b ratio. The last two could be attributed to the higher ligand concentration, since this lead to more of the rhodium being present as $[RhH(CO)_2L_2]$ or $[RhH(CO)L_3]$ (L = $P(4\text{-}C_6H_4C_6F_{13})_3$), which are known to give higher linear selectivity and lower isomerisation. The increase in rate appeared to be delayed somewhat because the samples for analysis were taken from the exit of the separator. Since the liquid volume in the separator and tubing was of the order of 70 ml, it was expected that changes occurring in the reactor would not start to be observed for some 100 min.

After peaking, the reaction again slowed down towards a steady state at about 40% conversion with significant isomerisation, but a high l:b ratio (11.7). More catalyst solution was then added at 15 h 50 min (5.7 ml) and at 18 h 50 min (9.0 ml) with very similar effects although the conversion rose to 70%, because of the larger increase in catalyst concentration. Here, the l:b ratio decreased as the conversion increased, suggesting that the main problem at these higher conversions was ligand rather than catalyst leaching. Hydroformylation using rhodium triarylphosphine complexes is negative order in [phosphine] [van Leeuwen *et al.*, 2000], so that loss of phosphine leads to an increase in rate (conversion), and the l:b ratio decreases as the phosphine concentration decreases, exactly as it was observed over the period 15-21 h. More catalyst solution (5.7 ml) was added at 22 h 20 min, again leading to increased conversion and increased l:b ratio, together with decreased isomerisation.

Confirmation that it was the added catalyst solution that lead to the beneficial changes in rate and selectivity was provided by adding pure fluorous solvent at 24 h (9.6 ml), 33 h 23 min (7.8 ml) and 36 h 34 min (9.6 ml). Apart from a slight rise in rate at 34 h, this period was characterised by a steady reduction in conversion and l:b ratio together with an increase in isomerisation, all of which could be attributed to the formation of unliganded rhodium species which give more isomerisation and are more soluble in the organic phase so are extracted faster leading to a reducing catalyst concentration. These would all be expected if loss of phosphine to the organic phase had occurred to such an extent that unliganded rhodium was present, which itself then leached into the organic phase.

Overall, from the last three experimental runs, several conclusions can be drawn. Firstly, it is possible to run the hydroformylation of 1 – octene under fluorous biphasic conditions in a continuous flow reactor, with activity being maintained over 40 h. Catalyst or fluorous solvent replenishment have been demonstrated and had the expected effects on conversion to aldehydes and selectivity to the desired nonanal. It is clear that, in this system the ligand leached into the product phase at a significant rate. It also appears that loss of rhodium to the organic phase was severe at low conversions. Both these facts are examined in detail in the following paragraph. One other interesting observation is that the l:b ratio in hydroformylation reaction could be much higher under flow conditions (12:1) than in batch reactions (6.3:1). This mainly arose because the isomerisation was higher in the flow system. Both the branched aldehyde and the isomerised alkene arise from the branched alkyl intermediate formed by insertion of alkene into the Rh–H bond (Figure 7.4). Reaction of this branched alkyl with CO leads to the branched aldehyde, whilst $\alpha$ - hydride abstraction leads to isomerised alkene. Since only the formation of the aldehydes is CO dependent,

increased isomerisation suggests that the gas mixing was not as efficient as in the batch reactions. An indication of the intrinsic selectivity of the reactions is given by Equation 7.4. The highest values of this parameter (4.0 – 4.4) were obtained at around 25-27 h for run No.8 and were almost as good as those from optimised batch reactions loadings (4.9). However, the amount of isomerised alkene (9 – 10%) and the l:b ratio (10 - 11.5) were both significantly higher than in the batch reactions (4% and 6.3).

### *7.3.4 Phosphine and catalyst leaching*

The leaching of phosphine and catalyst to the organic phase in the continuous experiments has been examined in detail through the effect of their change in concentration on the product selectivity. In order to investigate the issue quantitatively samples of the organic phase from batch and continuous runs were analysed by ICPMS.

As long as the phosphine leaching is concerned, ICPMS from batch experiments has shown that 2.8% (4.5% for a 1:1 ratio of organic: fluorous phases) of the phosphine leached when at 100% conversion [Foster *et al.*, 2002, b]. Partition studies suggest that 3% of the ligand partitioned into pure nonanal, but that this rose to 8% in pure 1 – octene, so the loss of phosphine was more severe at low conversion, see Table 7.2.

Studies of batch reactions of different conversions suggest that Rh leaching could increase 10 fold in reducing the conversion from 80 – 20 %, see Figure 7.10.

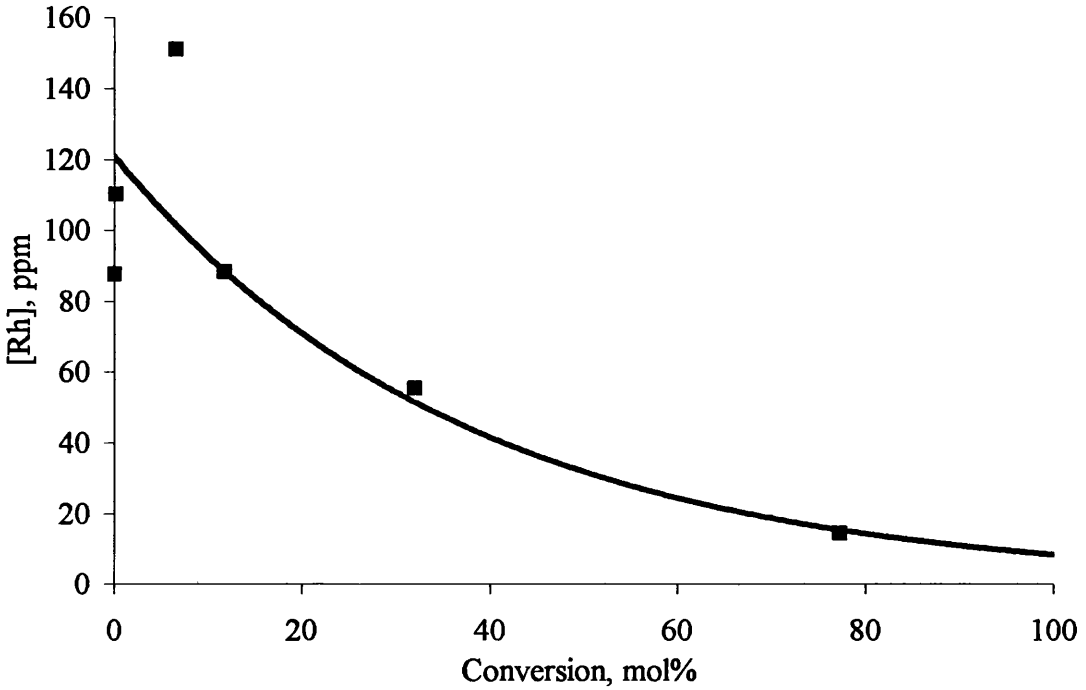


**Figure 7.10:** Concentration of rhodium in the organic phase at different conversions from batch reactions.

Figure 7.11 shows the rhodium leaching during the continuous reaction run No.4. According to the results, rhodium leaching was quite high at the beginning of the experiment, reaching values up to 563 ppm. This value dropped to around 100 ppm within two hours and there was a slight decrease in [Rh] to 70 ppm, as the conversion increased to 30%. For almost the same conversion, 32%, in batch experiments rhodium concentration in the organic phase was 55 ppm.

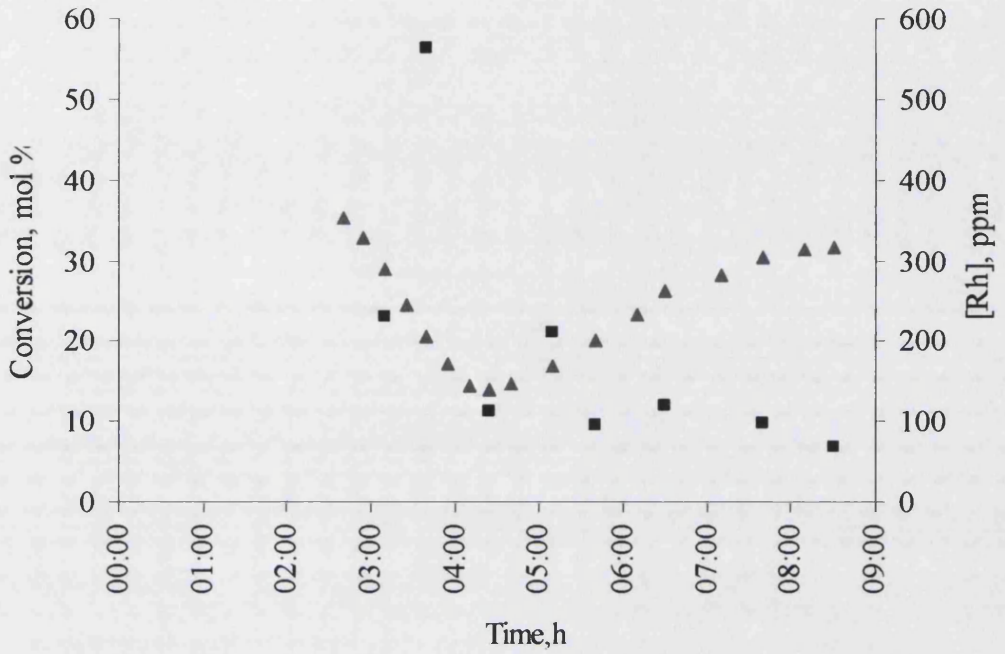


**Figure 7.11:** Concentration of rhodium in the organic phase at different conversions from continuous reactions for experimental run No.4 (▲: conversion to aldehydes, ■: concentration of Rh ).

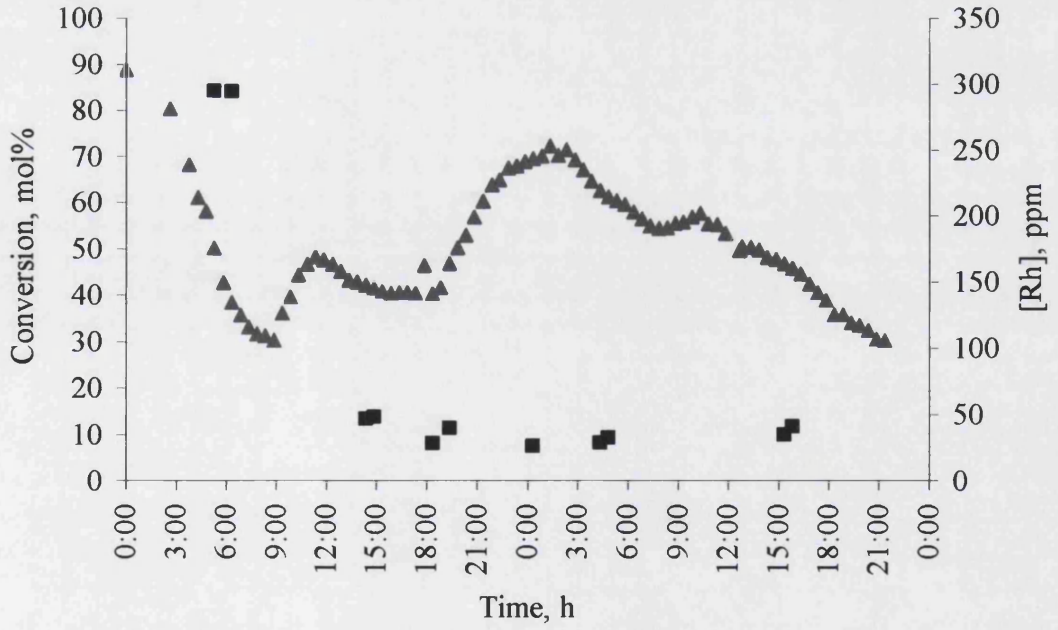


**Figure 7.12:** Concentration of rhodium in the organic phase at different conversions from continuous reactions for experimental run No.8 (▲: conversion to aldehydes, ■: concentration of Rh ).

Figure 7.12 shows the concentration of rhodium in the organic samples during the continuous experiment No.8. Again, rhodium leaching was much higher at the beginning of the experiment reaching values of 294 ppm. Nevertheless, rhodium leaching dropped to *ca.* 48 ppm, within the next 9 h and remained between 25 and 48 ppm during the whole run regardless of the alkene conversion. This behaviour was quite peculiar as one would expect rhodium leaching to be higher in later times as less and less phosphine was present in the system. On the other hand as less rhodium was present in the system in later times it was stronger retained by the fluorous phase leading to less leaching to the organic phase.

Though, the effect of alkene conversion in the continuous runs is not obvious in each separate run, conclusions can be drawn when comparing experimental runs No.4 and No.8. In run No.4 the initial rhodium concentration was 563 for conversion ranging from 35 to 25%, while it is almost half, 298 ppm, for conversion ranging from 90 to 45%, run No.8. Again, in later times, rhodium concentration was between 25 to 40 ppm, for conversion levels between 45 and 70 %, run No.8, while it was around 100 ppm for conversion ranging between 15 and 35 %, run No.4. Keeping in mind that double the catalyst concentration was used in run No.8 in comparison to No.4, the above observations are even more significant.

## 7.4 CONCLUSIONS

Overall, we have demonstrated for the first time the successful operation of a pressurised continuous flow reaction system that enables catalyst separation and recycling in a fluorous biphasic system using pressurised gases.

- The continuous system that has been developed has been successfully used for the long term testing of hydroformylation in a fluorous biphasic system.
- Conversion levels could be as high as 70%, but were somewhat lower than those observed in batch experiments. Under the best conditions, the isomerisation was kept at low levels, <10%, while very good linear to branched aldehydes ratios up to 12:1 were achieved.
- Efficient mixing of the three phases of the system is essential for obtaining high conversions and avoiding excessive alkene isomerisation.
- Leaching of the modifying phosphine, the rhodium catalyst and the fluorous solvent are the main issues. In principle the recovery of the fluorous solvent and ligand could be achieved by distillation, but the catalyst would decompose under most distillation conditions, so much higher retention of the catalyst into the fluorous phase would be required for this system to be able to approach commercial realisation. This will probably require significant redesign of the fluorinated ligand.

# CHAPTER 8:

# Conclusions – Future Work

We have demonstrated for the first time the successful operation of a pressurised continuous flow reaction system that enables catalyst separation and recycling under fluorous biphasic conditions.

The initial tests in the absence of chemical reaction verified the efficient separation of the system. The two well distinct phases settled quickly at room temperature in the separator. The organic phase ascended through the fluorous phase creating a top organic – rich phase, while the fluorous phase descended through the organic phase creating a bottom fluorous – rich phase. The partition of nonanal in the fluorous phase and of PFMC in the organic phase was kept at low levels, at room temperature, provided that conversion was high (>60%) – more polar products present in the organic phase. With reference to the simulated conversion levels, the higher the conversion, the less the leaching of the expensive fluorous solvent in the product phase.

An increase in temperature caused an increase in the partition of the nonanal in the fluorous phase and vice versa. Moreover, at reaction temperature, 70 °C (343K) only one phase was present up to 15% conversion. For higher conversion levels the distribution of 1 – octene in the organic phase reached a maximum of 85% (at 90.6% conversion). As most 1 – octene is present in the organic phase it is possible that longer reaction times will be needed to achieve full conversion in this biphasic system in comparison to homogeneous systems. This assumption was verified with the

modelling of a first order reaction happening in a homogeneous system (model 1) and in a system that phase separates at reaction temperature with increasing conversion (model 2). The partition coefficient of the reactant used in the second model was obtained from the phase separation experiments. Simulation results comparing the two models for various values of reaction rate constant showed that the predicted time needed for a conversion value in model 2 is longer than in model 1.

The continuous separation experiments have furthermore shown that the reactor pressure had no effect on the efficiency of the separation. Moreover, it was proven that the composition of both phases in the separator reached the equilibrium values. However, a method should be developed to recover the fluorous solvent from the exhaust gas stream.

Furthermore, the developed set – up has been successfully used for the long term testing of hydroformylation of higher olefins in a fluorous biphasic system. Conversion levels could be as high as 70%, but were somewhat lower than those observed in batch experiments. Under the best conditions, the isomerisation was kept at low levels, < 10%, while very good l:b ratios up to 12:1 were achieved. Efficient mixing of the three phases of the system was essential for obtaining high conversions and avoiding excessive alkene isomerisation, but even spurging of the gases did not achieve results as good as the batch experiments. Repositioning of the stirrer's level, as well as, change of the reactor dimensions could enhance these results.

The leaching of the modifying phosphine, the rhodium catalyst and the fluorous solvent were the main issues. In principle, the recovery of the fluorous solvent and ligand could be achieved by distillation, but the catalyst would decompose under most distillation conditions, so much higher retention of the catalyst into the fluorous phase

would be required for this system to be able to approach commercial realisation. This will probably require significant redesign of the fluorinated ligand.

To summarise, the successful long term testing of hydroformylation reaction under fluorous biphasic conditions has been demonstrated. For the further optimisation of the system, both modelling, engineering and chemistry developments are required.

In order to get more insight about the reaction kinetics in the fluorous biphasic system an advanced model should be developed. Factors such as phase dispersion due to stirring, as well as the partition of the catalyst in the product phase affect the reaction kinetics and should be taken into account in the advanced model.

From an engineering point of view redesigning of the CSTR shape, as well as, repositioning of the stirrer, will lead to better mixing and higher conversion, thus less phosphine and catalyst leaching. Furthermore, the use of a novel tubular reaction system, i.e. an oscillating baffled reactor, could enhance the reaction productivity. For the successful use of this kind of system very good mixing of the two phases and good contact of the gas and the liquid reactants should be guaranteed.

From a chemical point of view, the design and use of a fluorous ligand with higher fluorine content is necessary. Higher fluorine content will lead to decreased solubility of the ligand and the catalyst in the organic phase which could lead in turn to a continuous process with high potentials of commercialisation.

# References

Adams D.J., Gudmunsen D., Hope E.G., Stuart A.M., West A., (2003). "Phosphorous (III) compounds incorporating perfluoroalkyl – derivatised biphenolic units", *J. Fluorine Chem.*, **121**, 213 – 217

Alexander F.J., Chen S., Grunau D.W. (1993). "Hydrodynamic spinodal decomposition: Growth kinetics and scaling functions." *Phys. Rev. B*, **48**, 634 – 637

Arnoldy P. (2000) Process aspects of rhodium-catalysed hydroformylation in "Rhodium Catalysed Hydroformylation", Eds. van Leeuwen P. W. N. M. and Claver C, Dordrecht

Barthel-Rosa L.P. and Gladysz J.A. (1999). "Chemistry in fluorous media: a user's guide to practical considerations in the application of fluorous catalysts and reagents." *Coordin. Chem. Rev.*, **192**, 587-605

Benvenuti F., Carlini C., Marchionna M., Galletti A.M.R., Sbrana G., (2002). "Propylene oligomerisation by nickel catalysts in biphasic fluorinated systems", *J. Mol. Catal. A: Chem.*, **178**, 9 – 22

Bergbreiter D.E., (1998). "The use of soluble polymers to effect homogeneous catalyst separation and reuse", *Catal. Today*, **42**, 389 – 397

Bhanage B.M., Divekar S.S., Deshpande R.M. and Chaudhari R.V., (1997). "Kinetics of hydroformylation of 1-dodecene using homogeneous $HRh(CO)(PPh_3)_3$ catalyst", *J. Mol. Cat. A: Chem.*, **115**, 247-257

Bhattacharyya P., Croxtall B., Fawcett J., Fawcett J., Gudmunsen D., Hope E.G., Kemmitt R.D.W, Paige D.R., Russel D.R., Stuart A.M., Wood D.R.W., (2000). "Phosphorus (III) ligands in fluorous biphase catalysis", *J. Fluorine Catal.*, **101**, 247 –

255

Bhattacharyya P., Gudmunsen D., Hope E.G., Kemmit R.D.W., Paige D.R., Stuart A.M., (1997). "Phorphorous (III) ligands with fluorous ponytails", *J. Chem. Soc., Perkin Trans.*, **1**, 3609 -3612

Bird R.B., Stewart W.E. and Lightfoot E.N. (2002). Transport Phenomena, John Wiley and Sons, New York.

Bischoff S., Kant M., (2001). "Water soluble rhodium/phosponate-phosphine catalysts for hydroformylation", *Catal. Today*, **66**, 183-189

Bonafoux D., Hua Z., Wang B., Ojima I., (2001). "Design and synthesis of new fluorinated ligands for the rhodium-catalysed hydroformylation of alkenes in supercritical $CO_2$ and fluorous solvents", *J. Fluorine Chem.*, **112**, 101-108

Buhling A., Kamer P.C.J., van Leeuwen P.W.N.M, (1995). "Rhodium catalysed hydroformylation of higher alkenes using amphiphilic ligands"., *J. Mol. Catal. A: Chem.*, **98**, 69-80

Cavazzini M., Montanari F., Pozzi G., Quici S., (1999). "Perfluorocarbon –soluble catalysts and reagents and the application of FBS (fluorous biphase system) to organic synthesis", *J. Fluorine Chem.*, **94**, 183 – 193

Chaudhari R.V., Seayad A. and Jayasree S.,(2001). "Kinetic modelling of homogeneous catalytic processes", *Catal. Today*, **66**, 371-380

Cole – Hamilton D.J., (2003). "Homogeneous Catalysis – New Approaches to Catalyst Separation, Recovery and Recycling", *Science*, **299**, 1702-1706

Cornils B., (1998). "Industrial Aqueous Biphasic Catalysis: Status and Directions". *Org. Process Res. Dev.*, **2**, 121 – 127

Curran D.P (2000). "Fluorous mehods for synthesis and separation of organic molecules", *Pure Appl. Chem.*, **72**, 1649 – 1653

de Wolf E., van Koten G., and Deelman B.J. (1998). "Fluorous biphase separation techniques in catalysis." *Chem. Soc. Rev.*, **28**, 37-41

Debenedetti P.G. (1996). Metastable Liquids: Concepts and Principles, Princeton University Press, Princeton

Deshpande R.M., Purwanto and Delmas H., (1996), "Kinetics of Hydroformylation of 1-Octene Using $[Rh(COD)Cl]_2$-TPPS Complex Catalyst in a Two-Phase system in the Presence of a Cosolvent", *Ind. Eng. Chem. Res.*, **35**, 3927-3933

Divekar S.S., Deshpande R.M. and Chaudhari R.V. (1993). "Kinetics of hydroformylation of 1-decene using homogeneous $HRh(CO)(PPh_3)_3$ catalyst: a molecular level approach." *Catal. Lett.*, **21**, 191-200

Dobbs A.P., Kimberley M.R., (2002). "Fluorous phase chemistry: a new industrial technology", *J. Fluorine Chem.*, **118**, 3-17

Dupont J., de Souza R.F., and Suarez P.A.Z., (2002). "Ionic Liquid (Molten Salt) Phase Organometallic Catalysis", *Chem. Rev.*, **102**, 3667 - 3691

Dupont J., Silva S.M. and de Souza R.F. (2001). "Mobile phase effects in Rh/sulfonated phosphine/molten salts catalysed the biphasic hydroformylation of heavy olefines." *Catal. Lett.*, **77**, 131-133

Evans D., Osborn A. and Wilkinson G., (1968). "Hydroformylation of Alkenes by Use of Rhodium Complex Catalysts", *J. Chem. Soc. (A)*, 3133 - 3142

Fish R.H. (1999). "Fluorous Biphasic Catalysis: A New Paradigm for the Separation of Homogeneous Catalysts from Their Reaction Substrates and products." *Chemical European Journal*, **5**, 1677-1680

Fogler H.Scott. (2002). Elements of chemical reaction engineering, Prentice Hall, New Jersey.

Foster D.F., Adams D.J., Gudmunsen D., Stuart A.M, Hope E.G., Cole-Hamilton D.J., (2002). "Hydroformylation in fluorous solvents", *Chem. Commun.*, 722 - 723

Foster D.F., Gudmunsen D., Adams D.J., Stuart A.M, Hope E.G., Cole-Hamilton D.J., Schwarz G.P. and Pogorzelec P. (2002). "Hydroformylation in perfluorinated solvents; improved selectivity, catalyst retention and product separation." *Tetrahedron*, **58**, 3901-3910

Frohling C.D and Kohlpaintner C.W., 1996, Hydroformylation in "Applied Homogeneous Catalysis with Organometallic Compounds", Eds. Cornils B. and Herrmann W.A., Weinheim

Gladysz J.A. and Curran D.P. (2002). "Fluorous Chemistry: from biphasic catalysis to a parallel chemical universe and beyond." *Tetrahedron*, **58**, 3823-3825

Green S.W., Slinn D.S.L., Simpson R.N.F., Woytek A.J. (1994). Perfluorocarbon Fluids in "Organofluorine Chemistry: Principles and Commercial Applications", Eds. Banks R.E., Plenum Press, New York

Guillevic M.A., Arif A.M., Horvath I.T. and Gladysz J.A. (1997). "Synthesis, Structure and Oxidative Additions of a Fluorous Analogue of Vaska's Complex, *trans*-[IrCl(CO){P[$CH_2CH_2(CF_2)_5CF_3]_3$}$_2$] – Altered Reactivity in Fluorocarbons and Implications for Catalysis." *Angew. Chem. Int. Edit.*, **36**, 1612 -1615

Gupta R., Mauri R., Shinnar R. (1999). "Phase Separation of Liquids Mixtures in the Presence of Surfactants.", *Ind. Eng. Chem. Res.*, **38**, 2418-2424

Hanson B.E., Zoeller J.R., (1998). "Preface: Phase separable homogeneous catalysis", *Catal. Today*, **42**, 371 – 372

Hanson E.B., Ding H., Kohlpaintner W., (1998). "Amphiphilic phosphines for

catalysis in the aqueous phase", *Catal. Today*, **42**, 421-429

Haumann M., Koch H., Hugo P. and Schomacker R. (2002). "Hydroformylation of 1-dodecene using Rh-TPPTS in a microemulsion." *Appl. Catal. A: Gen.*, **225**, 239-249

Heck, R.S., Breslow D.S, (1961). "The Reaction of Cobalt hydrotetracarbonyl with olefins", *J. Am. Chem. Soc.*, **83**, 4023 - 4027

Herrmann W.A., Kohlpaintner C.W., Bahrmann H., Konkol W., (1992). "Water soluble metal complexes and catalysts. 6. A new efficient water soluble catalyst for 2 – phase hydroformylation of olefins", *J. Mol. Catal.*, **73**, 191 – 201

Hohenberg P.C (1977). "Theory of dynamic critical phenomena", *Rev. Modern Phys.*, **49**, 435-479

Hope E.G. and Stuart A.M. (1999). "Fluorous biphase catalysis." *J. Fluorine Chem.*, **100**, 75-83

Hope E.G., Kemmitt R.D.W., Paige D.R. and Stuart A.M. (1999). "The rhodium catalysed hydrogenation of styrene in the fluorous biphase." *J. Fluorine Chem.*, **99**, 197 – 200

Horvath I.T. (1998). "Fluorous Biphase Chemistry." *Accounts Chem. Res.*, **31**(10), 641-650

Horvath I.T. and Rabai J. (1994). "Facile Catalyst Separation Without Water: Fluorous Biphase Hydroformylation of Olefines." *Science*, **266**(5182), 72-75

Horvath I.T., (1990). "Hydroformylation of olefins with the water soluble $HRH(CO)[P(m\text{-}C_6H_4SO_3Na)_3]_3$ in supported aqueous – phase – Is it really aqueous?", *Catal. Lett.*, **6**, 43 – 48

Horvath I.T., Kiss G., Cook R.A., Bond J.E., Stevens P.A., Rabai J. and Mozeleski

E.J. (1998). "Molecular Engineering in Homogeneous Catalysis: One-Phase Catalysis Coupled with Biphase Catalyst Separation. The Fluorous-Soluble $HRh(CO)\{P[CH_2CH_2(CF_2)_5CF_3]_3\}$ Hydroformylation System." *J. Am. Chem. Soc.*, **120**, 3133-3143

Juliette J.J.J., Horvath I.T. and Gladysz J.A. (1997)."Transition Metal Catalysis in Fluorous Media: Practical Application of a New Immobilization Principle to Rhodium – Catalyzed Hydroboration" *Angew. Chem. Int. Ed. Eng.*, **36**, 1610-1612

Kalck P., Miquel L. and Dessoudeix M. (1998). "Various approaches to transfers inprovement during biphasic catalytic hydroformylation of heavy alkenes." *Catal. Today*, **42**, 431-440

Kamer P.C.J., Reek J.N.H., van Leeuwen P.W.N.M (2000). Rhodium Phosphite Catalysts in hydroformylation in "Rhodium Catalysed Hydroformylation", Eds. van Leeuwen P. W. N. M. and Claver C, Dordrecht

Klement I., Lutjens H., Knochel P., (1997). "Transition Metal Catalyzed Oxidations in Perfluorinated Solvents", *Angew. Chem. Int. Ed. Eng.*, **36**, 1454 – 1456

Kohlpaintner C.W., Fischer R.W. and Cornils B. (2001). "Aqueous biphasic catalysis:Ruhrchemie/Rhone-Poulenc oxo process." *Appl. Catal. A: Gen.*, **221**, 219-225

Laradji M., Toxvaerd S. and Mouritsen O.G. (1996). "Molecular Dynamics of Spinodal Decomposition in the Three-Dimensional Binary Fluids", *Phys. Rev. Lett.*, 77, 2253 – 2256

Lekhal A., Chaudhari R.V., WilhelmA.M. and Delmas H. (1999). "Mass transfer effects on hydroformylation catalyzed by water soluble complex." *Catal. Today*, **48**, 265-272

Leptoukh G., Strickland B., Roland C., (1995). "Phase Separation in Two-

Dimensional Fluid Mixtures." *Phys. Rev. Lett.*, **74**, 3636 – 3639

Ma W.J., Maritan A., Banavar J.R. and Koplik J. (1992). "Dynamics of phase separation of binary fluids", *Phys. Rev. A*, **45**, R5347 - R5350

Mac Dougall J.K., Simpson M.C., Green M.J., Cole-Hamilton D.J., (1996). "Direct formation of alcohols by hydrocarbonylation of alkenes under mild conditions using rhodium trialkylphosphinecatalysts", *J. Chem. Soc., Dalton T.*, 1161 – 1172

Mathivet T., Monfelier E., Castanet Y., Montreux A., Couturier J.L., (2002), a. "Hydroformylation of higher olefins by rhodium/tris-((1*H*,1*H*,2*H*,2*H*-perfuorodecyl)phenyl)phosphates complexes in a fluorocarbon/hydrocarbon biphasic medium: effects of fluorinated groups on the activity and stability of the catalytic system", *Tetrahedron*, **58**, 3877 - 3888

Mathivet T., Monfelier E., Castanet Y., Montreux A., Couturier J.L., (2002), b. "Perfluorooctyl substituted triphenylphosphites as ligands for hydroformylation of higher olefins in fluorocarbon/hydrocarbon biphasic medium", *C.R. Chimie*, **5**, 417 – 424

Mauri R., Shinnar R., Trantafyllou G., (1996). "Spinodal decomposition in binary mixtures", *Phys. Rev. E*, **53**, 2613 – 2623

Monteil F., Queau R., Kalck P., (1994). "Behaviour of water – soluble dinuclear rhodium complexes in the hydroformylation reaction of oct-1-ene", *J. Organomet. Chem*, **480**, 177 – 184

Niu Y., Crooks R.M., (2003). "Dendrimer – encapsulated metal nanoparticles and their applications to catalysis", *C. R. Chimie*, **6**, 1049 – 1059

Nozaki K., Itoi Y., Shibahara F., Shirakawa E., Ohta T., Takaya H., Hiyama T., (1998). "Asymmetric hydroformylation of olefins in a highly cross – linked polymer matrix", *J. Am. Chem. Soc.*, **120**, 4051 – 4052

Oosterom G.E., Reek J.N.H., Kamer P.C.J., Van Leeuwen P.W.N.M., (2001). "Transition metal catalysis using functionalised dendrimers", *Angew. Chem. Int. Ed.*, **40**, 1828 – 1849

Osuna B.A.M., Chen W., Hope E.G., Kemmitt R.D.W., Paige D.R., Stuart A.M., Xiao J., Xu L., (2000). "Effects of the ponytails of arylphosphines on the hydroformylation of higher olefins in supercritical $CO_2$", *J. Chem. Soc., Dalton Trans.*, 4052 – 4055

Paganelli S., Zanchet M., Marchetti M. and Mangano G. (2000). "Hydroformylation of functionalized olefins catalyzed by water-soluble rhodium carbonyl complexes." *J. Molec. Catal. A: Chem.*, **157**, 1-8

Palo D.R. and Erkey C. (1999). "Kinetics of the Homogeneous Catalytic Hydroformylation of 1-Octene in Supercritical Carbon Dioxide with HRh(CO)[P-(*p*-CF3C6H4)3]3." *Ind. Eng. Chem. Res.*, **38**, 3786-3792

Parsall G.W and Ittel S.D (1992). Homogeneous Catalysis, Wiley, New York

Perry R.H., Green D.W. (1997). Perry's Chemical Engineers'Handbook, Eds. Perry R.H., Green D.W., Maloney J.O., McGraw-Hill, New York

Pinault N., Bruce D.W., (2003). "Homogeneous catalyst based on water – soluble phosphines", *Coord. Chem. Rev.*, **241**, 1-25

Prausnitz J.M. and Lichtenthaler R.N. (1986). Molecular thermodynamics of Fluid-Phase Equilibria, Prentice-Hall Inc., New Jersey

Purwanto P. and Delmas H., (1995). "Gas-liquid-liquid reaction engineering: hydroformylation of 1-octene using a water soluble rhodium complex catalyst", *Catal. Today*, **24**, 135-140

Reek J.N.H., Kamer P.C.J., Van Leeuwen P.W.N.M., (2000). Novel developments in hydroformylation in "Rhodium Catalysed Hydroformylation", Eds. van Leeuwen P. W. N. M. and Claver C, Dordrecht

Reid R.C., Prausnitz J.M. and Poling B.E. (1987). Properties of gases and liquids, McGraw-Hill, New York

Richter B., de Wolf E., van Koten G., Deelman B.J., (2000). "Synthesis and Properties of a Novel Family of Fluorous Triphenylphosphine Derivatives", *J. Org. Chem.*, **65**, 3885 – 3893

Richter B., Deelman B.J. and van Koten G. (1999). "Fluorous biphasic hydrogenation of 1-alkenes using novel fluorous derivatives of Wilkinson's catalyst." *J. Molec. Catal. A: Chem.*, **145**, 317-321

Sandee A.J., Ubale R.S., Makkee M., Reek J.N.H., Kamer P.C.J., Moulijin J.A. and.Van Leeuwen P. W.N.M. (2001). "ROTACAT: A Rotating Device Containing a Designed Catalyst for Highly Selective Hydroformylation." *Adv. Synth. Catal.*, **343**(2), 201-206

Sellin M.F., Webb P.B. and Cole-Hamilton D.J., (2001). "Continuous flow homogeneous catalysis: hydroformylation of alkenes in supercritical fluid-ionic liquid biphasic mixtures", *Chem. Com.*, 781 -782

Sinnott R.K. (1996). Chemical Engineering Design, Butterworth-Heinemann, Oxford.

Sorensen J.M., (1979). Chemistry Data Series Vol. 5, DECHEMA, Frankfurt

Spetseris N., Hadida S., Curran D.P., Meyer T.Y., (1998). "Organic/Fluorous Phase Extraction: A New Tool for the Isolation of Organometallic Complexes", *Organometallics*, **17**, 1458 – 1459

Stephen & Stephen (1963). Solubilities of inorganic and organic compounds,

Pergamon, Oxford

Suomalainen P., Laitinen R., Jaaskelainen S., Haukka M., Pursiainen J.T., Pakkanen T.A., (2002). "Multidentate phosphanes as ligands in rhodium catalysed hydroformylation of 1-hexene", *J. Mol. Cat. A: Chem.*, **179**, 93-100

Tanaka H., Araki T., (1998). "Spontaneous Double Phase Separation Induced by Rapid Hydrodynamic Coarsening in Two-Dimensional Fluid Mixtures." *Phys. Rev. Lett.*, **81**, 389 – 392

Tic W., Miesiac I. and Szymanowski J. (2001). "Hydroformylation of Hexene in Microemulsion." *J. Colloid Interf. Sci.*, **244**, 423-426

Trzeciak A.M., Ziolkowski J.J., (1999). "Perspectives of rhodium organometallic catalysis. Fundamental and applied aspects of hydroformylation", *Coordination Chem. Rev.*, **190 -192**, 883 – 900

Tzschucke C.C., Markert C., Bannwarth W., Roller S., Hebel A., and Haag R., (2002). "Modern Separation Techniques for the Efficient Workup in Organic Synthesis", *Angew. Chem. Int. Ed.*, **41**, 3964 – 4000

Ullmann A., Ludmer Z., Shinnar R., (1995). "Phase Transition Extraction Using Solvent Mixtures with Critical Point of Miscibility", *AIChE Journal*, **41**, 488 – 500

Van Elk E.P., Borman P.C., Kuipers J.A.M., Versteeg G.F., (2001). "Modelling of gas – liquid reactors – stability and dynamic behaviour of a hydroformylation reactor, influence of mass transfer in the kinetics controlled regime", *Chem. Eng. Sc.*, **56**, 1491-1500

van Leeuwen P. W. N. M., Casey C.P, Whiteker G.T. 2000, Phosphines as ligands in "Rhodium Catalysed Hydroformylation", Eds. van Leeuwen P. W. N. M. and Claver C., Dordrecht

van Leeuwen P. W. N. M., 2000, Introduction to Hydroformylation in "Rhodium Catalysed Hydroformylation", Eds. van Leeuwen P. W. N. M. and Claver C., Dordrecht

van Leeuwen P.W.N.M. (2000) Catalyst preparation and decomposition in "Rhodium Catalysed Hydroformylation", Eds. van Leeuwen P. W. N. M. and Claver C, Dordrecht

Van Rooy A., de Bruijin J.N.H., Roobeek K.F., Kamer P.C.J. and Van Leeuwen P.W.N.M. (1996). "Rhodium-catalysed hydroformylation of branched 1-alkenes; bulky phosphite vs. triphenylphosphine as modifying ligand." *J. Organomet. Chem.*, **507**, 69-73

Van Rooy A., Orij E.N., Kamer P.C.J., Van Leeuwen P.W.N.M, (1995). "Hydroformyaltion with Rhodium/Bulky Phosphite Modified Catalyst. Catalyst Comparison for 1-Octene, Cyclohexene and Styrene", *Organometallics*, **14**, 34-43

Vladimirova N, Malagoli A. and Mauri R. (1999). "Two-dimensional model of phase segregation in liquid binary mixtures", *Phys. Rev. E*, **60**, 6968 – 6977

Vladimirova N. , Malagoli A., Mauri R., (2000). "Two – dimensional model of phase segregation in liquid binary mixtures with an initial concentration gradient" *Chem. Eng. Science*, **55**, 6109 – 6118

Vladimirova N., Malagoli A. and Mauri R. (1998). "Diffusion-driven phase separation of deeply quenched mixtures", *Phys. Rev. E*, **58**, 7691 – 7699

Wachsen O., Himmler K. and Cornils B., (1998). "Aqueous biphasic catalysis: Where the reaction takes place", *Cat. Today*, **42**, 373 – 379

Wang Y., Jiang J., Zhang R., Liu X. and Jin Z. (2000). "Thermoregulated Phase Transfer Ligands and Catalysis IX. Hydroformylation of higher olefins in organic monophase catalytic system based on the concept of critical solution temperature of the nonionic tensioactive phosphine ligand." *J. Molec. Catal. A: Chem.*, **157**, 111-115

Webb P.B., Sellin M.F., Kunene T.E., Williamson S., Slawin A.M., Cole – Hamilton D.J., (2003). "Continuous Flow Hydroformylation of Alkenes in Supercritical Fluid – Ionic Liquid Biphasic Systems", *J. Am. Chem. Soc.*, **125**, 15577 – 15588

Xiang J., Orita A. and Junzo Otetra (2002). "Fluoroalkyldistannoxane Catalysts for Transesterification in Fluorous Biphase Technology." *Advanced Synthesis Catalysis*, **344**(1), 84-90

Xiaodong Li S.L. and Wang A. (2000). "A new chiral diphosphine ligand and its asymmetric induction in catalytic hydroformylation of olefins." *Catal. Today*, **63**, 531-536

Yang C., Bi X., Mao Z. S., (2002), a. "Effect of reaction engineering factors on biphasic hydroformylation of 1-dodecene catalysed by water-soluble rhodium complex", *J. Mol. Cat. A: Chem.*, **187**, 35-46

Yang C., Mao Z. S., Wang Y., Chen J., (2002), b. "Kinetics of hydroformylation of propylene using $RhCl(CO)(TPPTS)_2$/TPPTS complex catalyst in aqueous system", *Catal. Today*, **74**, 111-119

Yoshida A., Hao X., Nishikido J., (2003). "Development of the continuous –flow system based on the Lewis acid-catalysed reactions in a fluorous biphasic system", *Green Chem.*, **5**, 554 – 557

Zhang Y., Mao Z.S., Chen J., (2002). "Macro-kinetics of biphasic hydroformylation of 1-dodecene catalysed by water-soluble rhodium complex", *Cat. Today*, **74**, 23-35

Zheng X., Jiang J., Liu X., Jin Z., (1998). "Thermoregulated phase transfer ligands and catalysis III. Aqueous/Organic two-phase hydroformylation of higher olefins by thermoregulated phase transfer catalysis", *Catal. Today*, **44**, 175 -182

Zhu D.W. (1993). "A Novel reaction Medium: Perfluorocarbon Fluids." *Synthesis*,**10,** 953- 954

# Appendix 1:

# Fluorocarbons used as oxygen carriers

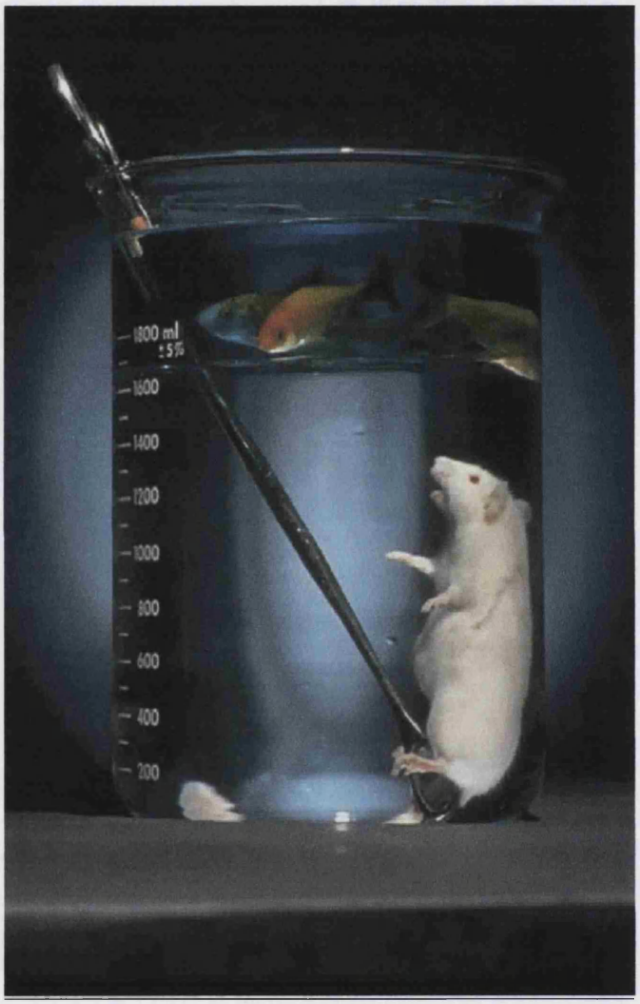


Dr. Leland Clark of Cincinnati invented a blood substitute allowing this living mouse to breathe in the liquid, while goldfish inhabit the water floating on top. After the mouse was removed from the fluid 90 min later, it went happily on its way.[a] The fluid used as a blood substitute is a perfluorocarbon – based oxygen carrier.

[a] Source: www.gbphoto.com

# Appendix 2:

# Calculation of $r_{max}$ for mixture PFMC – toluene

According to Equation A1.1, in order to calculate $r_{max}$ for the mixture,

$$r^2_{max} = O(\sigma / g\Delta\rho) \qquad \text{(Eq. A1.1)}$$

it is necessary to know the surface tension, and the densities of the pure components, and to calculate the surface tension, $\sigma$, and the density difference, $\Delta\rho$, of the mixture. Table A1.1 shows the properties of the pure components at room temperature, 25 °C.

**Table A1.1:** Properties of pure toluene and perfluoromethylcyclohexane.

| Component | Density, kmol/m$^3$ | Density, kg/m$^3$ | Surface tension, mN/m | Reference |
|---|---|---|---|---|
| Toluene | 9.38 | 863 | 47.9 | [Reid et al., 1987] |
| PFMC | 5.11 | 1788 | 15.4 | [Green et al, 1994] |

The surface tension of a non aqueous mixture can be calculated from Equation A1.2 [Perry and Green, 1997]

$$\sigma_m = \sum_{i=1}^{n}\sum_{j=1}^{n}\rho^2\left(\frac{x_i}{\rho_{Li}}\right)\left(\frac{x_i}{\rho_{Li}}\right)\left(\sigma_i\sigma_j\right)^{1/2} \qquad \text{(Eq. A1.2)}$$

$$\frac{1}{\rho} = \sum_{i=1}^{n}\frac{x_i}{\rho_{Li}} \qquad \text{(Eq. A1.3)}$$

where, $\sigma_m$ is the mixture surface tension, mN/m,

$x_{i,j}$ is the mole fraction of component *i* or *j* in the liquid mixture,

$\rho_{Li,j}$ is the pure component liquid density of component *i* or *j*, kmol/m$^3$,

$\sigma_{i,j}$ is the pure component surface tension of component *i* or *j*, mN/m

Substituting the values from Table A1.1 in Equations A1.2 and A1.3, the surface tension of the mixture toluene – perfluoromethycyclohexane for the critical composition, 26.7%mol PFMC is:

$\sigma_m = 26.1$ mN/m

Moreover, $\Delta\rho = 925$ kg/m$^3$, and g = 9.8 m/s$^2$. Substituting these values in Equation A1.1 we obtain

$r_{\max} \approx O(1mm)$.

# Appendix 3:

# Calculation of settling velocity vs. drop radius

The settling velocity of a fluid drop of radius $d$, in a fluid of density $\rho_l$ can be calculate according to Equation 4.4,

$$U = 2\sqrt{\frac{d * \Delta\rho * g}{3 * C_d * \rho_l}} \qquad \text{(Eq.4.4)}$$

where, $\Delta\rho$, is density difference between the two fluids, $g$ is gravity acceleration, 9.81 m/s and $C_d$ is the drag coefficient [Bird *et al.*, 2002].

The drag coefficient of spherical particles is a function of Reynolds number [Perry and Green, 1997],

$$\mathrm{Re} = \frac{d\rho_l U}{\mu_l} \qquad \text{(Eq. A3.1)}$$

where, $\mu_l$ is the fluid viscosity.

At low Reynolds number Re < 0.1 the drag coefficient is given by Equation A3.2

$$C_d = \frac{24}{\mathrm{Re}} \qquad \text{(Eq. A3.2)}$$

In the intermediate regime, 0.1 < Re < 1,000

$$C_d = \left(\frac{24}{\mathrm{Re}}\right)\left(1 + 0.14\,\mathrm{Re}^{0.70}\right) \qquad \text{(Eq. A3.3)}$$

and when 1,000 < Re < 350,000

$$C_d = 0.445 \qquad \text{(Eq. A3.4)}$$

Thus, to calculate the settling velocity of a PFMC drop in the organic mixture of 13 % mol 1 - octene and 87% nonanal, as well as the settling velocity of an organic

drop in pure PFMC, it is necessary to know the density and the viscosity of the pure components. These values are given in Table A3.1

**Table A3.1:** Properties of pure PFMC, 1 – octene and nonanal at 25 °C.

| Component | Density, kmol/m$^3$ | Viscosity, Pa s | Reference |
|---|---|---|---|
| PFMC | 1.788 | 1.561 $10^{-3}$ | [Green et al., 1994] |
| 1-octene | 0.715 | 0.457 $10^{-3}$ | [Reid et al., 1987] |
| Nonanal | 0.827 | 1.349 $10^{-3}$ | [Reid et al., 1987] |

The density and viscosity of the organic mixture were calculated to be 0.812 gr/cm$^3$ and 1.2 $10^{-3}$ Pa s respectively using the average molecular composition.

When we assume the worse case scenario, with the fluorous phase containing 20% mol organics and the organic phase containing 20% PFMC, the density and viscosity of both phases are again calculated using the average molecular composition.

To calculate the settling velocity according to Equations 4.4 and A3.1 to A3.4 we developed an algorithm in Excel using the trial and error method. For a given $C_d$ we calculated the settling velocity, $U$ and Reynolds number, Re. For that Re we calculated a new $C_d$, and we repeated the calculations until the two values converged.

The calculated velocities vs. drop radius are shown in Table A3.2.

Table A3.2: Calculated settling velocities vs. drop radius.

| d( um) | 500 | 750 | 1000 | 1100 | 1200 | 1300 | 1400 | 1500 |
|---|---|---|---|---|---|---|---|---|
| U fluorous100%, cm/s | 7.5 | 13.8 | 21.3 | 24.5 | 28.0 | 31.6 | 35.3 | 39.1 |
| U fluorous 80%, cm/s | 4.6 | 8.4 | 12.9 | 14.9 | 17.0 | 19.1 | 21.4 | 23.7 |
| U organic 100%, cm/s | 5.7 | 10.5 | 16.2 | 18.6 | 21.2 | 24.0 | 26.8 | 29.7 |
| U organic 80%, cm/s | 3.8 | 7.0 | 10.8 | 12.4 | 14.2 | 16.0 | 17.8 | 19.8 |

# Appendix 4:

# List of Publications and Presentations

***Publications***

1. Perperi E., Huang Y., Angeli P., Manos. G., Mathison C.R., Cole-Hamilton D.J., Adams D.A., Hope E.G., (2004). "A Novel Continuous Homogeneous Catalytic Process for Fluorous Biphasic Systems", *Chem. Eng. Sc.*, In press.
2. Perperi E., Huang Y., Angeli P., Manos. G., Mathison C.R., Cole-Hamilton D.J., Adams D.A., Hope E.G., (2004). "The Design Of A Continuous Reactor For Fluorous Biphasic Reactions Under Pressure And Its Use in Alkene Hydroformylation", *Dalton Trans.*, **14**, 2062 – 2064
3. Perperi E., Huang Y., Angeli P., Manos G., Cole-Hamilton D.J., (2004). "Separation studies in a continuous flow fluorous biphasic system. Proof of concept", *J. Molec. Catal. A: Chem*, **221**, 19 – 27
4. Huang Y., Perperi E., Manos G. and Cole – Hamilton D.J., (2004) "Performance of Octene in Fluorous Biphasic Hydroformylation: Octene Distribution and Reversible Transfer between Perfluoromethylcyclohexane and Nonanal", *J. Molec. Catal. A: Chem*, **210**, 17-21

***Presentations***

1. Perperi E., Huang Y., Manos G., Angeli P., Adams D.A., Mathison C.R., Hope E.G., Cole-Hamilton D.J., 18$^{th}$ International Symposium of Chemical reaction Engineering, Chicago (2004). (Presentation)

2. Huang Y., Perperi E., Manos G., Cole – Hamilton D.J., Phase Behaviour in Fluorous Biphasic Systems, Proc. 11th International Symposium on Relation between Homogeneous and Heterogeneous Catalysis, Evanston, Illinois (2003). (Poster)
3. Perperi E., Huang Y., Adams D.A., Mathison C.R., Manos G., Hope E., Cole-Hamilton D.J., Integrated Process Design For the Long Term Testing of Catalytic Reactions In Fluorous Biphasic Systems, 3rd RSC Fluorine Subject Group, Postgraduate Meeting, St. Andrews (2003). (Presentation)
4. Huang Y., Perperi E., Manos G. and Cole – Hamilton D.J., Performance of Octene in Fluorous Biphasic Hydroformylation: Octene Distribution and Reversible Transfer between Perfluoromethylcyclohexane and Nonanal, 3rd RSC Fluorine Subject Group, Postgraduate Meeting, St. Andrews (2003). (Poster)
5. Perperi E., Huang Y., Manos G. and Angeli P., Integrated Process Design for Catalytic Reactions in Fluorous Biphasic Systems, Proc. 4th Panhellenic Conference of Chemical Engineering, Patra (2003). (Presentation)
6. D.J. Adams, D. Gudmunsen, E.G. Hope, A.M. Stuart, D.J. Cole-Hamilton, D.F. Foster, G. Manos, P. Angeli & E. Perperi, Hydroformylation Under Fluorous Biphasic Solvent Conditions, Proc. Annual Conference of Royal Society of Chemistry, Symposium on Fluorous Biphasic Catalysis, Birmingham (2001). (Presentation)